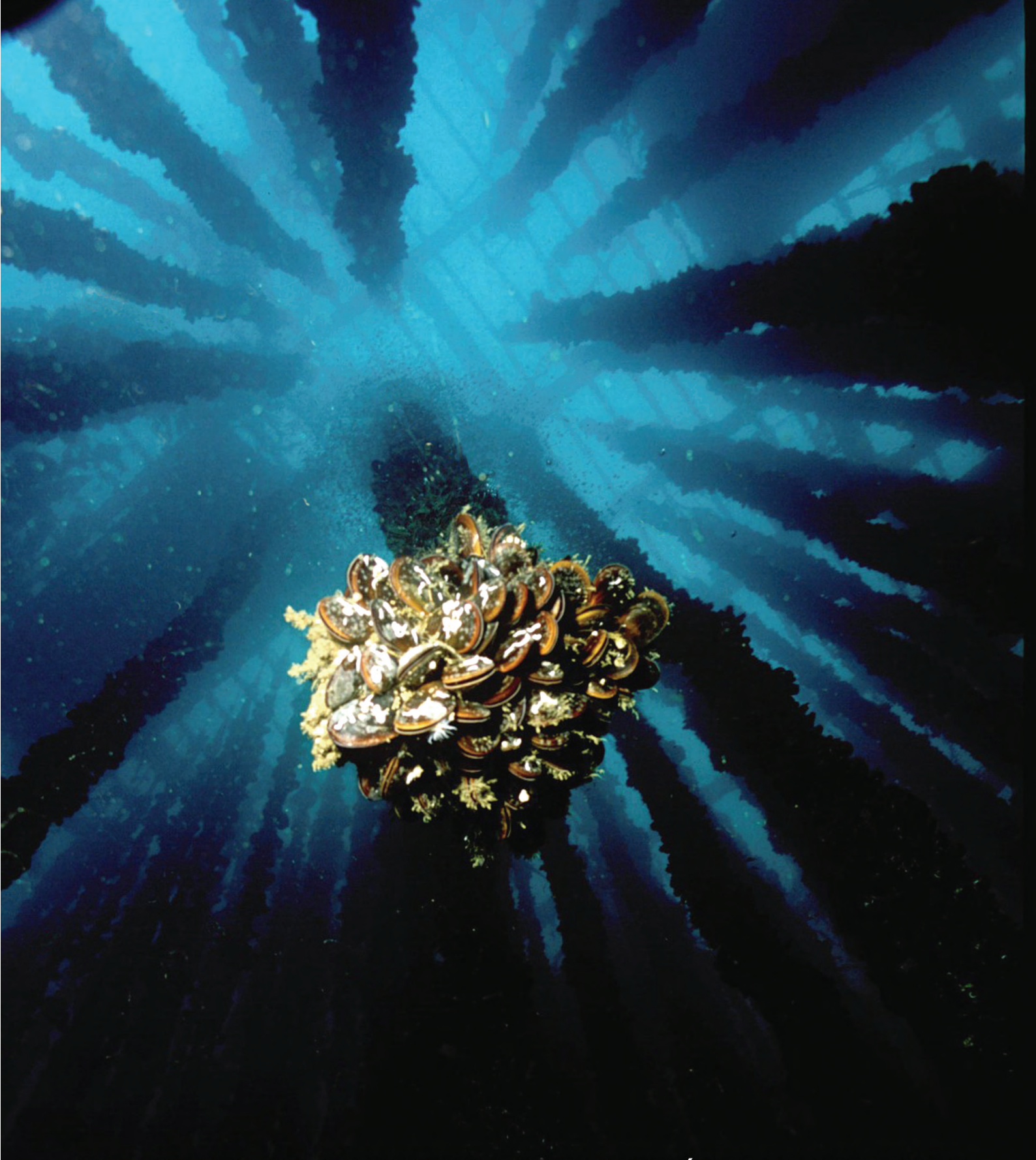

Relaciones de competencia intraespecífica y auto-raleo de Mytilus galloprovincialis en sistemas de cultivo suspendido

Instituto de Investigacións Mariñas

Alhambra gadea martínez cubillo

Tesis Doctoral 2012

Consejo Superior de Investigaciones Científicas
Instituto de Investigacións Mariñas

Universidade de Vigo

Relaciones de competencia intra-específica y auto-raleo del mejillón *Mytilus galloprovincialis* en sistemas de cultivo suspendido

Alhambra Gadea Martínez Cubillo

TESIS DOCTORAL

2012

Alhambra Gadea Martínez Cubillo fue contratada con cargo al Programa I3P del Fondo Social Europeo (CSIC-I3P-PC 2008) y con el contrato CSIC 201030E071. Esta tesis se ha realizado bajo la financiación del contrato-proyecto PROINSA-CSIC 20061089 y 0704101100001 y de los proyectos de la Xunta de Galicia PGIDIT06RMA018E y PGIDIT09MMA038E.

Fotografías portada: Manuel E. Garci. Para cualquier reproducción de la misma será necesario obtener el permiso del autor.

Procesamiento gráfico y diseño portada: Elia Muriel Martínez Cubillo.

Consejo Superior de Investigaciones Científicas
Instituto de Investigacións Mariñas

Universidade de Vigo

Intraspecific competition and self-thinning relationships of the mussel *Mytilus galloprovincialis* grown in suspended culture systems

Alhambra Gadea Martínez Cubillo

TESIS DOCTORAL

2012

To carry out this work Alhambra Gadea Martínez Cubillo was funded by a CSIC-I3P-PC 2008 contract, from the European Social Fund, and a CSIC 201030E071 contract. This study was supported by the PROINSA Mussel Farm contract-project (Codes CSIC 20061089 and 0704101100001) and Xunta de Galicia PGIDIT06RMA018E and PGIDIT09MMA038E projects.

Cover image: Manuel E. Garci.
Cover design: Elia Muriel Martínez Cubillo.
All rights reserved. No part of this cover may be reproduced without the prior permission of the authors.

Consejo Superior de Investigaciones Científicas

Instituto de Investigacións Mariñas

UXÍO LABARTA FERNÁNDEZ, Doctor en Ciencias Biológicas. Profesor de Investigación del CSIC.

MARÍA JOSÉ FERNANDEZ REIRIZ, Doctora en Biología. Investigador Científico del CSIC.

CERTIFICAN:

Que la presente Tesis Doctoral titulada: **Relaciones de competencia intra-específica y auto-raleo del mejillón *Mytilus galloprovincialis* en sistemas de cultivo suspendido**, que presenta ALHAMBRA GADEA MARTÍNEZ CUBILLO para optar al grado de Doctora por la Universidad de Vigo, ha sido realizada bajo nuestra dirección en el Grupo de Fisiología, Nutrición y Cultivo de Moluscos Bivalvos del Instituto de Investigacións Mariñas (IIM-CSIC), y una vez concluida, autorizamos su presentación ante el tribunal correspondiente, con el visto bueno del tutor, Gonzalo Méndez Martínez, profesor titular de la Universidad de Vigo.

Vigo, Enero de 2012

Fdo. Dra. María José Fernández Reiriz Fdo. Dr. Uxío Labarta Fernández

Fdo. Dr. Gonzalo Méndez Martínez

Agradecimientos

Y por fin la última sección de la tesis, una de las que más me apetecía escribir, lo cual me hace dudar de mi vocación como científica, o quizá simplemente es que hacía mucho tiempo que sentía la necesidad de agradecer a toda la gente todo lo que me han aportado de una u otra manera, o porque en mi casa siempre he escuchado aquello de "es de bien nacido ser agradecido"…

En primer lugar, me gustaría agradecer a mis directores de tesis, María José Fernández-Reiriz y Uxío Labarta, la confianza que tuvieron en mí, incluso en los momentos en los que yo misma la había perdido, la paciencia, y por supuesto su apoyo económico a lo largo del desarrollo de esta tesis.

Quiero agradecer al grupo PROINSA, en especial a Dolores Fernández Vázquez y a Juan Fernández Arévalo, ya que sin su apoyo a la ciencia, su tiempo y sus recursos este trabajo nunca hubiera podido llevarse a cabo. Además, tengo que dar las gracias a todos los trabajadores de la empresa por las molestias que hayamos podido causarles y su inestimable ayuda en cada muestreo. Todos ellos han aportado un grano de arena para que este trabajo llegara a buen puerto.

Quiero dedicar un agradecimiento especial a Laura García Peteiro, Helena Regueiro y María García, por todas las horas invertidas en el laboratorio (contar, pesar, medir, y vuelta a empezar…), el frío, las olas, la lluvia y hasta el granizo de los muestreos, por los agobios y las prisas, esas comidas "tragadas" en segundos que encima nos parecían largas… Pero también por esa profesionalidad, esa capacidad de organización, todas las risas y sobre todo, por ser tan buena gente y haberme hecho sentir como en casa, MIL GRACIAS…

Quiero agradecer a todo el grupo de moluscos bivalvos por el buen ambiente que se respira siempre en el laboratorio, que consiguen hacer mucho más agradable el día a día. A Ana, la voz de la experiencia, por saber de todo un poco, a Lourdes que desde el primer día ya estaba dispuesta a ayudarme en todo, a Bea por todos sus buenos consejos y atreverse con todo (incluida la danza oriental), a Babarro por leerse todo lo que le enviaba y por sus valiosísimas correcciones, a Elsi que aporta siempre buen humor y es una mamá estupenda, y a todas las personas que han pasado por allí: José Luis, David, Noelia, Javi, Cris, y a las nuevas incorporaciones: Jade y Vanessa,… porque siempre tienen buenas palabras y da gusto teneros por ahí. En especial, me gustaría dar las

gracias a Rocío por ser una estupenda compañera de piso durante tres años y una cuaderna leal por muchos más, por todos los chapuzones, los paseos, las pláticas, los desmadres y las crudas. Porque no sé qué voy a hacer sin ti cuando te regreses a México, una cosa es segura, te voy a extrañar de a madres…

Otra mención especial la merece Lau, que además de ayudarme en los muestreos siempre me ha echado una mano con mis dudas tanto en el análisis de datos como en la redacción del texto. Porque a parte de ser una excelente compañera de trabajo también es una buena amiga, sin ti esta tesis no sería lo que es…

También me gustaría agradecerle a Isabel su gran ayuda con la parte matemática del self-thinning, así como con la redacción y la traducción de esos dos capítulos, y qué decir de sintetizar todo a la mitad, que parecía imposible!

Gracias también a todo el personal del IIM, en especial a Marigel, por su ayuda en la búsqueda de los artículos perdidos y por ese gran sentido del humor y a Garci por esas increíbles fotos de las cuerdas en la batea. Agradecer también a mis amigos del Instituto: Elsi, Waldo, Berto, Roci, Miguel, Javi Chuliño, Beliña, Aldo, Sheila, Fernando, Fernandinho, Tere, ... por hacer del IIM un sitio mucho más alegre. Tampoco quiero olvidarme de mis amigos de fuera del instituto y en especial a Migui, Gelo, Roi y Buisqui, porque me acogisteis como una más desde el principio y porque me lo paso increíble con vosotros, nunca cambiéis!!

Gracias a mis amigos de Burgos: Mari, Jelenai, Dianepo, Carmen, Cou, Laurens, Ane, Reichi, Elena, Marga y Lauris y a mis coleguillas de la universidad de Salamanca: Lemur, Regi, Estefa, Rebecal, Cris, Sandra y Laura por todos los buenos momentos juntos y porque haya muchos más…

Otras mil gracias son para Isma, que a pesar de la distancia siempre me apoyó en todo y me animó para hacer esta tesis aunque ello supusiese estar separados durante tres largos años, gracias por toda la paciencia, el cariño y los muchos buenos ratos juntos. ¡Ojalá no perdamos esta buena amistad!

Un agradecimiento especial va para mi familia: a mis padres, por todo lo que han hecho por mí, qué duda cabe que sin ellos este trabajo no sería posible, a mi madre por haberme ayudado tantas veces a hacer la tarea (qué paciencia!), a mi padre por aportarme el lado arquitectónico y artístico (todo el que he sido capaz de desarrollar…), a mis hermanos Elia y Mauro, que son lo que más quiero en este mundo, por tantos años de juegos y peleas... y a mi July, mi segunda mamá, por querernos y criarnos desde que éramos enanos.

También deseo agradecer de todo corazón a Miguel por su gran apoyo sentimental y de todo tipo durante estos últimos tiempos, por su paciencia, su cariño y su comprensión, por ser un gran compañero de la vida y por que lo siga siendo durante mucho tiempo más…

Finalmente, me gustaría dedicar esta tesis a mis abuelitos Felisa, Jesús, Aurelia y Leonardo, por todo vuestro cariño y atenciones y por representar la parte más bondadosa y entrañable de este mundo, quiero que sepáis que siempre os llevo en mi corazón y que no me olvidaré de vosotros nunca.

Índice

Capítulo 1. Introducción general.....3

1.1. Contexto general: El cultivo del mejillón en Galicia.....3

1.2. Implicaciones ecológicas de la elevada densidad poblacional.....4

1.3. Estudio del fenómeno de auto-raleo o self-thinning (ST).....5

1.4. Implicaciones de la densidad poblacional y la competencia intraespecífica en el cultivo.....10

1.5. Área de estudio.....11

1.6. Hipótesis y objetivos..... 12

Capítulo 2. Influence of stocking density on growth of mussels (*Mytilus galloprovincialis*) in suspended culture.....15

2.1. Introduction.....16

2.2. Material and Methods.....18

2.3. Results.....22

2.4. Discussion.....34

Capítulo 3. Density-dependent effects on morphological plasticity of *Mytilus galloprovincialis* in suspended culture.....37

3.1. Introduction.....38

3.2. Material and Methods.....40

3.3. Results.....42

3.4.Discussion..... 49

Capítulo 4. Evaluation of self-thinning models and estimation methods in multilayered sessile animal populations.....55

4.1. Introduction.....56

4.2. Material and Methods.....58

4.3. Results and Discussion.....64

4.4. Conclusions.....79

4.5. Appendix.....83

Capítulo 5. Dynamic self-thinning model for sessile animal populations with multilayered distribution.....89
5.1. Introduction.....90
5.2. Material and Methods.....92
5.3. Results.....96
5.4. Discussion.....105
5.5. Appendix.....109

Capítulo 6. Conclusiones generales.....117

Bibliografía.....125

Capítulo 1. Introducción general

1.1. Contexto general: El cultivo de mejillón en Galicia

El cultivo de mejillón tiene una gran importancia ecológica y socio-económica en las Rías Gallegas. Las condiciones oceanográficas de las Rías constituyen el marco idóneo para su cultivo, ya que la interacción entre el afloramiento costero y los patrones de circulación internos tienen como resultado una alta producción fitoplanctónica en el interior de las mismas (Figueiras et al. 2002).

En Galicia se desarrolla la mayor producción de mejillón cultivado en Europa y una de las más extensivas del mundo (Labarta, 2004). Esta producción se desarrolla en cultivo suspendido, mayoritariamente en estructuras flotantes ancladas al fondo marino (bateas), de donde cuelgan las cuerdas de mejillón. Este cultivo está condicionado por la variabilidad de las condiciones ambientales en el ecosistema Rías y, muy particularmente, por las variaciones interanuales y espaciales que tienen lugar en ellas. Así, como en toda cosecha en medio natural, es posible observar una variabilidad en aspectos como el crecimiento y el rendimiento en función de las características de la zona de cultivo y de las condiciones ambientales y oceanográficas que se suceden en distintos años (Labarta et al. 2004).

Desde una perspectiva de optimización del proceso de cultivo, además de las labores propias del cultivo, es preciso conocer las condiciones ambientales de la zona de producción, sobre todo en lo que a disponibilidad de alimento se refiere, y adaptar la densidad de cultivo a estas características, para que la producción y la rentabilidad económica de la explotación sean lo más altas posibles (Labarta et al. 2004).

La disponibilidad de alimento en una batea viene determinada por la concentración de clorofila y por la velocidad de la corriente a través de ella. Son precisamente estos dos factores los que explican más de un 75% de la varianza de las tasas de crecimiento del mejillón en las Rías (Pérez-Camacho et al. 1995). Ambos factores vienen determinados en primer lugar por las condiciones oceanográficas de las Rías, a lo que hay que sumar los aportes de agua continental de los ríos que desembocan en estas.

Además de las características ecológicas y oceanográficas, el cultivo de mejillón se encuentra determinado en gran medida por la densidad de las unidades de cultivo (bateas) y su distribución espacial en el área de producción. Además, la densidad en cada unidad de cultivo (número de cuerdas) y la densidad por cuerda (individuos por cuerda) son factores fundamentales que afectan al rendimiento y la productividad de la

cosecha y por lo tanto, son de extrema importancia para el desarrollo de estrategias de explotación y gestión de los cultivos.

La acuicultura en cultivo suspendido representa un caso extremo de agregación donde se maximiza la densidad de estos suspensívoros para conseguir un mayor rendimiento comercial. Sin embargo, el efecto negativo de las elevadas densidades de cultivo sobre el crecimiento del mejillón es bien conocido por los bateeiros. Por este motivo, en el cultivo tradicional de mejillón en Galicia se realizan sucesivas reducciones de la densidad de las cuerdas, procesos conocidos como "Partida" y "Desdoble". La "Partida" se realiza debido a las elevadas densidades de asentamiento en las cuerdas colectoras y consiste en el desprendimiento del mejillón de los colectores para plantarlo a las mismas densidades que la semilla recogida del litoral rocoso (Labarta, 2004). El "Desdoble" se lleva a cabo después de 4-7 meses, cuando el mejillón ha alcanzado tallas alrededor de 40-60 mm y el peso de las cuerdas ha aumentado considerablemente haciendo que el crecimiento sea más lento y heterogéneo. Este proceso consiste en desprender el mejillón de las cuerdas para volverlo a encordar con el objetivo de homogeneizar las tallas y disminuir la densidad (Pérez-Camacho et al. 1991).
El "desdoble" permite a los bateeiros controlar la densidad de mejillón en las cuerdas con el fin de optimizar su crecimiento, minimizando el tiempo de cultivo y las pérdidas de producto, ya que además de limitar la disponibilidad de alimento, las altas densidades también aumentan el riesgo de mortalidad denso-dependiente y desprendimientos de mejillón de las cuerdas ocasionando pérdidas económicas. Este es un método comúnmente empleado, a pesar de que representa una inversión considerable respecto a costes operativos y mano de obra, dando una idea de la importancia de la densidad sobre el crecimiento del mejillón y el rendimiento de los cultivos.

1.2. Implicaciones ecológicas de la elevada densidad poblacional

Desde el punto de vista ecológico, la densidad juega un papel importante en la dinámica poblacional de los organismos sésiles. El comportamiento gregario de algunos invertebrados bentónicos suspensívoros como los bivalvos conlleva una serie de ventajas, que incluyen protección ante predadores (Bertness & Grosholz 1985; Lin 1991; Reimer & Tedengren 1997), éxito reproductivo (Okamura 1986) y optimización de los regímenes hidrodinámicos que generan un mayor flujo de seston (Gibbs et al. 1991). Sin embargo, las elevadas densidades poblacionales pueden causar limitaciones

de los recursos (espacio/alimento) disponibles para los organismos provocando la aparición de fenómenos de competencia intraespecífica (Alvarado & Castilla 1996; Boromthanarat & Deslous-Paoli 1988; Fréchette et al. 1992; Gascoigne et al. 2005; Guiñez 1996; Guiñez & Castilla 1999; Mueller 1996; Okamura 1986; Taylor et al. 1997). Estas limitaciones pueden causar reducciones en el crecimiento (Alunno-Bruscia 2000; Boromthanarat & Deslou-Paoli 1988; Dowd et al. 2001; Fréchette & Bourget 1985[ab]; Gascoigne et al. 2005; Guiñez & Castilla 1999; Grant 1999; Kautsky 1982[a]; Newel 1990; Peterson 1989; Scarrat 2000) y cambios en la morfología del mejillón (Alunno-Bruscia et al. 2001; Lauzon-Guay et al. 2005[b]; Seed et al. 1968). Además, la interferencia física entre individuos genera presiones laterales que restringen la eficacia de la apertura valvar, provocando reducciones en la tasa de aclaramiento y por tanto, del crecimiento (Jørgensen et al. 1988).

A medida que los individuos crecen, los procesos de competencia intraespecífica se intensifican, provocando la aparición de una mortalidad denso-dependiente (Griffiths & Hockey 1987; McGrorty et al. 1990; Richardson & Seed 1990; Stillman et al. 2000; Stiven & Kuenzler 1979). Este proceso, denominado auto-raleo o self-thinning (ST), determina finalmente el tamaño poblacional en función de la disponibilidad de recursos (Westoby et al. 1981; Yoda et al. 1963).

1.3. Estudio del fenómeno de auto-raleo o self-thinning (ST)

El fenómeno de self-thinning describe la correlación negativa entre tamaño corporal y densidad de la población cuando el crecimiento de los individuos provoca mortalidad por competencia intraespecífica (Weller 1987; Westoby 1984). Este proceso ha sido observado en poblaciones de elevada densidad de plantas y animales y juega un papel importante determinando la dinámica poblacional y la estructura de la comunidad (Fréchette & Lefaivre 1995; Fréchette et al. 1996; Guiñez & Castilla 1999, 2001; Guiñez et al. 2005; Marquet et al. 1995; Petraitis 1995; Puntieri 1993; Westoby 1984). El self-thinning se estudia mediante el seguimiento del crecimiento de grupos de la misma edad y diferente densidad a través de muestreos secuenciales en el tiempo, que se representan en diagramas biomasa vs. densidad (B-N), o de forma equivalente, masa media individual vs. densidad (m-N) (Alunno-Bruscia et al. 2000). En este tipo de diagramas podemos observar distintos patrones de respuesta a lo largo del tiempo y el incremento en tamaño de los organismos (Alunno-Bruscia et al. 2000; Fréchette et al. 1995; Fréchette et al. 1996; ver Figura 1). En un primer momento (t0), el ecosistema es

capaz de soportar un mayor número de individuos de menor tamaño y se puede observar un incremento lineal de la biomasa con la densidad, lo que indica ausencia de competencia y mortalidad incluso a elevadas densidades. Esto significa que el crecimiento y la mortalidad son independientes tanto de la densidad como de la biomasa. A tiempo t1 esto todavía sucede en todas las densidades. Con el tiempo, al incrementarse el tamaño de los individuos, se ralentiza el crecimiento en los grupos de mayor densidad, indicando la aparición de fenómenos de competencia intraespecífica (a partir de N5 en t2). Por último, los procesos de competencia observada en las poblaciones de mayor densidad dan lugar a la aparición de mortalidad (N5-N7 en t3), delimitando la biomasa máxima soportada por el ecosistema a una densidad determinada (fenómeno de auto-raleo o self-thinning).

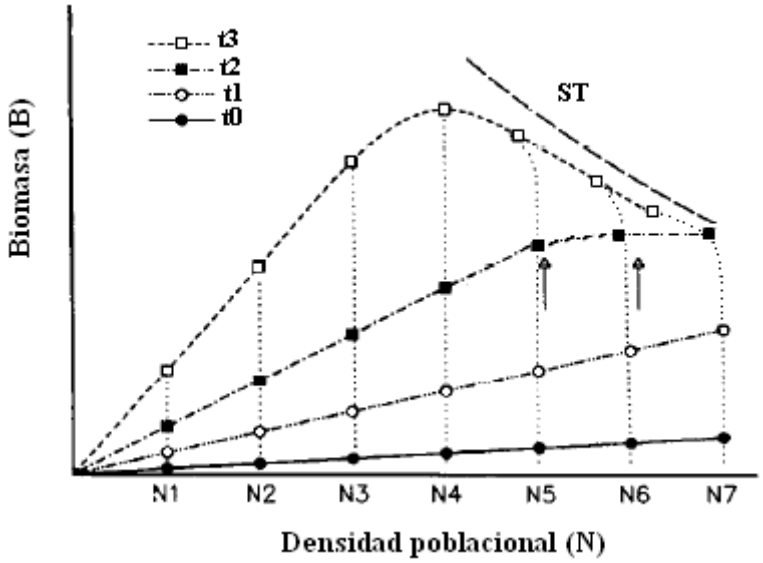

Fig. 1. Ejemplo del típico diagrama B-N, donde se representa la evolución de distintas densidades iniciales (N1-N7) en muestreos sucesivos a lo largo del tiempo (t0-t3). Las flechas indican la evolución del tiempo. ST: línea de self-thinning. Modificado a partir de Fréchette et al. (1995).

Tradicionalmente el self-thinning ha sido descrito a través de un modelo bidimensional, en el que se define la relación alométrica entre la biomasa (B) y la densidad (N) de la población:

$$B = k_2 N^{\beta_2} \tag{1.1}$$

donde k_2 y $ß_2$ son los parámetros del modelo.

Teniendo en cuenta que la masa media individual (m) se obtiene como el cociente entre biomasa y densidad, m=B/N, podemos obtener el equivalente para la relación masa-densidad:

$$m = k_2 N^{\beta-1} = k_2 N^{\gamma} \quad (1.2)$$

La mayor parte de los estudios experimentales y teóricos acerca de las relaciones de ST se han desarrollado en plantas, donde se supone competencia por espacio (SST) y se ha sugerido el exponente clásico de $ß_2$ = -1/2 para un amplio rango de especies (Westoby 1984; White 1981; Yoda et al. 1963). Este exponente se obtiene de las relaciones morfométricas de la superficie ocupada por un individuo (S) con respecto a su longitud (l) y su peso (m). Asumiendo un crecimiento isométrico ($S \alpha l^2$ y $m \alpha l^3$) y que la superficie es inversamente proporcional a la densidad (N), se obtiene la expresión: $m = k_2N^{-3/2}$ o su equivalente $B = k_2N^{-1/2}$ en relación a la biomasa de la población (B = Nm). Aunque esta teoría esta basada en estudios realizados con plantas, puede ser aplicable a poblaciones de animales sésiles y móviles (Hughes & Griffiths 1988; Steingrímsson & Grant 1999).

Begon et al. (1986) sugirieron que en animales móviles el proceso de ST se describía mejor como una consecuencia de la limitación de alimento (FST) y basándose en la hipótesis de la "equivalencia energética" proponen un exponente de $ß_2$ = -1/3 (ver a su vez Armstrong 1997; Bohlin et al. 1994; Dunham & Vinyard 1997; Elliot 1993; Latto 1994; Norberg 1988[a]). Esta hipótesis sugiere que la densidad poblacional está relacionada con la tasa metabólica de la población (TM), la cual está relacionada con el peso medio de los individuos ($TM \alpha N m^{3/4}$) y la energía disponible ($TM \alpha F$). Asumiendo que la cantidad de alimento consumido por la población es constante (F cte) en condiciones ambientales estables se obtendría que $m = k_2N^{-4/3}$ o su equivalente $B = k_2N^{-1/3}$.

Fréchette & Lefaivre (1990) tratan de distinguir el efecto de las limitaciones por espacio y alimento sobre la relación existente entre la máxima biomasa soportada por la población y la densidad de la misma (auto-raleo). Para ello se basan en las expresiones matemáticas descritas, atribuyendo el ajuste de la densidad derivado de limitaciones espaciales, SST, a la relación $m = kN^{-3/2}$ ($B = kN^{-1/2}$), y el derivado de las limitaciones de alimento, FST, a la relación $m = kN^{-4/3}$ ($B = kN^{-1/3}$). Sin embargo, distinguir el efecto de las limitaciones por espacio o por alimento en función del exponente (β_2) es

complicado ya que, además de poder existir interdependencia entre ambos factores en individuos sésiles y filtradores (Buss 1979; Fréchette et al. 1992), el exponente de ambas funciones puede desviarse del valor teórico (Alunno-Bruscia et al. 2000). De este modo, se ha observado una amplia variabilidad en el exponente de la relación tasa metabólica vs. peso (Latto 1994), que a su vez alteraría el valor teórico del exponente para la función del FST.

En el caso de las limitaciones por el espacio, las asunciones del modelo clásico son: (1) crecimiento isométrico, (2) la ocupación del 100% de la superficie muestreada (White 1981) y (3) la existencia de una relación inversa entre esta superficie y la densidad de los individuos ($N \alpha S^{-1}$, Hughes & Griffiths 1988). Sin embargo, el crecimiento no sigue una relación isométrica sino alométrica que provoca una desviación del exponente teórico (Hughes & Griffiths 1988; Weller 1987; Westoby 1984; White 1981). Además, los mejillones, al igual que otros bivalvos sésiles, son animales gregarios que forman habitualmente matrices muy densas y complejas estructuralmente que a veces se disponen formando múltiples capas sobre el sustrato (Alvarado & Castilla 1996; Guiñez 1996; Suchanek 1986; ver Figura 2). Esta disposición invalida la tercera de las asunciones enumeradas y altera el exponente teórico esperado al infraestimar la superficie disponible para los individuos (Hughes & Griffiths 1988). Todas estas desviaciones han sido incluidas en nuevos modelos (Frechette & Lefaivre 1990, 1995; Guiñez & Castilla 1999) que reformulan las relaciones clásicas para introducir el efecto del crecimiento alométrico, la disposición multicapa y la posible influencia de la rugosidad del sustrato como modificador de la superficie disponible para los individuos.

Guiñez and Castilla (1999) proponen un modelo tridimensional incorporando el grado de empaquetamiento (número de capas) en el modelo bidimensional, de tal modo que la densidad de individuos (N) es inversamente proporcional a la superficie que proyectan en el sustrato (S) y directamente proporcional al número de capas (L) que forman ($N \alpha L S^{-1}$). Así, la expresión matemática del modelo tridimensional B-N-L que define el auto-raleo puede expresarse como:

$$B = k_3 (n/S)^{\beta} L^{1-\beta} = k_3 N^{\beta} L^{1-\beta} = k_3 (N/L)^{\beta} L = k_3 N_e{}^{\beta} L \qquad (1.3)$$

$$m = k_3 (n/SL)^{\beta-1} = k_3 N^{\beta-1} L^{1-\beta} = k_3 (N/L)^{\beta-1} = k_3 N_e{}^{\gamma} \qquad (1.4)$$

donde m es la masa media individual, n el número de individuos, S la superficie total ocupada, N la densidad, L el número de capas, N_e=N/L la densidad por capa o densidad efectiva y (k_3,β_3) el vector de parámetros del modelo.

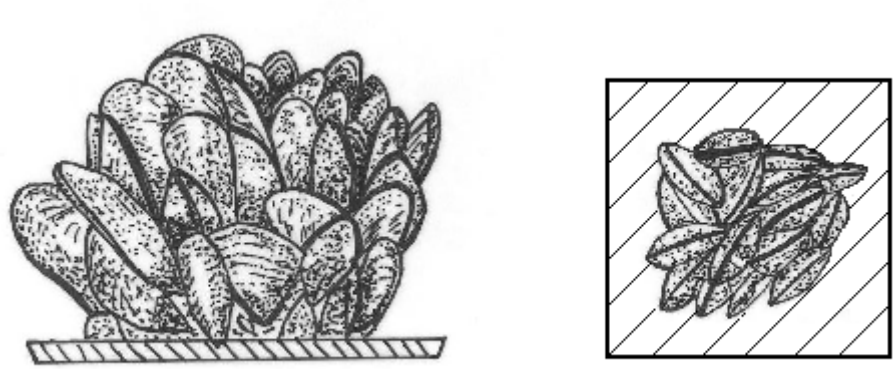

Fig. 2. Representación de la disposición de los mejillones en el sustrato desde la perspectiva de A) un corte longitudinal y B) una visión apical.

La principal debilidad de los modelos de self-thinning empleados actualmente (ecs. 1.1-1.4) es como se trata el tiempo, pues a pesar de que en la estimación de los parámetros (K,β) se incluye implícitamente al utilizar medidas secuenciales de masa y densidad, el efecto temporal no aparece explícitamente en el modelo. Esto restringe el análisis al comportamiento competitivo medio de la población y produce una estimación sesgada de los parámetros del modelo. Roderick & Barnes (2004) ponen de manifiesto esta situación y presentan una nueva formulación del self-thinning como un problema dinámico. En este nuevo modelo los parámetros K y β se estiman para cada intervalo de tiempo y el exponente de self-thinning (β) se define como el cociente entre las tasas de cambio de masa y densidad:

$$\beta = \frac{dm}{m}\frac{N_e}{dN_e} \tag{1.5}$$

Esta aproximación refleja la naturaleza dinámica del proceso de ST y facilita la interpretación ecológica del modelo.

1.4. Implicaciones de la densidad poblacional y la competencia intraespecífica en el cultivo

La existencia de competencia por espacio y alimento ha sido observada en poblaciones de mejillones, tanto naturales (en "mussel beds") como cultivadas (Ceccherelli & Barboni 1983; Fréchette & Lefaivre 1990; Fréchette et al. 1992; Mueller 1996; Taylor et al. 1997). Así, se ha observado una inhibición en la alimentación y descensos en las tasas de crecimiento y supervivencia en áreas con elevada densidad de mejillones cultivados (Fréchette & Despland 1999).

Por un lado, se ha observado que las limitaciones espaciales provocadas por elevadas densidades de bivalvos pueden dar lugar a unas tasas de crecimiento y unos rendimientos de cosecha menores (Scarratt 2000). Además, el aumento de la interferencia física entre individuos puede reducir los beneficios de la cosecha, bien por distorsiones en la concha (Bertness & Grosholz 1985), que pueden afectar la calidad y aceptabilidad del producto en el mercado, o por migraciones y desprendimientos denso-dependientes (McGrorty & Goss-Custard 1995), que conllevan pérdidas de producto comercializable.

Por otra parte, la especie *Mytilus galloprovincialis* tiene una gran capacidad de filtración que puede ocasionar la depleción de las partículas de seston en la columna de agua y provocar limitaciones de alimento en los emplazamientos de cultivo (Dolmer 2000; Gibbs et al. 1991; Grant 1996; Lesser et al. 1992; Mueller 1996; Navarro et al. 1991; Smaal & van Stralen 1990). En general, se ha podido establecer que el mejillón contenido en una batea retiene entre un 30 y un 40% de la materia orgánica particulada, y hasta un 60% del fitoplancton en términos de clorofila (Pérez-Camacho et al. 1991). La cantidad de alimento disponible a escala local depende de la densidad poblacional, la concentración de seston disponible y la hidrodinámica (Dame & Prins 1998). Así, la densidad tiene un efecto negativo creciente sobre el crecimiento de los individuos en zonas con tiempos de residencia elevados y/o en aguas menos profundas, originando un gradiente de crecimiento dentro de las Rías (Bacher et al. 2003; Iglesias et al. 1996). En las zonas donde se produce el cultivo extensivo de mejillón, la tasa de renovación del agua puede limitar la renovación del seston (Álvarez-Salgado et al. 2008; Álvarez-Salgado et al. 2011) causando limitaciones en el crecimiento y el rendimiento comercial (índice de condición) de los mejillones en cultivo suspendido (Lesser et al. 1992). Este fenómeno es más frecuente en las partes internas de las Rías donde el intercambio mareal es mucho menor (Álvarez-Salgado et al. 2008; Álvarez-Salgado et al. 2010). Se

necesitan estimadores de la capacidad de las Rías para sustentar los niveles de producción (capacidad de carga) con el fin de optimizar la gestión y definir la idoneidad de las localizaciones para el cultivo de mejillón.

La limitación por alimento puede afectar el crecimiento de los bivalvos a varios niveles. Las elevadas densidades en las cuerdas de cultivo pueden provocar una reducción del crecimiento en los individuos de la parte interna (Côte et al. 1994; Parsons & Dadswell 1992). Así mismo, la depleción de seston a través de las zonas de cultivo puede afectar de la misma manera al crecimiento de los bivalvos en el centro de estas (Pilditch et al. 2001). Por otra parte, los ciclos naturales de disponibilidad de alimento, asociados a una serie de fenómenos oceanográficos como el afloramiento costero, pueden modular los procesos de competencia intraespecífica y sus efectos sobre el crecimiento y la supervivencia (Figueiras et al. 2004).

1.5. Área de estudio

La Ría de Ares-Betanzos se encuadra dentro de las Rías centrales de Galicia, en el NW de la Península Ibérica y es una de las Rías en forma de V de la costa gallega (Fig. 1 del Capítulo 2). La topografía de este estuario es compleja, con una parte interna poco profunda (<10 m) dividida en dos ramales, Ares y Betanzos, y una parte externa más profunda donde convergen ambos, que está conectada con la costa adyacente (Sánchez-Mata et al. 1999). Se trata de una Ría relativamente pequeña (72 km^2) en comparación con las Rías Baixas, que presenta una longitud de 19 km de largo y 4.7 km de anchura máxima (Fraga 1996). La ría soporta un volumen total de 0.65 km^3, alcanzando una profundidad máxima de 43 m en el extremo abierto.

Desde el punto de vista hidrográfico, las dos ramas internas pueden ser consideradas como estuarios: siendo Ares el estuario del río Eume, con un caudal medio de 16.5 m^3 s^{-1} y Betanzos el estuario del río Mandeo, con un caudal medio de 14.1 m^3 s^{-1} (Gómez–Gesteira & Dauvin 2005; Prego et al. 1999; Sánchez–Mata et al. 1999). Por el contrario, la ría exterior se comporta como una extensión de la costa adyacente y responde a la intensidad, persistencia y dirección de los vientos costeros (Bode & Varela 1998).

Las áreas de cultivo del mejillón están localizadas en la zona sur de la ría, en concreto en Arnela y Lorbé, con un total de 40 y 107 bateas, respectivamente, que producen alrededor de 10.000 toneladas de mejillón al año (Labarta et al. 2004).

El cultivo experimental de este estudio se llevó a cabo en una de las bateas empleadas habitualmente para el cultivo de mejillón en la ría de Ares-Betanzos, concretamente en

el polígono de Lorbé, siguiendo los métodos de cultivo y manejo utilizados por la empresa propietaria de la explotación.

1.6. Hipótesis y objetivos

En base a lo expuesto anteriormente y en el contexto del cultivo de mejillón en las Rías Gallegas, se plantearon las siguientes hipótesis:

¿Las densidades habituales de plantado en el cultivo industrial de *M. galloprovincialis* provocan la aparición de fenómenos de competencia intraespecífica o de auto-raleo? ¿A partir de que densidad se desarrollan dichos procesos? ¿Se ve acentuada la competencia intraespecífica con el crecimiento de los individuos? ¿Se reflejan dichos procesos de competencia sobre el crecimiento, la morfología y la mortalidad de *M. galloprovincialis*? ¿La regulación del tamaño de la población es consecuencia de una limitación del espacio disponible para crecer o de una limitación de la disponibilidad de alimento? ¿Es posible caracterizar mediante modelos matemáticos clásicos dichos procesos de competencia intraespecífica y auto-regulación del tamaño poblacional? ¿Son capaces estos modelos de inferir el factor limitante que los desencadena (espacio/alimento)?

En la acuicultura, y en concreto en la producción de mejillón en cultivo suspendido en las Rías Gallegas, se maximiza la densidad de los organismos para conseguir un mayor rendimiento comercial. Además, el uso de sistemas de cultivo suspendido permite manipular la densidad en el medio natural y al mismo tiempo eliminar una serie de variables que pueden interferir en estudios en el intermareal y el fondo, tales como exposición al oleaje, desecación, etc. Esto nos proporciona un escenario ideal para el estudio de los efectos de la densidad y la competencia intraespecífica en el medio natural. Además, existen pocos estudios sobre la influencia de la densidad de plantado en el crecimiento de los mejillones en cultivo suspendido (Lauzon-Guay et al. 2005ª; Lauzon-Guay et al. 2006; Pérez-Camacho & Labarta 2004), a pesar de la importancia que tiene ésta en la industria miticultora. El estudio de la competencia intraespecífica en dicho escenario, permite estudiar las implicaciones ecológicas del tamaño poblacional y los recursos limitantes del mismo, así como una transferencia directa del conocimiento obtenido a la producción industrial de mejillón.

En base a todo lo expuesto se plantearon los siguientes objetivos:

- Evaluar el efecto de un gradiente de densidades de cultivo, y por tanto de diferentes niveles de competencia intraespecífica, sobre el crecimiento, la plasticidad morfológica y la supervivencia del mejillón (*Mytilus galloprovincialis*) en una situación de cultivo suspendido en la Ría de Ares-Betanzos.

- Establecer las relaciones de auto-raleo o self-thinning que delimitan la biomasa soportada por el ecosistema, evaluando qué variables del sistema (espacio y/o alimento) condicionan la competencia intraespecífica, los procesos de auto-raleo y por tanto determinan el tamaño de la población.

- Estudiar la evolución temporal de la competencia intraespecífica y aportar una interpretación más realista de la dinámica poblacional de *Mytilus galloprovincialis* mediante la extensión del modelo dinámico de self-thinning propuesto por Roderick & Barnes (2004).

El contenido de este capítulo se corresponde con el artículo:

Alhambra M. Cubillo, Laura G. Peteiro, María José Fernández-Reiriz, Uxío Labarta (2012) Influence of stocking density on growth of mussels (*Mytilus galloprovincialis*) in suspended culture. Aquaculture (in press).

Capítulo 2. Influence of stocking density on growth of mussels (*Mytilus galloprovincialis*) in suspended culture

Influencia de la densidad poblacional en el crecimiento del mejillón (*Mytilus galloprovincialis*) en cultivo suspendido

Summary

Crowding conditions in bivalve populations cause intraspecific competition processes, resulting in individual growth reduction. In aquaculture, density is usually maximized to obtain a greater commercial yield. Commercial farms provide an ideal scenario for studying the effect of density on mussel growth in suspended culture systems. In this study, different growth indicators for *Mytilus galloprovincialis* (growth rates, length and weight growth curves and size frequency distributions) were measured along a cultivation density gradient. Ropes cultured at different densities (220, 370, 500, 570, 700, 800 and 1150 ind/m) were hanged from a commercial raft and growth indicators were monitored monthly over the second phase of traditional culture in Galicia, from thinning-out to harvest (April to October 2008). A negative effect of density on individual growth was observed. Individuals cultured at lower densities presented higher growth rates and consequently reached greater weight and length values at the end of the experimental period than those cultured at higher densities. Differences in growth related to the cultivation density may suggest differences in intraspecific competition for limiting resources (space/food). Effects of density on growth started after 4 months of culture (August) when individuals reached sizes around 66 ± 1.3 mm. The increase in size of individuals in a population implies an increment of their food and space requirements, which in turn intensifies intraspecific competition. This fact should be considered in aquaculture management, since higher densities could be supported without effects on growth performance if cultured mussels are limited to a lower size.

2.1. Introduction

The gregarious behavior characteristic of many benthic suspension-feeding invertebrates such as bivalves is associated with certain advantages including protection from predators (Bertness & Grosholz 1985; Lin 1991; Reimer & Tedengren 1997), reproductive success (Okamura 1986) and optimization of hydrodynamic regimes leading to a higher flux of seston (Gibbs et al. 1991). However, high population densities may lead to food and space limitations inducing intraspecific competition phenomena (Alvarado & Castilla 1996; Boromthanarat & Deslous-Paoli 1988; Fréchette et al. 1992; Gascoigne et al. 2005; Guiñez 1996; Guiñez & Castilla 1999; Mueller 1996; Okamura 1986; Taylor et al. 1997). Intraspecific competition for limiting resources is usually reflected in growth reductions at the individual level (Alunno-Bruscia et al. 2000; Boromthanarat & Deslous-Paoli 1988; Gascoigne et al. 2005; Guiñez & Castilla 1999; Kautsky 1982; Newel 1990; Parsons & Dadswell 1992; Peterson 1989; Scarrat 2000). Furthermore, as population density increases, intraspecific competition can also cause density-dependent mortality (Griffiths & Hockey 1987; Richardson & Seed 1990; Stillman et al. 2000; Stiven & Kuenzler 1979). This mechanism, known as "self-thinning", can regulate the size of the population regarding to the available resources (Westoby et al. 1984; Yoda et al. 1963).

In bivalves, crowding conditions were shown to have negative impacts on growth due to spatial limitations, inducing shell distortion (Bertness & Grosholz 1985) or density-dependent migration (McGrorty & Goss-Custard 1995). Moreover, physical interference between neighbours can result in restrictions of shell gape and thus clearance rate, which in turn cause reductions in feeding and mussel growth (Jørgensen et al. 1988). In addition, the large filtering capacity of mussels can cause depletion of seston particles in the water column and food limitations in cultivation emplacements (Dolmer 2000; Gibbs et al. 1991; Grant 1996; Lesser et al. 1992; Mueller 1996; Navarro et al. 1991; Smaal & van Stralen 1990). The quantity of food available at local scale depends on mussel population density, seston availability and the hydrodynamic patterns (Dame & Prins 1998). In areas with extensive mussel cultivation, the water renewal time can limit the seston regeneration (Álvarez-Salgado et al. 2008; Álvarez-Salgado et al. 2011) with the subsequent growth reduction. Furthermore, natural cycles of food availability associated with oceanographic processes such as coastal upwelling,

may modulate intraspecific competition processes and their consequences in individual growth and survival (Figueiras et al. 2002).

Competition for space and food has been observed in both natural mussel beds and cultured mussel populations (Ceccherelli & Barboni 1983; Fréchette & Lefaivre 1990; Fréchette et al. 1992; Mueller 1996; Taylor et al. 1997). Aquaculture on suspended structures represents a particular case of aggregation where density of suspension-feeders is maximized to achieve a greater commercial yield and economic benefit. Inhibition in feeding and declines in growth and survival rates have been observed in areas with high density of cultivated mussels (Fréchette & Despland 1999).

Galicia is one of the largest mussel farming producers in the world, where mussels are grown in culture ropes suspended from raft systems (Gosling 2003; Labarta 2004). The productivity is sustained by coastal upwelling and the circulation patterns in the Rías that together stimulate high primary production rates (Figueiras et al. 2002). Nevertheless, the detrimental effect of density on mussel growth is well known by mussel producers. Aside from a reduction in food availability, crowding also increases the risk of mussel dislodgement from the ropes and subsequent financial losses. In traditional mussel cultivation, mussel density on culture ropes is reduced in a process called “thinning-out”. The “thinning-out” is carried out after 4-7 months when mussels reached shell lengths of 40-50 mm and growth slows down. This process consists of detaching the individuals from the ropes and replacing them in order to reduce the density and homogenize the size distributions (Pérez-Camacho et al. 1991). Mussel farmers can thus control mussel density on the ropes in order to optimize growth and minimize cultivation time and product losses. Although this method requires considerable labor and financial investment, it is commonly employed in the Galician Rías, thereby demonstrating the importance of mussel density on growth and commercial yield.

Studies on the effect of stocking density on mussel growth in suspended culture are scarce (Lauzon-Guay et al. 2005a; Lauzon-Guay et al. 2006; Pérez-Camacho & Labarta 2004) despite the obvious importance to the mussel industry. A better understanding of the effect of stocking density on mussel growth will enable more efficient management at rope, raft and, ultimately, ecosystem scale, allowing the implementation of carrying

capacity models (Rosland et al. 2011). The aim of this study is to determine the effect of mussel density on growth in a suspended culture situation, using the commercial culture techniques commonly employed in the Galician Rías. For this purpose, during the second phase of cultivation (from thinning-out to harvest), different growth indicators (shell length and weight growth rates, growth curves and size frequency distributions) were analyzed.

2.2. Materials and methods

2.2.1. Experimental design

Experimental suspended culture of *Mytilus galloprovincialis* was performed on a raft located at a commercial aquaculture polygon (Lorbé) in the Ría de Ares-Betanzos (NW Iberian Peninsula) (Fig. 1). Different growth indicators of mussels were measured on suspended culture ropes along a cultivation density gradient (220, 370, 500, 570, 700, 800 and 1150 individuals per meter of rope; ind/m). Experimental culture lasted six months, covering the second phase of commercial mussel culture in Galicia, from thinning-out to harvest (April to October 2008). The experimental culture was carried out following commercial protocols and handling techniques usually employed for mussel culture in Galician Rías.

In April, a total of 24 ropes for each experimental density were randomly distributed over a commercial raft. Mussels employed in the experimental culture were obtained from adjacent long-lines and presented a homogeneous size distribution. Initial shell length (mean ± SD) of mussels was 48.78 ± 1.27 mm, total dry weight was 2.52 ± 0.18 g., and tissue and shell dry weight were 0.41 ± 0.03 and 2.11 ± 0.15 g., respectively. No significant differences in initial length or dry weight values were observed between density treatments (ANOVA; $p > 0.05$).

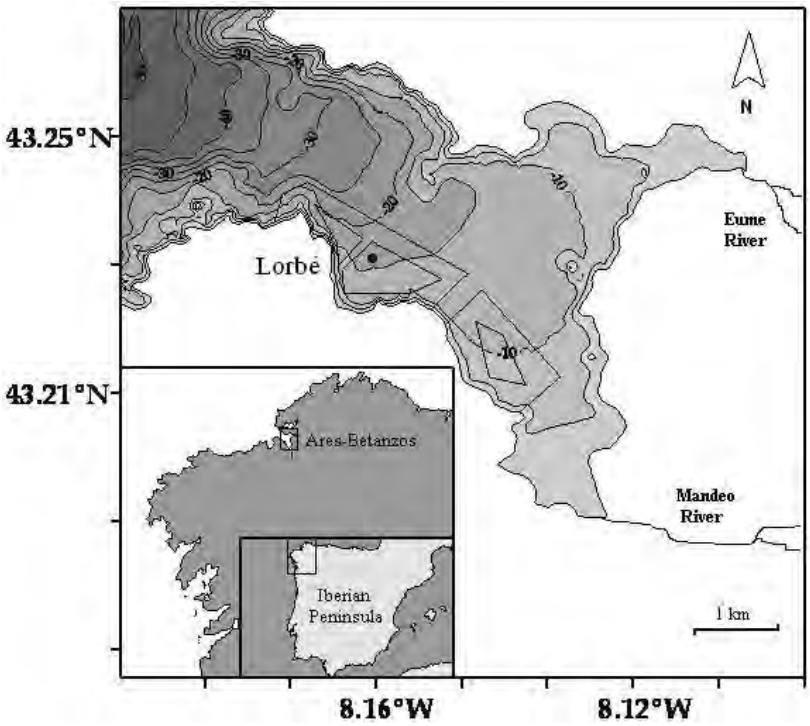

Fig. 1. Map of the Ría de Ares-Betanzos showing the topography of this inlet (contour lines -m-) and highlighting the commercial mussel culture areas (polygons) and the sampling station (●) of the present study. Modified from Álvarez-Salgado et al. (2011).

2.2.2. Mussel sampling

Four ropes per density treatment were sampled monthly, between 1 and 6m depth, during the experimental period (May to October). At each rope, a sample of known surface was scraped free of mussels. From each sample, the maximum length of the antero-posterior axis of a minimum of 250 individuals was measured for the calculation of the mean shell length ($\overline{L}$; mm). Length data were classified into 5 mm length classes in order to analyze the size frequency distribution of each sample. Subsamples of 15-20 mussels per rope, covering a range of 10 mm around the mean length ($\overline{L}$) were employed for total, tissue and shell dry weight (TDW, DWt and DWs) calculation. First, the adductor muscle was cut and the individuals were placed on their ventral edge on filter paper to remove internal water. After dissecting the tissue from the shell, both were dried at 110ºC until constant weight was obtained, then soft tissue and shell were weighed separately to obtain DWt and DWs. The total dry weight was calculated as the sum of tissue and shell dry weights.

2.2.3. Environmental conditions

At each sampling, measurements of temperature (T, ºC), salinity (S), pH and oxygen saturation (O_2, %) were made using a YSI 556MPS multiprobe system at 1 and 6 m depth. Water samples were collected at each sampling time to calculate the concentration of chlorophyll-a (Chl-a; μgl^{-1}) and suspended particulate matter (mgl^{-1}) including the organic and inorganic fraction.

Total particulate matter (TPM) and the organic (POM) and inorganic (PIM) fractions were determined gravimetrically. Three replicates of 1l seawater per sampling date were filtered on pre-combusted (450ºC for 4h) and pre-weighed 25 mm Whatman GF/C filters. Salts were removed by rinsing with isotonic ammonium formate (0.5 M). Filters were dried at 110ºC for 24h and weighed to determine the TPM concentration. The filters were then ashed at 450ºC for 4h to determine the inorganic fraction. The organic fraction was calculated by difference between the total and the inorganic fraction. The determination of chlorophyll-a concentration was performed by spectrophotometry following the method of Jeffrey and Humphrey (1975). Three replicates of 1l seawater per sampling date were filtered on 25 mm Whatman GF/C filters. The filters were frozen at -20ºC to facilitate cellular rupture and improve chlorophyll extraction. The extraction was carried out for 12h using 5ml of 90% acetone (SCOR-UNESCO, 1966). Thereafter, the solution was centrifuged at 4500 rpm at 10ºC for 10 min to separate the chlorophyll extract from the filter remains. The concentration was quantified using the equation developed by Jeffrey and Humphrey (1975): Chl-a = (11.85 (E_{664}-E_{750})-1.54 (E_{647}-E_{750})-0.08 (E_{630}-E_{750}) v)/V, where Chl-a is the chlorophyll-a concentration (μgl^{-1}), E_{750}, E_{664}, E_{647} and E_{630} are the absorbances at 750, 664, 647 and 630 nm respectively, v is the volume of acetone used in the extraction (ml) and V is volume of filtered seawater (ml).

2.2.4. Data analysis

For each density treatment and sampling date, weight values corresponding to the mean shell length were estimated by linear regression of log-transformed allometric relationship shell length (L) vs. total, tissue and shell dry weight (TDW, DWt and DWs).

Two-way factorial analyses of variance (Zar 1999) were used to test the effect of density treatment and sampling time on the mean shell length and weight values (L, TDW, DWt and DWs). Under normality (Shapiro-wilk test, p-value>0.05) and

homogeneity of variance (Levene test, p-value>0.05) conditions, parametric ANOVA followed by a Tukey-HSD (Honest Significant Difference) test were performed. Otherwise, the Kruskal-Wallis nonparametric test two-way ANOVA on ranked data was applied followed by the Wilcoxon test for pair-wise comparison between groups.

Shell length growth curves were fitted to a Gompertz (G) model: $L_t=L_\infty(e^{-e(-k(t-t'))})$, where L_t is shell length (mm) at time t (days), L_∞ is the maximum size, k is the growth parameter indicator of the speed at which maximum size is attained ($days^{-1}$) and t´ is the inflexion point of the curve, where growth is no longer linear (Ratkoskwy 1990). Similarly, the growth curves of total, tissue and shell dry weight were fitted to a Gompertz model: $DW_t=DW_\infty(e^{-e(-k(t-t'))})$, whose parameters are analogous to those for shell length growth curves. The Gompertz model parameters were estimated by non-linear regression, using the Levenberg-Marquardt algorithm and least squares as loss function. Comparisons between the estimated Gompertz model parameters for each density treatment were made using an extra sum of squares (Chen et al. 1992). This technique (Motulsky & Christopoulos 2004) facilitates comparing growth curves from estimated parameters directly between density treatments using a set of pairwise contrasts, by an F statistical test: $F = ((RSS_s)-(RSS_i)/(df_s - df_i))/(RSS_i/df_i)$, where RSS_s and RSS_i are the residual sum of squares of the curves fitted with and without a parameter shared, respectively, and df_s and df_i are their corresponding degrees of freedom.

Length and weight (total, tissue and shell) growth rates were calculated for the entire experimental period (May to October 2008) and the Spring-Summer (May-August) and Summer-Autumn (August-October) periods. Growth rates were calculated in mm day^{-1} and g day^{-1}, respectively, as the difference between length and weight values at the beginning and the end of each period. One-way analysis was used to determine the effect of density treatment on the growth rates of these periods. A Tukey test was performed as post hoc test.

The effect of density on the size frequency distribution of mussels was tested at the beginning (May) and at the end (October) of the experimental period. As normality and homogeneity assumptions were not met, a one-way non-parametric nested ANOVA with the random factor rope nested to density was applied. However, as differences

between ropes within each density were not found (p-value > 0.05), the nested effect was removed and a Kruskal-Wallis test, followed by a Wilcoxon post-hoc test were performed.

All data analyses were performed using the statistical software STATISTICA 6.0.

2.3. Results

2.3.1. Environmental conditions

Mean ± SD and ranges of the environmental variables registered at 1 and 6m depth during the experimental culture are presented in Table 1. The environmental parameters shown in this study presented seasonal patterns typical of temperate latitudes. Temperature values had been kept within a narrow range throughout winter months and until the end of April, when temperature showed a rapid increase which continued to rise until the end of summer. Since then temperatures decreased gradually. Salinity showed a seasonal pattern with lowest values during spring probably associated with the highest continental runoff. Chlorophyll-a concentration presented minimum values during winter and tended to increase during spring and summer periods, showing several peaks in spring, summer and autumn (Fig. 2A). The presence of a persistent phytoplankton bloom at the beginning of July corresponds to the highest peak in chl-a, TPM and POM (Fig. 2A-C). Oxygen saturation and pH are indicators of net ecosystem production and were correlated between them and with chl-a and POM concentration, presenting maximum values during summer (phytoplankton bloom associated to the upwelling season).

Table 1. Mean ± SD of the environmental parameters registered at 1 and 6 m depth during the experimental period (May to October 2008). Maximum and minimum values are specified in parentheses.

Depth	TPM (mg/l)	POM (mg/l)	PIM (mg/l)	Chla-a (µg/l)	T (ºC)	Salinity	Oxygen (% sat)	pH
1m	1.54±2.28 (0.36-10.38)	1.28±2.19 (0.23-9.95)	0.26±0.20 (0.09-0.87)	2.34±3.19 (0.29-16.35)	17.19±1.60 (13.45-19.38)	35.01±0.68 (34.0-35.82)	109.94±17.11 (79.9-153.8)	8.26±0.12 (8.0-8.49)
6m	0.96±0.88 (0.27-3.92)	0.76±0.85 (0.18-3.73)	0.20±0.14 (0.07-0.49)	2.14±2.23 (0.30-11.14)	16.19±1.43 (13.45-19.00)	35.42±0.50 (34.3-35.92)	103.20±14.97 (68.7-125.3)	8.26±0.11 (7.99-8.4)

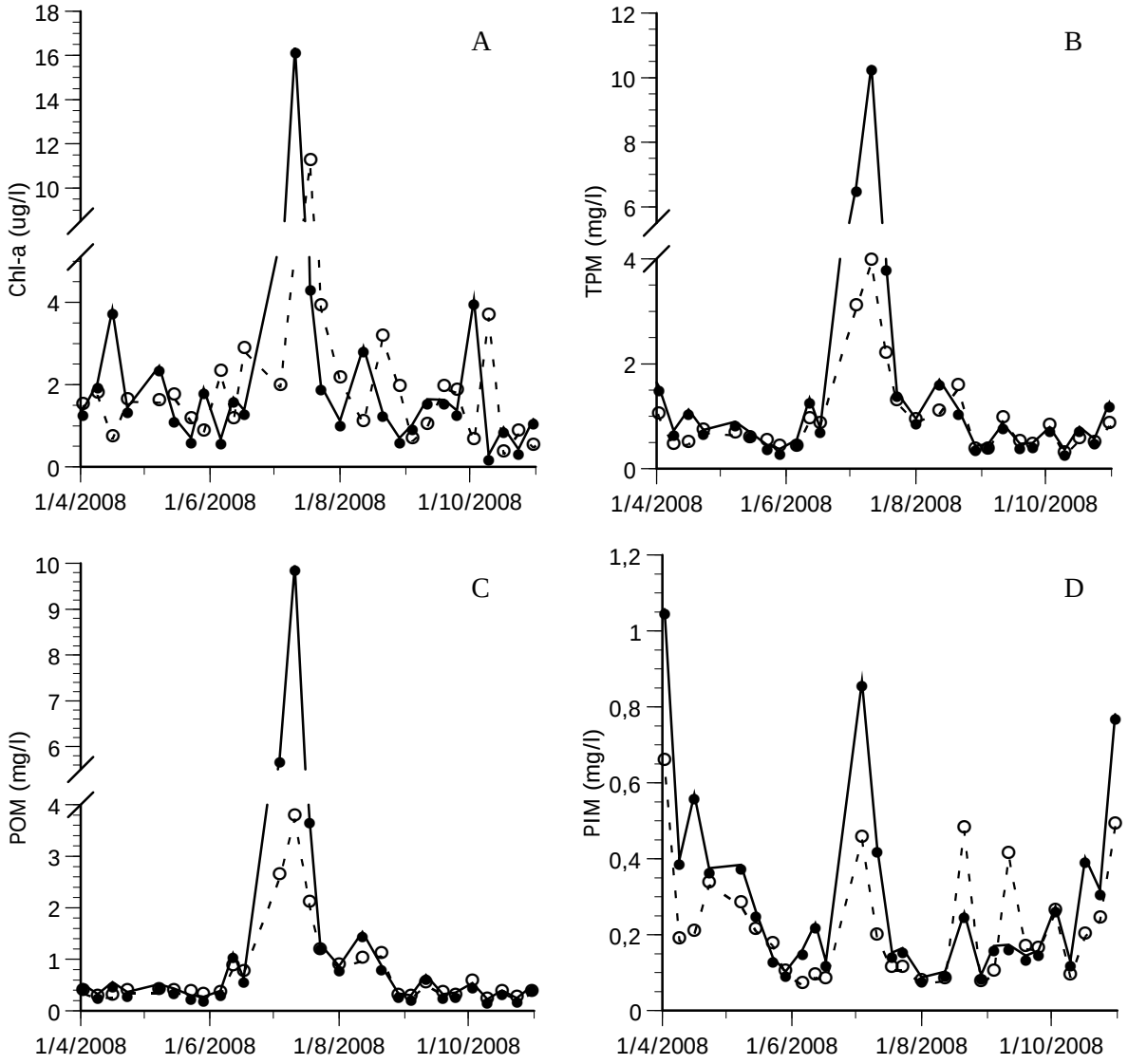

Fig. 2. Evolution of (A) chlorophyll a (Chl-a), (B) total particulate matter (TPM) and (C) particulate organic matter (POM) and (D) particulate inorganic matter (PIM), over the experimental period at 1 m (solid line) and 6 m (dashed line) depth.

2.3.2. Growth temporal evolution

The significant density×time interaction found for all the growth parameters evaluated (Table 2) revealed a different growth temporal evolution among density treatments (Fig. 3). There were no significant differences in any of the parameters studied (L, TDW, DWt and DWs) among density treatments during the first months of the experimental culture (May and June) ($p>0.05$; Fig. 3). However, in the following months an inverse relationship between size/weight mean values and density treatment was observed (Fig.

3), with the exception of August where the differences in growth indicators showed no relationship with density.

Tissue dry weight (DWt) increased significantly from May until August, then growth ceased in all the density treatments (Fig. 3). Significant increases in length (L), total dry weight (TDW) and shell dry weight (DWs) were observed from May to September for all treatments, except for the highest mussel density (1150 ind/m) where growth ceased in August (Fig. 3).

Table 2. Two-way ANOVA results testing the influence of density treatment and sampling time on the mean values of shell length (L; mm), total dry weight (TDW; g), tissue dry weight (DWt; g) and shell dry weight (DWs; g) of mussels grown in suspended culture.

Source of variation	d.f.	S.S.	M.S.	F	p-value
Talla					
Density	6	198	33	21.16	< 0.001***
Month	5	8792	1758.5	1126.42	< 0.001***
Density:Month	30	187	6.20	4.00	< 0.001***
Residuals	126	197	1.60		
TDW					
Density	6	40.30	6.72	20.07	< 0.001***
Month	5	1276.4	255.29	762.88	< 0.001***
Density:Month	30	26	0.87	2.59	< 0.001***
Residuals	126	42.20	0.33		
DWt					
Density	6	13131	2189	5.30	< 0.001***
Month	5	307100	61420	148.69	< 0.001***
Density:Month	30	22356	745	1.80	0.0131**
Residuals	126	52046	413		
DWs					
Density	6	24.90	4.16	25.41	< 0.001***
Month	5	792.5	158.51	968.95	< 0.001***
Density:Month	30	14	0.47	2.86	< 0.001***
Residuals	126	20.60	0.16		

(*) p<0.1; (**) p<0.05; (***) p<0.001

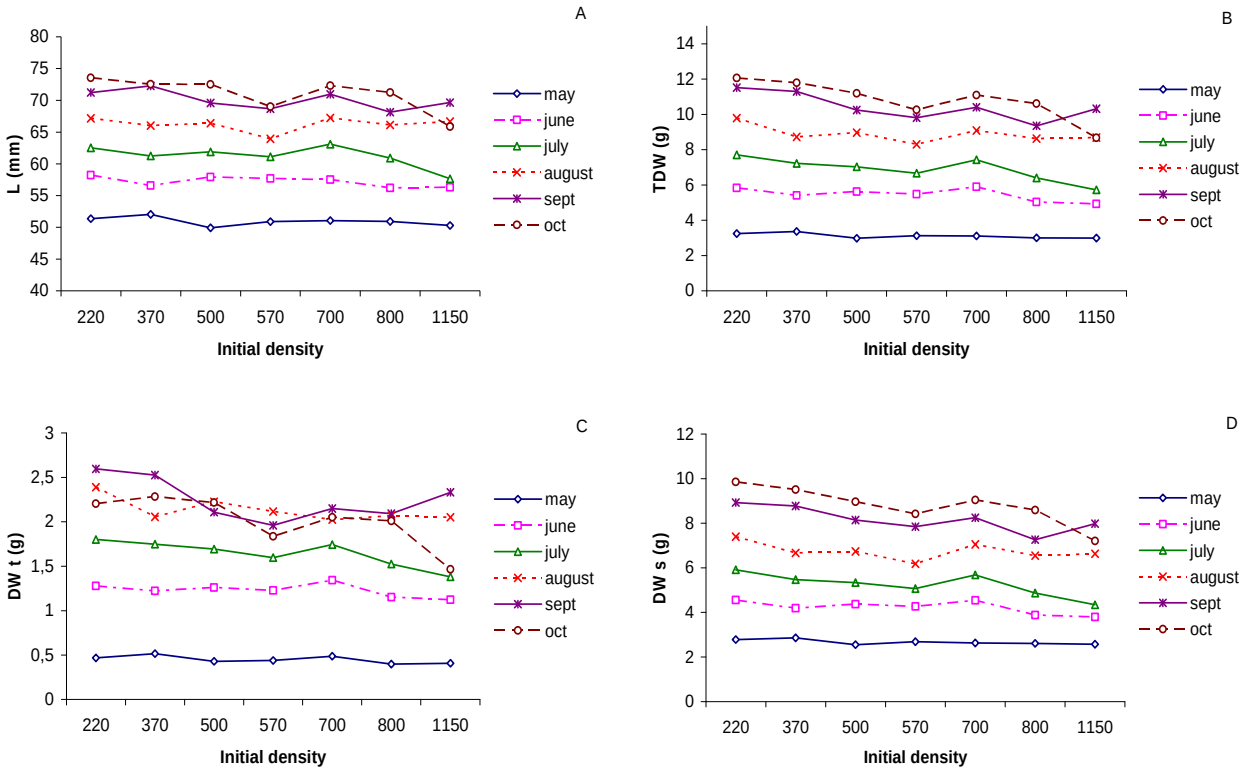

Fig. 3. Evolution of mean (A) length (L; mm), (B) total dry weight (TDW; g), (C) dry tissue weight (DWt; g) and (D) shell weight (DWs; g) values for each density treatment throughout the experimental period.

2.3.3. Size frequency distribution

Throughout the experimental period the size frequency distributions of all densities fitted a unimodal curve. No differences were observed in the size frequency distributions among experimental densities in the first culture month (May; Kruskal-Wallis test; p-value > 0.05). At harvest (October), size distribution showed a leftward displacement as density increased (Fig. 4 and Table 3), where the 220 ind/m density treatment presented the greatest mean shell length and the 1150 ind/m the lowest (Table 3).

Table 3. Mean differences between the size frequency distributions (L_{column}-L_{row}) of the different density treatments, at the end of the experimental period (October). Asterisks indicate p-values for the respective unilateral pair-wise Wilcoxon test.

	220	**370**	**500**	**570**	**700**	**800**
370	2.31 **					
500	2.81**	0.25				
570	11.87***	8.59***	9.19***			
700	2.17*	-0.14	-0.40	-8.76***		
800	7.84***	4.89***	5.11***	-4.04***	5.06***	
1150	21.64***	17.48***	19.06***	9.73***	17.69***	13.79***

(*) p-value < 0.1, (**) p-value < 0.05, (***) p-value < 0.01

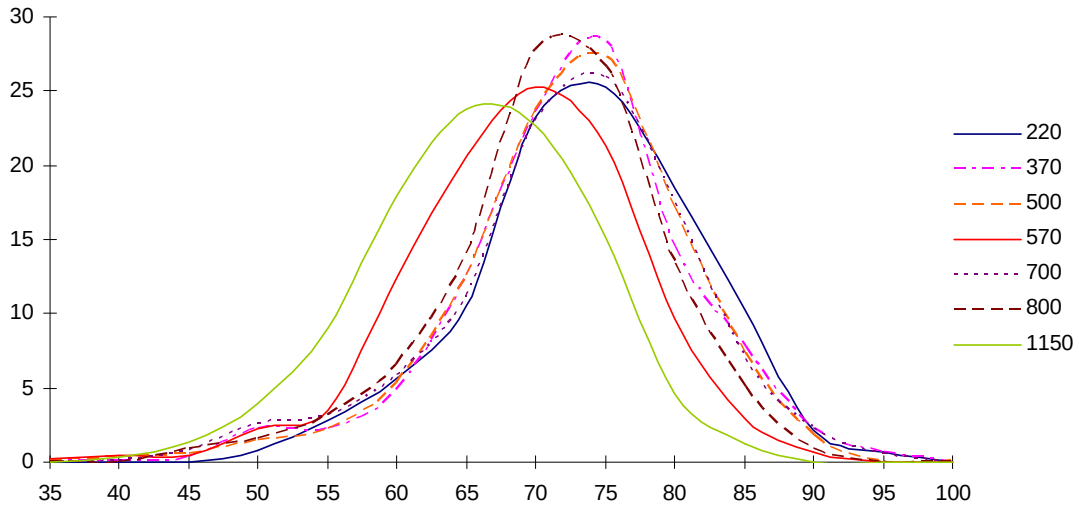

Fig. 4. Size frequency distributions for the seven density treatments at harvest (October).

2.3.4. Gompertz growth curves

A gradual decrease in mussel asymptotic size, total, tissue and shell weight as density increases was observed (Table 4). Asymptotic sizes (L_∞) were significantly different between extreme density treatments ($p<0.05$; Table 4). The lowest values were observed for the 1150 ind/m treatment (71.3 mm) and the highest in the 220 and 370 ind/m treatments (90.2 and 96.9 mm, respectively; Table 4 and Fig. 5A). Accordingly, in the lowest densities the maximum estimated length was 21 and 26.4% larger (for 220 and

370 ind/m, respectively) than the estimated for the highest density (1150 ind/m). Furthermore, we found significant differences in the growth factor (k) of shell length growth curves between the highest values observed for 370 ind/m mussels, and the lowest for 1150 ind/m ($p<0.05$; Table 4).

The individuals cultured at the highest density (1150 ind/m) also reached a significantly lower total weight than those for the other densities ($p<0.05$; Table 4 and Fig. 5B). Concurrently, the intermediate densities (570, 700 and 800 ind/m) reached lower total weights than those for 220 and 370 ind/m ($p<0.05$; Table 4). This implies differences up to 35.8% in the maximum total weight estimated between the extreme density treatments (1150 and 220-370 ind/m). In addition, significant differences related to density were observed at the inflexion point (t´) of TDW growth curves, showing an earlier change from linear to asymptotic growth in the higher density treatments (Table 4).

In concordance, individuals cultured at higher densities (between 570 and 1150 ind/m) reached significantly lower estimated tissue weights than those cultured at lower densities (220 and 370 ind/m) ($p<0.05$; Table 4 and Fig. 5C). Differences up to 22.5% in the estimated maximum tissue weight attainable by individuals were observed among extreme density treatments (1150 and 220-370 ind/m). Similarly, asymptotic shell weights (DWs_{∞}) were significantly different between the lowest values observed for the density of 1150 ind/m (8.9g) and the highest values for 220 and 370 ind/m mussels (15.4 and 17.0g, respectively; Table 4 and Fig. 5D). Therefore, in the lowest density treatments, individuals achieved a shell weight 41.9 and 47.4% higher, respectively, than those at the highest density.

Table 4 Estimated parameters and determination coefficients of the shell length (L, mm) and weight growth curves (TDW, DWt and DWs, g) fitted to a Gompertz model, for the different densities under study. All parameters are statistically significant ($p<0.001$). Significant differences between estimated parameters are shown with different letters ($p<0.05$).

Density	Asymptotic value	k	t´	R^2
Shell length				
220	90.2^{a}	-0.007^{ab}	66.4	0.98
370	96.9^{a}	-0.005^{a}	63.3	0.97
500	80.0^{ab}	-0.010^{ab}	70.6	0.98
570	77.7^{ab}	-0.009^{ab}	50.9	0.97
700	79.8^{ab}	-0.010^{ab}	70.1	0.97
800	82.2^{ab}	-0.008^{ab}	55.3	0.96
1150	71.3^{b}	-0.015^{b}	66.6	0.91
Total dry weight				
220	15.6^{a}	-0.013	181.6^{a}	0.98
370	16.2^{a}	-0.011	190.2^{a}	0.98
500	13.6^{ab}	-0.014	176.8^{ab}	0.97
570	12.2^{b}	-0.014	169.1^{ab}	0.98
700	12.4^{b}	-0.017	166.6^{bc}	0.97
800	12.1^{b}	-0.014	172.4^{ab}	0.96
1150	10.4^{c}	-0.018	163.9^{c}	0.91
Tissue dry weight				
220	2.50^{a}	-0.030	167.1	0.85
370	2.53^{a}	-0.024	168.0	0.90
500	2.27^{ab}	-0.031	164.7	0.86
570	2.05^{b}	-0.033	161.3	0.88
700	2.14^{b}	-0.033	159.4	0.92
800	2.08^{b}	-0.028	164.9	0.94
1150	1.96^{b}	-0.034	165.1	0.73
Shell dry weight				
220	15.4^{a}	-0.009	204.8	0.98
370	17.0^{a}	-0.008	226.0	0.98
500	12.2^{ab}	-0.011	188.4	0.97
570	12.9^{ab}	-0.009	198.5	0.98
700	11.2^{ab}	-0.012	176.0	0.97
800	11.9^{ab}	-0.010	192.6	0.97
1150	8.9^{b}	-0.016	173.1	0.90

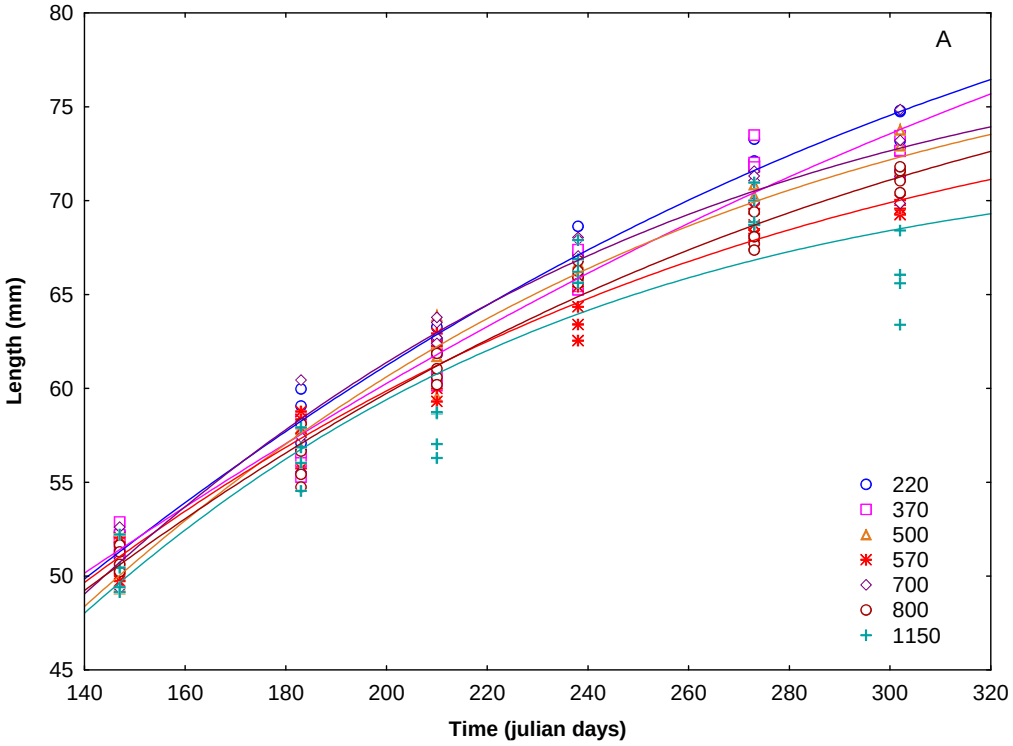
A
Length (mm)
Time (julian days)
220
370
500
570
700
800
1150

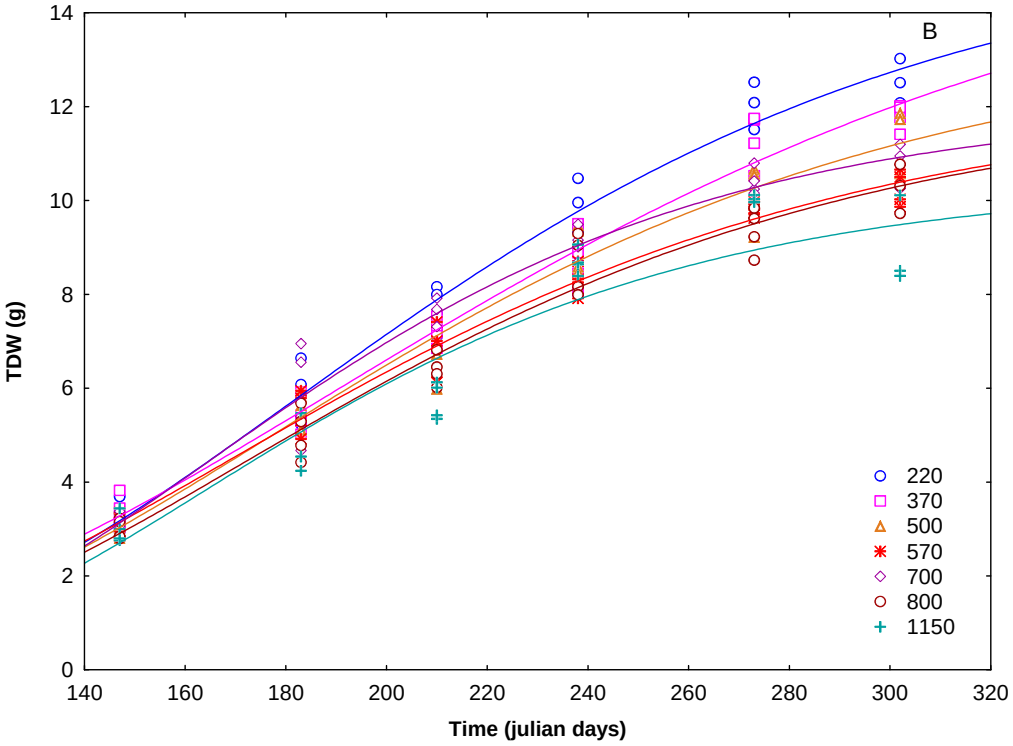
B
TDW (g)
Time (julian days)
220
370
500
570
700
800
1150

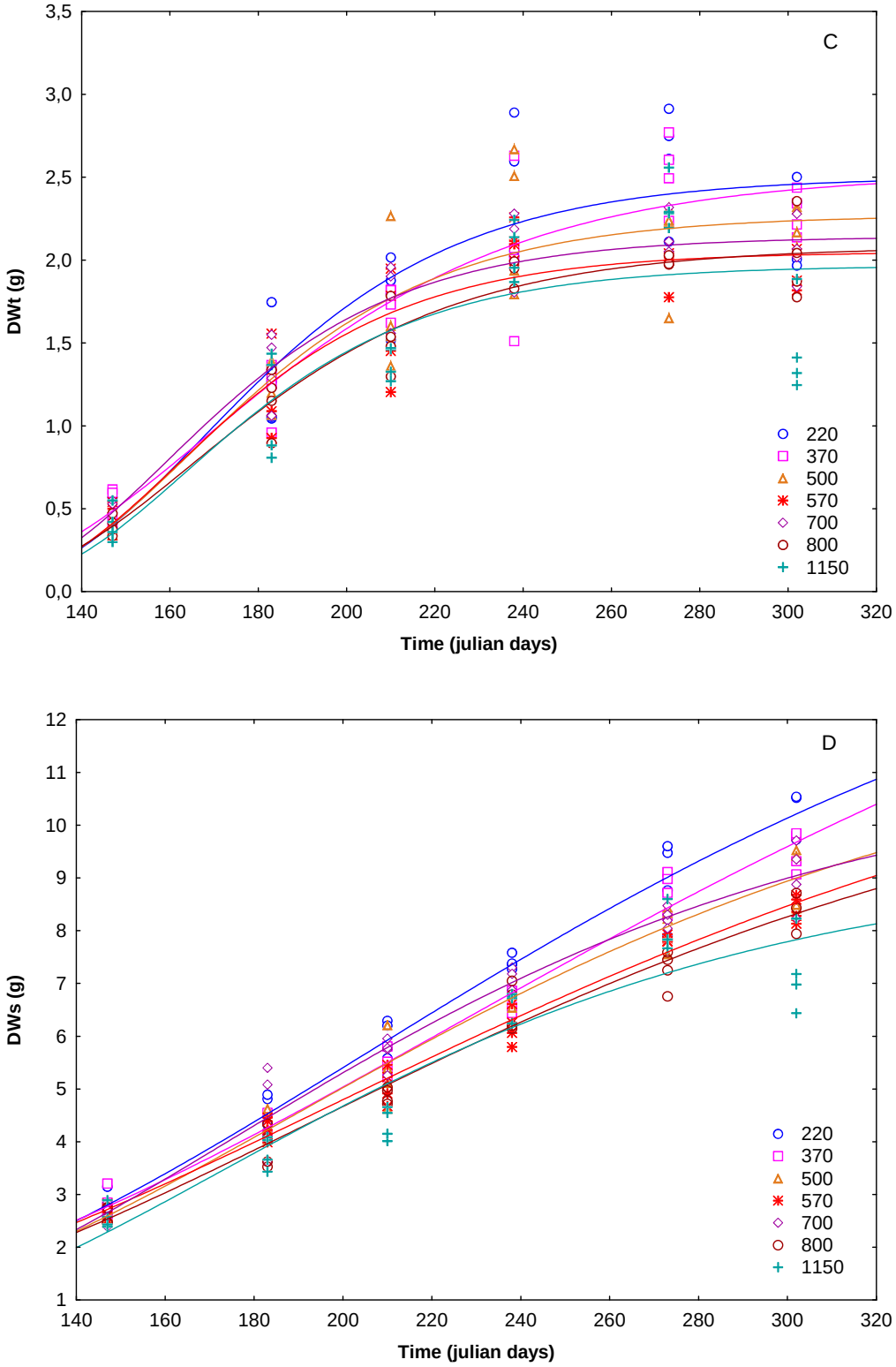

Fig. 5. Growth curves fitted to the Gompertz model for the seven density treatments over the experimental period (May to October 2008) in terms of (A) shell length, (B) total dry weight, (C) tissue dry weight and (D) shell dry weight. Growth curve parameters are shown in Table 4.

2.3.5. Growth rates

Growth rates of the entire experimental period (May-October) showed significant differences among density treatments for all the parameters studied ($p<0.05$; Table 5). During this period, a decrease of growth rates with increasing culture density was observed (Table 6). Accordingly to the post hoc test results, the highest density (1150 ind/m) showed significantly lower length growth rates than those for 220 and 500 ind/m (Table 6). A similar trend was observed for weight growth rates, whereby the density of 1150 ind/m presented lower TDW rates than the densities of 220, 370, 500 and 700 ind/m (Table 6). Similarly, the highest density treatment showed lower DWt growth rates than 220, 370, and 500 ind/m treatments and lower DWs growth rates than 220 and 370 ind/m (Table 6).

Table 5 One-way ANOVA results testing the influence of culture density on the shell length growth rate (mm day^{-1}) and dry weights growth rates, i.e. total, tissue and shell weight (TDW, DWt and DWs, respectively; g day^{-1}), for the entire culture period (May-October 2008) and for the May-August and August-October periods.

May-October	**d.f.**	**S.S.**	**M.S.**	**F**	**p-value**
Length	6	0.0034	0.0006	4.52	0.004**
TDW	6	0.0008	0.0001	5.21	0.002**
DWt	6	0.0001	0.0000	4.97	0.003**
DWs	6	0.0005	0.0001	4.30	0.006**
May-August					
Length	6	0.0050	0.0008	3.71	0.011**
TDW	6	0.0006	0.0001	2.72	0.041**
DWt	6	0.0001	0.00001	0.65	0.690
DWs	6	0.0004	0.0001	6.26	0.001***
August-October					
Length	6	0.0379	0.0063	9.89	<0.001***
TDW	6	0.0052	0.0009	3.72	0.011**
DWt	6	0.0004	0.0001	1.68	0.176
DWs	6	0.0030	0.0005	4.48	0.005**

(*) $p<0.1$; (**) $p<0.05$; (***) $p<0.001$

However, when the Spring-Summer and Summer-Autumn periods were analyzed separately (May-August and August-October, respectively) we observed that the differences in growth rates between density treatments were specifically located during

the second period (Fig. 6 and Table 6). Although significant differences were observed among some density treatments during May-August (Table 5), those differences did not show a pattern related with density gradient (Table 6 and Fig. 6). However, during August-October a decrease of growth rates with increasing density was observed (Table 6 and Fig. 6). Specifically, the highest density (1150 ind/m) showed significantly lower shell length growth rates than the other densities. Similarly, the 1150 ind/m density treatment presented lower TDW growth rates than density treatments between 220 and 500 ind/m and lower DWs growth rates than the densities between 220 and 570 ind/m. Furthermore, during this period, the 1150 ind/m density showed no growth in all observed parameters (Fig. 6). Differences in the tissue weight growth rates between densities were no longer observed when these two periods were analyzed separately (Table 6 and Fig. 6).

Table 6 Growth rates (mean ± SD) of the different culture densities in terms of shell length (mm day^{-1}), total, tissue and shell weight (TDW, DWt and DWs; g day^{-1}), for the periods May-October, May-August and August-October. Different letters indicate significant differences between groups ($p<0.05$).

		220	370	500	570	700	800	1150
May-October	Mean L	**0.143^{a}**	**0.135^{a,b}**	**0.146^{a}**	**0.117^{b}**	**0.137^{a,b}**	**0.131^{a,b}**	**0.115^{b}**
	SD	0.015	0.009	0.004	0.007	0.021	0.007	0.005
	Mean TDW	**0.057^{a}**	**0.054^{a}**	**0.053^{a}**	**0.046^{a,b}**	**0.052^{a}**	**0.049^{a,b}**	**0.039^{b}**
	SD	0.009	0.003	0.004	0.003	0.006	0.004	0.005
	Mean DWt	**0.011^{a}**	**0.011^{a}**	**0.012^{a}**	**0.009^{a,b}**	**0.010^{a,b}**	**0.010^{a,b}**	**0.007^{b}**
	SD	0.002	0.001	4.0e-04	0.002	0.001	0.001	0.002
	Mean DWs	**0.046^{a}**	**0.043^{a}**	**0.041^{a,b}**	**0.037^{a,b}**	**0.041^{a,b}**	**0.039^{a,b}**	**0.032^{b}**
	SD	0.007	0.003	0.003	0.002	0.005	0.003	0.004
May-August	Mean L	**0.173^{a,b}**	**0.154^{a,b}**	**0.181^{a}**	**0.143^{b}**	**0.178^{a}**	**0.167^{a,b}**	**0.180^{a}**
	SD	0.018	0.018	0.012	0.004	0.024	0.007	0.012
	Mean TDW	**0.072^{a}**	**0.059^{a,b}**	**0.066^{a,b}**	**0.057^{b}**	**0.066^{a,b}**	**0.062^{a,b}**	**0.063^{a,b}**
	SD	0.004	0.010	0.007	0.002	0.005	0.008	0.003
	Mean DWt	**0.021**	**0.017**	**0.020**	**0.018**	**0.017**	**0.018**	**0.018**
	SD	0.004	0.006	0.005	0.002	0.003	0.003	0.001
	Mean DWs	**0.051^{a}**	**0.042^{b,c}**	**0.046^{a,b,c}**	**0.038^{c}**	**0.049^{a,b}**	**0.043^{a,b,c}**	**0.045^{a,b,c}**
	SD	0.003	0.004	0.002	0.002	0.002	0.005	0.004
August-October	Mean L	**0.100^{a}**	**0.102^{a}**	**0.096^{a}**	**0.079^{a}**	**0.079^{a}**	**0.079^{a}**	**-0.012^{b}**
	SD	0.024	0.015	0.015	0.017	0.031	0.018	0,043
	Mean TDW	**0.036^{a}**	**0.048^{a}**	**0.035^{a}**	**0.031^{a,b}**	**0.031^{a,b}**	**0.031^{a,b}**	**-3.0e-04^{b}**
	SD	0.021	0.011	0.012	0.008	0.010	0.020	0.018
	Mean DWt	**-0.003**	**0.004**	**-1.4e-04**	**-0.004**	**4.1e-04**	**-0.001**	**-0.009**
	SD	0.008	0.008	0.006	0.002	0.002	0.007	0.007
	Mean DWs	**0.038^{a}**	**0.044^{a}**	**0.035^{a}**	**0.035^{a}**	**0.031^{a,b}**	**0.032^{a,b}**	**0.009^{b}**
	SD	0.015	0.006	0.009	0.006	0.010	0.013	0.012

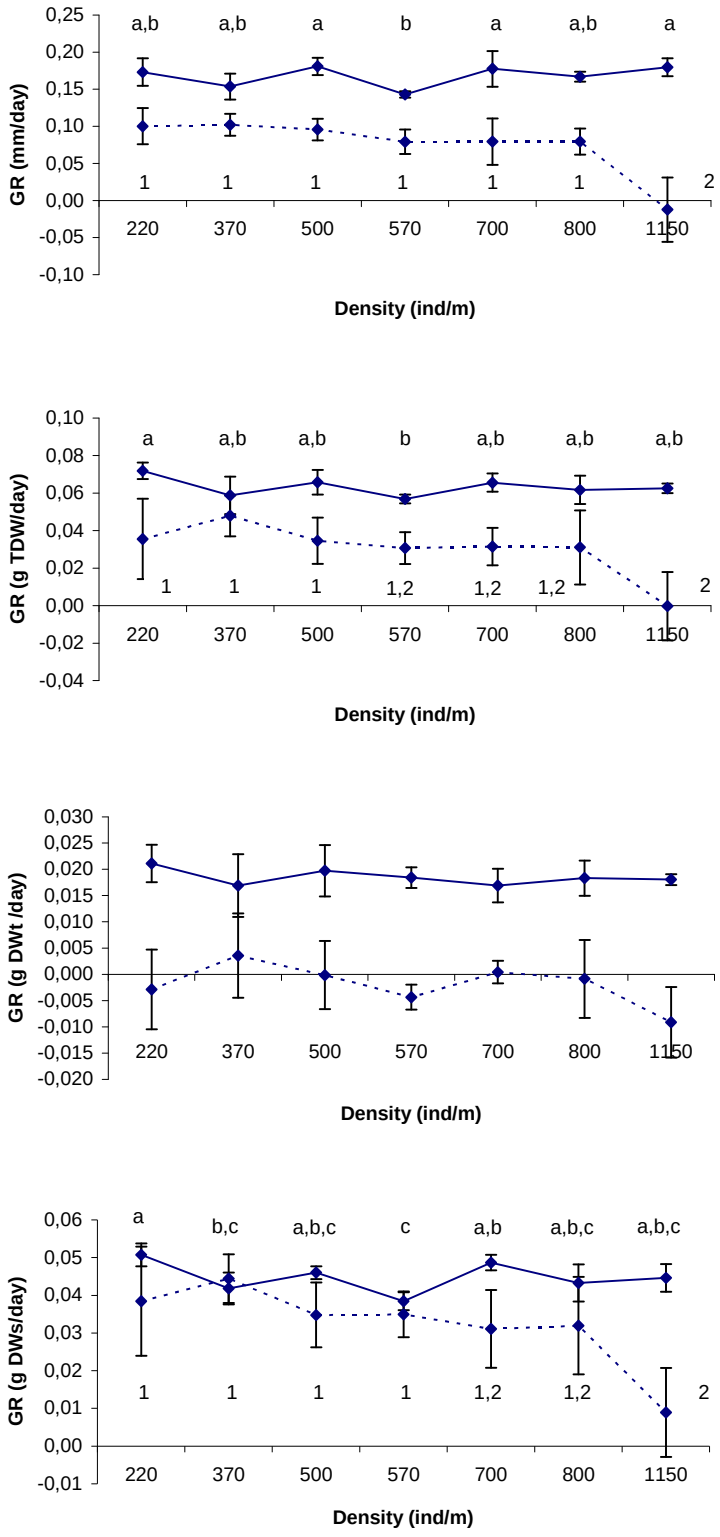

Fig. 6. Growth rates (mean ± SD) of the different culture densities in terms of shell length (mm day^{-1}) and weights, i.e. total, tissue and shell weight (TDW, DWt and DWs; g day^{-1}), for the periods May-August (solid line) and August-October (dotted line). Different letters and numbers indicate significant differences between groups ($p<0.05$) for the periods May-August and August-October, respectively.

2.4. Discussion

The present study showed the negative effect of high population density on mussel growth in suspended culture. Significant differences in the asymptotic values of the growth curves were observed among the different cultivation densities in all the growth parameters studied. Individuals cultured at lower density reached significantly higher maximum length and weight values than those at higher densities. This suggested that lower growth is a result of stronger intraspecific competition at high density populations.

Our results agree with those of Xavier et al. (2007) who observed that the mean size of *M. galloprovincialis* in "mussel beds" was larger in sites with lower densities. Widman & Rhodes (1991) and Côté et al. (1993) also found a greater growth in shell and tissue weight at low densities for pectinids in suspended culture. These authors have suggested that this could be due to the individuals acquiring a greater proportion of limiting resources (food/space). This would stimulate growth and enhance survivorship, either directly, through a reduction of competitive pressure (Griffiths & Hockey 1987) or indirectly, through an increase of growth rate to a larger size (Xavier et al. 2007), reducing the risk of predation (Branch & Steffani 2004; Griffiths & Hockey 1987; Paine 1974).

Significant differences between extreme densities were also observed in the growth factor (k) of the shell length growth curves, with highest values at lowest densities. Therefore, the individuals at lower densities, aside from reaching larger sizes, grow faster. Significant differences in the inflexion point (t´) among densities were only observed in the total dry weight (TDW) growth curves, where individuals cultured at higher densities reached the inflexion point faster than those cultured at lower densities, that is, growth was linear for less time and asymptotic growth was reached sooner. These support ANOVA results on the mean individual L, TDW and DWs, where growth in size and weight ceased earlier in the highest densities than at the lowest (August c.f. September). This was also reflected in the leftward displacement of the size frequency distribution with increasing culture density, with the highest densities showing a slower growth and thus a greater proportion of small individuals and less of larger ones, and vice versa.

Over the entire experimental period (May-October) there was a negative effect of density on the growth rates in size and weight of individuals. This is in agreement with previous studies on *Mytilus* spp. (Alunno-Bruscia et al. 2000; Gascoigne et al. 2005; Parsons & Dadswell 1992; Scarrat 2000). However, when growth rates were analyzed in two different periods (Spring-Summer and Summer-Autumn), we observed that the differences associated to density treatment were concentrated in the second culture period. During the first period (May-August) there was no influence of density on growth. However, from August, when the individuals had reached a considerable size (66.2 ± 1.3 mm), a reduction in growth rates at higher density populations was observed. This may indicate that as individuals grow their requirements for limiting resources increase and intraspecific competition becomes more pronounced. Furthermore, ageing decreases the absorption efficiency and slows growth (Pérez-Camacho et al. 2000) due to the achievement of the stationary phase of growth. These effects would be intensified by the decrease in food availability during these months (August-October; Fig 2). In summary, we can conclude that individual growth seems to intensify intraspecific competition, which in turn establishes the limits on mussel coverage and biomass reached by the population.

Our results pointed out the influence of density on mussel growth in suspended cultivation which seems to be related to competition for limiting resources (space/food). The effect of stocking density on the growth rate of bivalves has been well-documented in several species under different culture and environmental conditions. In most of these studies, a negative relationship between growth rate and density has been established (Alunno-Bruscia et al. 2000; Boromthanarat & Deslou-Paoli 1988; Cigarría & Fernández 1998; Cotê et al. 1993; Gascoigne et al. 2005; Kautsky 1982; Newell 1990; Peterson 1989; Román et al. 1999; Scarrat 2000; Taylor et al. 1997; Waite et al. 2005). Nevertheless, other studies have found limited evidence for such a negative effect on mussel growth (Fuentes et al. 2000; Lauzon-Guay et al. 2005a,b; Mallet & Carver 1991; Sénéchal et al. 2008). The lack of a negative effect of density on growth has been explained by the use of insufficient crowded populations (Lauzon-Guay et al. 2005a,b; Sénechal et al. 2008) or the greater influence of macroenvironmental factors in determining mussel growth, such as food availability or current speed (Fuentes et al. 2000; Gascoigne et al. 2005; Mueller 1996; Sénéchal et al. 2008). It has also been speculated that density-dependent reduction in the number of mussels (i.e.

dislodgements and mortality), would alleviate competitive pressures and could mask the effect of density on mussel growth (Alunno-Bruscia et al. 2000; Boromtharanat & Deslous-Paoli 1988; Fréchétte et al. 1992; Fuentes et al. 2000; Lauzon-Guay et al. 2005a,b; Maximovich et al. 1996), while laboratory experiments where densities were maintained constant, detected a negative effect of density on growth and condition index (Alunno-Bruscia et al. 2000). In the present study we have recorded a negative effect of density on growth even when experimental densities were not kept constant throughout the experimental period. Decreases in density were also positively related to density treatment and resulted in a greater mortality at elevated densities (Cubillo et al. In preparation). This has also been observed in other studies in suspended culture (Fuentes et al. 1998; Fuentes et al. 2000; Lauzon-Guay et al. 2005a), and leads to the convergence of the densities with time that seems to mitigate the effect of density on individual growth.

In summary, the results from the present work have established for the first time the effect of stocking density on mussel growth in suspended culture applying the cultivation techniques used by mussel producers, during the period from thinning-out to harvest. Our study suggests that density influences the maximum size and weight attainable by individuals, as well as their growth rate. Although seasonal changes in food availability can modulate the effect of density on growth, lowering densities could reduce its detrimental effect along the culture. This is in concordance with previous results obtained using traditional cultivation techniques (thinning-out) in Ría de Ares-Betanzos, which suggested that adjusting mussel density to the characteristics of the cultivation area could yield an increase of 10-15% in biomass production and at least 20% in economic benefits (Labarta & Pérez-Camacho 2004). In addition, our results showed an increased effect of intraspecific competition with mussel size. This fact should be considered in aquaculture management, since higher densities could be supported without effects on growth performance if the final culture product is limited to a lower size.

El contenido de este capítulo se corresponde con el artículo:

Alhambra M. Cubillo, Laura G. Peteiro, María José Fernández-Reiriz, Uxío Labarta (2012) Density-dependent effects on morphological plasticity of *Mytilus galloprovincialis* in suspended culture. Aquaculture (2012), doi: 10.1016/j.aquaculture.2012.01.028.

Capítulo 3. Density-dependent effects on morphological plasticity of *Mytilus galloprovincialis* in suspended culture

Evolución temporal y efecto de la densidad sobre la morfología y distribución energética del mejillón *Mytilus galloprovincialis* en cultivo suspendido

Summary

Bivalve molluscs are characterized by high morphological plasticity in response to variations in local environmental conditions. In the present study, we evaluate this capacity in the mussel *Mytilus galloprovincialis* with regard to intra-specific competition caused by cultivation density. Suspended cultivation ropes at different initial densities (220, 370, 500, 570, 800 and 1150 individuals per meter of rope) were placed on a raft in the Ría Ares-Betanzos, following standard cultivation techniques. From May to October, covering the period from thinning out to harvest, various morphological indicators (length/width, length/height and height/width ratios) and allometric relationships (Volume-Length and Projected area-Length) in addition to energy distribution (dry tissue weight/dry valve weight) were analyzed. Differences in morphological indicators due to cultivation density were observed while no influence on the energy distribution was detected. From the second cultivation month (June), a decrease was recorded in the length/height ratio of individuals due to cultivation density. Similarly, there was also a decrease in the length/width ratio, although this decrease only became statistically significant from September. In addition, the allometric relationships studied (Volume-Length and Projected area-Length) suggested asymmetric competition processes. Differences in volume or projected area between densities were only detected at the end of the experimental culture (October) and only in the smaller individuals. These morphological adaptations can be understood as a strategy to mitigate the effects of intra-specific competition, palliating the consequences of physical interference at high densities.

3.1. Introduction:

Marine invertebrates exhibit a wide range of morphological variations in the natural environment. In bivalves, such variations can be caused by ontogenetic processes (Dickie et al. 1984; Karayucel & Karayucel 2000; Stirling & Okumus 1994) or a plastic response to environmental conditions, such as wave exposure (Akester & Martel 2000; Funk & Reckendorfer 2008; Steffani & Branch 2003), exposure to predators (Caro & Castilla 2004; Leonard et al. 1999; Reimer & Tedengren 1996) and population density (Alunno-Bruscia et al. 2001; Bertness & Grosholz 1985; Briones & Guiñez 2005; Brown et al. 1976; Richardson & Seed 1990; Seed 1968).

Cultivation density appears to be a particularly important environmental factor on the shell shape of the genus *Mytilus* (Brown et al. 1976; Seed 1968, 1973). Similar effects have also been observed in other species of molluscs, such as oysters (Chinzei et al. 1982; Tanita & Kikuchi 1957) and clams (Cigarria & Fernández 1998; Ohba 1956). Alunno-Bruscia et al. (2001) noted that density influenced shell morphology and the condition index of *Mytilus edulis* cultivated in laboratory growth chambers. High densities lead to more elongated and less triangular shells with a lower height/length ratio (Briones & Guiñez 2005; Brown et al. 1976; Coe 1946; Lent 1967; Richardson and Seed 1990) and a lower width/length ratio (Alunno-Bruscia et al. 2001; Lauzon-Guay et al. 2005[a]). Bertness & Grosholz (1985) observed extreme distortions of more than 30º in the angle of the shells in *Geukensia demissa* at extremely high densities.

The previously cited studies suggest that morphological plasticity is a strategy to mitigate the effects of intra-specific competition at the individual level. Generally, these effects have been attributed to limitations in the availability of food, available substrate or the interaction of both of these factors (Fréchette & Lefaivre 1990; Fréchette et al. 1992).

The negative effect of density on the growth of mussels has been widely studied (Alunno-Bruscia et al. 2000; Boromthanarat & Deslous-Paoli 1988; Filgueira et al. 2008; Fréchette & Bourget 1985a,b; Gascoigne et al. 2005; Grant 1999; Guiñez & Castilla 1999; Kautsky 1982; Newell 1990; Peterson & Beal 1989). However, there are few studies on the effect of density on bivalve shell morphology in the field (Bertness &

Grosholz 1985; Briones & Guiñez 2005; Lauzon-Guay et al. 2005a; Richardson & Seed 1990; Seed 1968). Of the aforementioned studies, only Lauzon-Guay et al. (2005a) focussed on the effect of density in a suspended culture system.

Mussels in suspended culture are exposed to different growing conditions than bottom or intertidal-cultivated mussels and wild or laboratory-grown mussels (due to differences in air exposure, wave action, temperature, food availability, currents, etc.). Therefore, the effect of crowding on morphological variations of individuals in suspended culture is not easy to predict from previous studies in different environments. Furthermore, the use of suspended culture systems allows the effect of crowding in the natural environment to be isolated, since it eliminates the interference of other variables, such as wave exposure, desiccation, etc.

Galicia is an important mussel producing region where most mussel farming occurs in suspended culture using rafts. In the traditional mussel culture as individuals increase their size, successive reductions in the density of mussels on the ropes are made. One of these reductions is called the “thinning out”. The "thinning out" process is carried out after 4-7 months, when the mussels have reached about 40-60 mm length and the weight of the ropes have increased significantly making mussel growth slower and heterogeneous. This process consists of detaching individuals from the ropes and re-attaching them in order to standardize the size and decrease the density on the ropes. The "thinning out" allows growers control of the density of mussels on the ropes in order to enhance their growth, while minimizing culture time and density-dependent losses (Pérez-Camacho & Labarta 2004). This method represents a considerable investment of working hours and labor costs, however, is a method commonly used in the Galician Rías. This highlights the importance of density on mussel growth and optimizing production in aquaculture.

The aim of this study is to analyze the effect of intra-specific competition on the morphological plasticity of *Mytilus galloprovincialis* (Lamarck 1819) in suspended culture by monitoring different morphological indexes in populations grown at different densities. For that purpose, we use commercial raft cultivation techniques that allow the manipulation of density in the natural field and facilitate the applicability of the results to the aquaculture industry.

3.2. Material and methods:

3.2.1. Experimental design

The study area was located in the raft polygon of Lorbé, in the Ría de Ares-Betanzos (NW of Spain), which is used intensively for the mussel *Mytilus galloprovincialis* cultivation (see Fig. 1 in Chapter 2). The study employs the same standard culture and handling techniques as those used by the local industry. Mussels (*Mytilus galloprovincialis*) were placed on culture ropes at seven density levels (220, 370, 500, 570, 750, 800 and 1150 individuals/m of rope). The ropes were suspended from a raft in April in order to study the period from thinning out to harvest (from May to October of 2008). Four ropes (replicates) were used by combination of 6 months and 7 density treatments (168 ropes), which were randomly distributed at the prow of the raft. Initial measures of shell length, weight and morphological characteristics are detailed in Table 1. Monthly samplings were performed until harvesting in October. Each month, a sample of known length of rope was taken from 4 ropes of each density treatment (28 ropes per sampling date) at an average depth of 2-4 m.

3.2.2. Sampling procedure

Individuals from each sample were counted to estimate density (individuals/m). The maximum length of the antero-posterior axis of a minimum of 200 individuals was measured for the calculation of the mean length ($\overline{L}$; mm). Sub-samples of 14 individuals per rope (56 mussels per density), covering a range of 30 mm around the average length, were used for morphometric measurements using callipers with a precision of 0.1mm. Length (L; mm) was calculated as the maximum distance of the antero-posterior axis. Height (H; mm) was considered as the maximum distance of the dorso-ventral axis and Width (W; mm) as the maximum lateral axis (Fig. 1). These measurements were used to calculate the morphological W/L, H/L and H/W ratios.

Table 1. Mean and standard deviation of mean length ($\overline{L}$; mm), dry tissue weight (DWt; g), total dry weight (TDW; g) and morphological ratios (H/L, W/L and H/W) of mussels at the beginning of the experimental culture.

$\overline{L}$	DWt	TDW	H/L	W/L	H/W
46.15±3.76	0.39±0.08	2.60±0.32	0.53±0.03	0.31±0.02	1.68±0.14

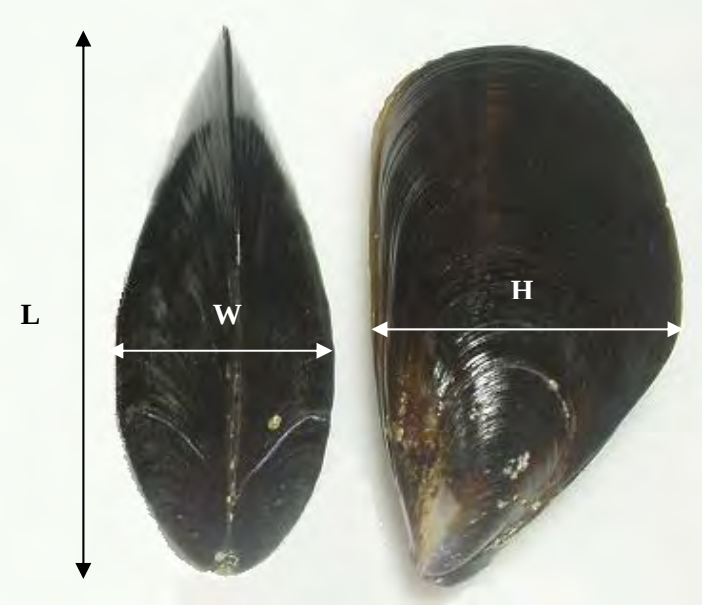

Fig. 1. Shell dimensions of *Mytilus galloprovincialis*: Length (L; mm), Height (H; mm) and Width (W; mm) used to calculate the morphological W/L, H/L and H/W ratios.

Sub-samples of 15-20 mussels, covering a range of 10 mm around the mean length, were gathered from each rope replicate (60 to 80 mussels per density level) to calculate the total dry weight (TDW; g), tissue dry weight (DWt; g) and shell weight (DWs; g). After cutting adductor muscles and allowing intrapallial water to drain, mussels were dissected and both shell valves and soft tissues were weighed after drying at 110ºC for 48 h. The total dry weight was calculated as the sum of the dry weights of tissue and shell. The condition index or meat yield was estimated as the ratio between the dry weight of soft tissues and the dry weight of the shell, according to the equation: CI = (DWt/ DWs).

Volume (V; ml) was calculated as the volume of water displaced after placing the mussel with the valves tightly shut in a vessel containing a known volume of seawater. To obtain the surface area occupied or projected area (S; cm^2) by the mussels in the rope, dorsal photographs of 28 to 56 individual mussels from each experimental density were taken perpendicular to the antero-posterior axis, using a Nikon Coolpix 4500. The size range of mussel used was at least 15 mm around the mean length. The projected area on the substrate was calculated using image analysis software (ImageJ 1.37v).

We assumed an allometric relationship between the volume, projected area and the shell length of mussels. These allometries were established for each density and sampling period using power equations of the form: $V = aL^b$ and $S = aL^b$, where a and b are the intercept and the allometric coefficient, respectively.

3.2.3. Statistical analysis

Analysis of covariance was applied to test the effect of initial density and sampling time on the intercepts and allometric coefficients for the log-transformed relationship Volume-Length and Projected area-Length (Snedecor & Cochran 1989). Post hoc Tukey tests (t-tests) were used for pair-wise comparisons.

Analysis of variance (factorial ANOVA) was used to determine the effect of the initial density, time (month) and their interaction on each morphological ratio (W/L, H/L, H/W) and condition index (DWt/DWs). The homocedasticity assumption was met (Levene test, p-value>0.05) for the three morphological variables. As ANOVA analysis is robust under slight deviations from the model hypothesis, the departure from normality found for some densities in each variable (Shapiro-Wilk test, p-value<0.01) should not affect the results. For the condition index (DWt/DWs), hetereogenity of variances (Levene test, p.value < 0.001) in addition to non-normality for some densities (Shapiro-Wilk test, p-value<0.01) were found, therefore a two way ANOVA on ranked data was applied. In cases where normality or homocedasticity assumptions were met, the Tukey HSD (Honest Significant Difference) test was used as a post-hoc, otherwise the Wilkoxon non-parametric test was performed.

Statistica 6.0 software was used for all analyses, considering a significance level of α=0.05.

3.3. Results

3.3.1. Width-length ratio

Density treatment and time showed a significant effect on the W/L ratio (Table 2). Nevertheless, the significant interaction between those variables revealed a variable effect of density over the study period. At the beginning of the study, the width/length ratio (W/L) was similar for all densities (ANOVA; p-value>0.05). From May to August a common tendency of an increase in this ratio was observed for all density treatments, without significant differences between densities (Fig. 2). After August, the W/L ratio

continued to increase linearly in mussels cultivated at lower densities (220, 370 and 500 ind/m) (Table 3 and Fig. 2). For higher densities (570, 700, 800 and 1150 ind/m), the increase ceased and this ratio was maintained nearly constant until October, implying that these relationships were better described as second order polynomial functions (Table 3 and Fig. 2). Therefore, the lower densities (220 and 370 ind/m) reached significantly higher W/L values than the highest ones (800 and 1150) at the end of the experimental culture (September and October).

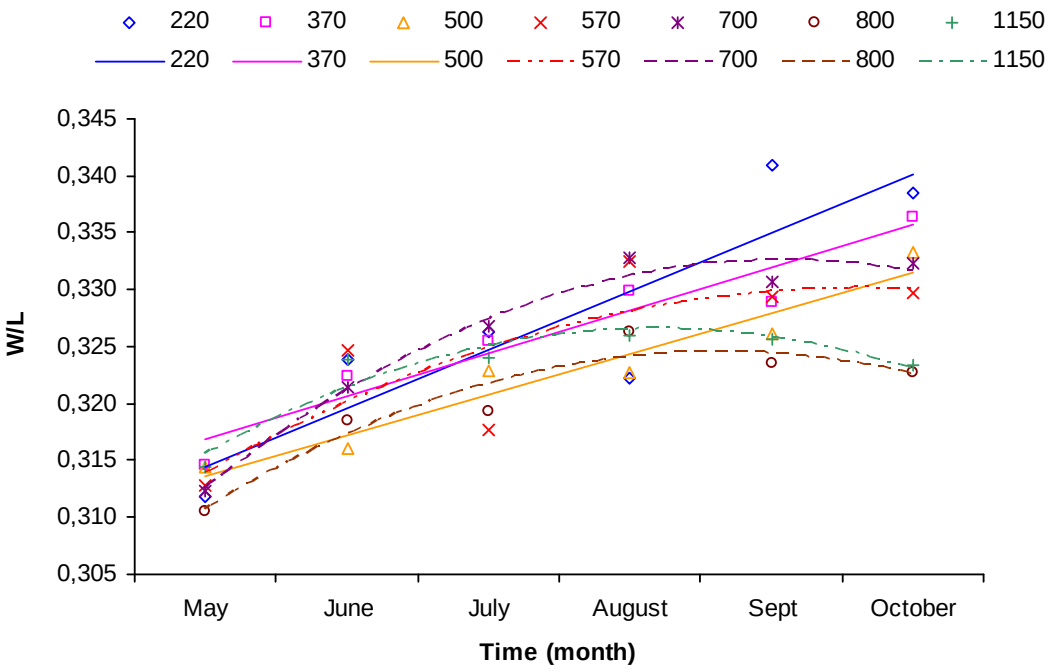

Fig. 2. Linear and polynomial fits to the average width-length (W/L) ratios of *M. galloprovincialis* throughout the experimental culture at different densities: 220, 370 and 500 (linear); 570, 700, 800 and 1150 ind/m (polynomial).

Table 2. Two way ANOVA results testing the effect of sampling time and density treatment on the different ratios analysed in the study (W/L, H/L, H/W and DWt/DWs).

Source of variation	df	S.S.	M.S.	F	p-value
W/L					
Time	5	0.074	0.015	37.72	<2e-16***
Density	6	0.014	0.002	5.96	3.4e-06***
Time:Density	30	0.026	8.7e-04	2.22	1.6e-04***
Residuals	2229	0.876	3.9e-04		
H/L					
Time	5	0.115	0.023	24.76	<2e-16***
Density	6	0.063	0.010	11.22	2.3e-12***
Time:Density	30	0.046	0.002	1.65	1.4e-02*
Residuals	2226	2.071	9.3e-04		
H/W					
Time	5	4.786	0.957	64.27	<2e-16***
Density	6	0.288	0.048	3.22	0.004**
Time:Density	30	0.683	0.023	1.53	0.034*
Residuals	2231	33.226	0.015		
IC					
Time	5	57628599	11525720	253.26	<2e-16***
Density	6	70412	70412	1.55	0.160
Time:Density	30	43723	43723	0.96	0.528
Residuals	1045	45510	45510		

(*) p<0.05; (**) p<0.01; (***) p<0.001

Table 3. Parameters of the linear ($W/L = a + bx$) and second-order polynomial regression ($W/L = a + bx – cx^2$) describing the changes in the mean W/L index as a function of time.

W/L	a	b	c	R^2 adjusted	F	p-value	N
220	0.309	0.005**		0.737	15.03	0.018*	6
370	0.313	0.004**		0.898	45.21	0.003**	6
500	0.310	0.004**		0.917	55.96	0.002**	6
570	0.306***	0.0085	-0.0008	0.683	6678.44	3.1e-06***	6
700	0.301***	0.0123**	-0.0012**	0.977	88894.48	6.4e-08***	6
800	0.302***	0.0097**	-0.0010*	0.911	45734.57	1.7e-07***	6
1150	0.308***	0.0091**	-0.0011**	0.900	68226.59	9.5e-08***	6

(*) p<0.05; (**) p<0.01; (***) p<0.001

3.3.2. Height-length ratio

The H/L ratio was influenced by density treatment and sampling time, but not independently since the density × time interaction was significant ($p<0.05$) (Table 2). At the start of the study (May), the height-length ratio presented similar values for all densities (ANOVA p-value>0.05). There was a tendency towards a decrease in the H/L ratio with time for all densities, which was most pronounced toward the end of the cultivation period (Fig. 3). However, post hoc analysis showed that this decrease was only significant for the densities lower than 1150 ind/m.

From the second month of cultivation (June), a negative effect of density on the H/L ratio was observed (Fig. 3). This tendency was maintained until the end, leading to more elongated shells in mussels cultivated at greater densities.

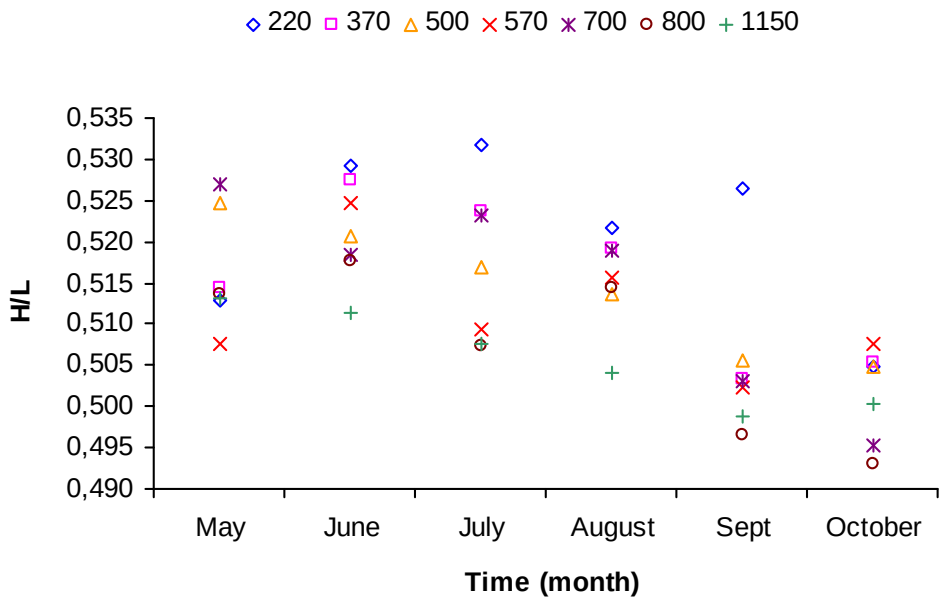

Fig. 3. Average height-length (H/L) ratios of the different density treatments tested (N= 220, 370, 500, 570, 700, 800 and 1150 ind/m) along the experimental culture.

3.3.3. Height-width ratio

Density treatment and time showed a significant effect on the H/W ratio (ANOVA; $p<0.05$; Table 2). The mussels always grew more in height than width (H/W>1), but at decreasing rates, since the H/W decreased significantly with time (Fig. 4 and Table 4). Nevertheless, the significant interaction between density and time (ANOVA; $p<0.05$; Table 2) revealed a variable effect of density over the study period. Accordingly, no

significant effect of the initial density on the H/W ratio was detected, with the exception of August where a decrease of this ratio with increasing density was observed.

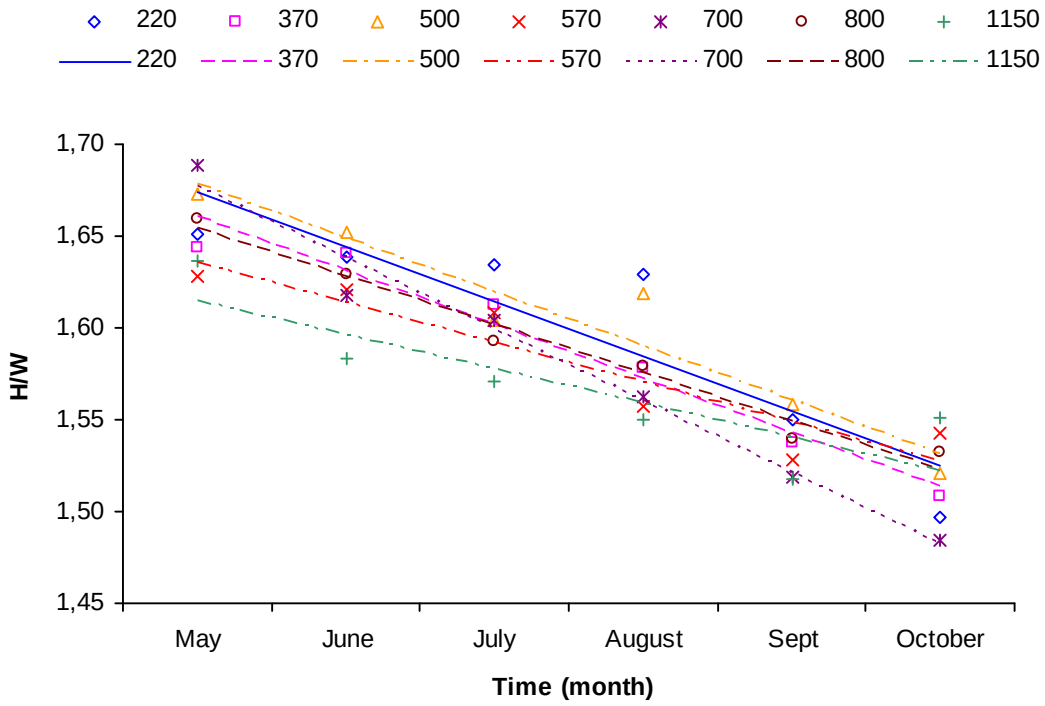

Fig. 4. Linear fits of the mean height-width (H/W) ratio for the different density treatments (N = 220, 370, 500, 570, 700, 800 and 1150 ind/m) along the experimental culture.

Table 4. Linear regression parameters describing changes in the mean H/W index as a function of time, by means of the equation: $H/W = a + bx$.

H/W	Intercept	Slope	R^2 adjusted	F	p-value	N
220	1.704	-0.030	0.756	16.50	0.015*	6
370	1.689	-0.029	0.955	107.77	4.9e-04***	6
500	1.708	-0.029	0.907	49.61	0.002**	6
570	1.657	-0.022	0.838	26.95	0.007**	6
700	1.716	-0.039	0.972	175.23	1.9e-04***	6
800	1.681	-0.026	0.969	155.22	2.4e-04***	6
1150	1.633	-0.018	0.671	11.18	0.029*	6

(*) p<0.05; (**) p<0.01; (***) p<0.001

3.3.4. Energy distribution

The condition index was influenced by time (ANOVA; p>0.05), while density treatment (p=0.259) and the density-time interaction were not significant (p=0.492; Fig. 5 and Table 2). There was a significant increase in meat yield from May to June. Such increase was maintained, though not significantly, until summer (July/August) when maximum values were reached (Fig. 5). Thereafter, the condition index decreased until the end of the study to values closed to those observed in May (Fig. 5).

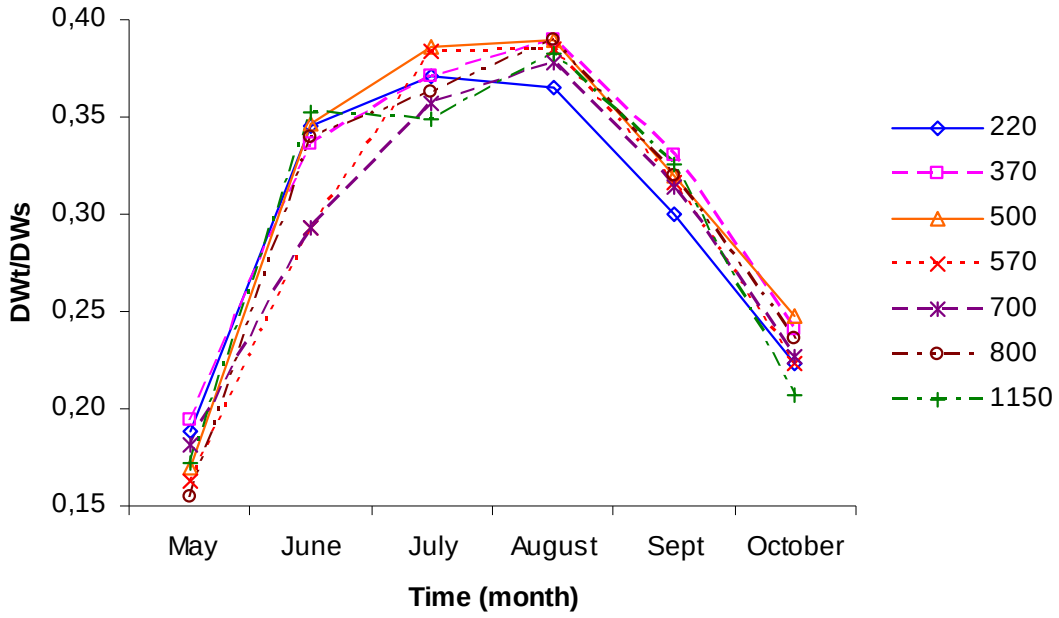

Fig. 5. Average energy distribution (DWt/DWs) of the different density treatments tested along the experimental culture.

3.3.5. Volume-Length relationships

Volume-Length relationships showed similar slopes between density treatments until October (ANCOVA; F=2.21, p=0.042). Differences observed between intercepts during that period (May-September) did not show a relationship with the density gradient. At the end of the experimental period (October) the pairwise comparisons t-test showed significant lower slopes for Volume-Length relationships for the 220 density treatment compared to the 800 and 1150 densities (p< 0.05). Similarly, the slopes observed for the allometric relationships for the 370 and 500 densities showed significantly lower values than that for the 800 density (Table 5). However, the intercepts followed an inverse trend than the slope values, decreasing with an increase in initial density (t-test; p<0.05;

Table 5). The lowest densities produced a significantly lower increase in volume per size increment compared to the highest densities, which indicates a smaller difference in volume between the individuals of different sizes at lower density.

Table 5. Parameter values of the allometric relationship Volume-Length at the end of the study period for each of the density treatments (log V = a + b log L). All the regressions were highly significant in all cases ($p<0.001$).

	Intercept	**Slope**	**R^2 adjusted**	**F**	**N**
All data	-3.45±0.06***	2.59±0.03***	0.94	5560.47***	384
220	-3.17±0.15***	2.44±0.08***	0.94	908.61***	55
370	-3.24±0.20***	2.49±0.11***	0.91	554.04***	55
500	-3.29±0.15***	2.51±0.08***	0.95	961.08***	55
570	-3.53±0.19***	2.63±0.10***	0.93	669.43***	54
700	-3.37±0.15***	2.56±0.08***	0.95	1036.39***	56
800	-3.89±0.16***	2.82±0.09***	0.95	1038.24***	56
1150	-3.60±0.15***	2.67±0.08***	0.96	1115.32***	53

(*) $p<0.05$; (**) $p<0.01$; (***) $p<0.001$

3.3.6. Projected area-Length relationships

Differences between densities in the slopes of the Projected area-Length relationships were only observed for the last month of cultivation (October) (ANCOVA; $F=3.10$, $p=0.007$). With regard to the intercepts, significant differences were observed among density treatments in every sampling ($p<0.05$), but those differences did not follow a density gradient until the end of the study (October). In October, an inverse relationship between the intercept magnitude and the initial density was observed (Table 6). In addition, in this month there was a progressive decrease in the slopes related with the decrease in the initial cultivation density (Table 6). The pairwise t-test found significantly lower slopes for the lower density treatments ($p<0.05$). Specifically, the 220 ind/m density showed significantly lower slopes than the densities of 700, 800 and 1150, whereas the 370 ind/m slope was lower than those of 800 and 1150 and that of 500 was lower than the slope for 800 ind/m.

Table 6. Parameters of the allometric relationship Projected area-Length in October for the different densities (log S = a + b log L). All the regressions were highly significant in all cases ($p<0.001$).

	Intercept	Slope	R^2 adjusted	F	N
All data	-2.94±0.10***	2.08±0.05***	0.89	1539.07***	1219
220	-2.31±0.20***	1.74±0.11***	0.90	246.78***	193
370	-2.69±0.23***	1.96±0.12***	0.91	256.90***	187
500	-2.64±0.25***	1.90±0.14***	0.88	189.98***	194
570	-2.88±0.19***	2.04±0.10***	0.94	412.36***	153
700	-3.10±0.21***	2.17±0.11***	0.93	363.33***	180
800	-3.40±0.23***	2.33±0.12***	0.93	352.89***	158
1150	-3.33±0.24***	2.28±0.13***	0.92	300.04***	154

(*) $p<0.05$; (**) $p<0.01$; (***) $p<0.001$

3.4. Discussion

In our studies we observed a growth-related variation in the morphology of mussels. As for the majority of organisms, mussels exhibit gradual changes in their relative proportions as they increase their size. From a physiological perspective, these changes can be associated with the maintenance of optimal proportions (Banavar et al. 1999; West et al. 1997) or may reflect an adaptive response to changes in environmental conditions (Akester & Martel 2000; Reimer et al. 1995; Seed 1980; Seed & Suchanek 1992; Steffani & Branch 2003). The effect of growth on morphology is consistent in all the experimental densities evaluated in this study, showing a decrease in the H/L and H/W ratios and an increase in W/L along the study period. However, during the final month of cultivation these ratios tended to stabilize. Despite growth in all dimensions (length, width, height), changes in morphological ratios indicate a gradual change in the relative proportions of the mussels with time. In other words, the rate of growth in height decreases over time with respect to length or width, whereas the growth in width occurs at higher rates than growth in length. Due to this differential growth of shell dimensions, the larger (older) mussels have more elongated morphology where height exceeds width in ever decreasing proportions.

These results agree with previous studies on mussel growth and morphology where variations in mussel shape were attributed to age (Alunno-Bruscia et al. 2001; Brown et al. 1976; Lauzon-Guay et al. 2005[a]; Seed 1968). This allows us to isolate the effect of normal growth on morphology from that related to intra-specific competition. Our results agree with those of Seed (1968) who observed that the H/L and H/W ratios decreased with increasing size, whereas the W/L ratio increased. Similarly, Lauzon-Guay et al. (2005[a]) recorded a decrease in H/L and an increase in W/L with time. Alunno-Bruscia et al. (2001) also noted similar tendencies as the observed in the present study for W/L and H/W ratios, but an increase in H/L ratio with the increase in size. These discrepancies may be related to different experimental conditions (laboratory versus field), cultivation method (growth chambers versus suspended cultivation), or the growth period studied (juveniles -2cm- versus adults -4.62±3.8cm-).

The present study also showed a significant effect of cultivation density on various morphological indicators. From June onwards the mussels cultured at higher densities showed a decrease in the height-length (H/L) ratio and, from September, a decrease in the width-length ratio (W/L) was also observed. Thus, mussels cultivated at higher densities showed at the end of the study more elongated and narrower shells than those growing at low densities, which tend to be wider and higher. The density effect on both ratios (H/L and W/L) became more pronounced with time, showing the largest differences between densities at the end of the cultivation period. This may be related to the increasing limitations by food and space as the individuals grow and increase their requirements, which in turn increase intra-specific competition (Alunno-Bruscia et al. 2000; Boromthanarat & Deslous-Paoli 1988; Fréchette & Lefaivre 1995; Marquet et al. 1990; Petraitis 1995). However, the effect of density on the H/W ratio was only detected in August. This would suggest that the decrease in height and width of the mussels caused by intra-specific competition occurs evenly over the density gradient.

These results agree with previous studies that reported more elongated and less triangular mussels with a lower height/length ratio (Briones & Guiñez 2005; Brown et al. 1976; Coe 1946; Lent 1967; Richardson & Seed 1990) and a lower width/length ratio (Alunno-Bruscia et al. 2001; Lauzon-Guay et al. 2005[a]) at higher mussel densities. Together, this suggests that morphological plasticity is a strategy to mitigate the effects of intra-specific competition at the individual level (Brown et al. 1976; Seed 1968,

1973). There is a great controversy of the limiting factor that determines the appearance of intra-specific competition mechanisms in bivalves. Some authors suggest limitation by the concentration of available food ("exploitative competition"; Alunno-Bruscia et al. 2001; Seed 1968), whereas others attributed intra-specific competition mechanisms to physical spatial limitations ("interference competition"; Fréchette et al. 1992; Okamura 1986). The morphological changes observed in the mussels cultivated at higher densities could be a strategy to reduce physical interference between individuals. Although it is not clear if physical interference has an effect on growth (Fréchette & Lefaivre 1990; Fréchette & Despland 1999), such interference may cause a reduction in valve gaping, clearance rate and food uptake (Jørgensen et al. 1988). Mussels cultured at high densities and laterally constricted will encounter more restriction to valve opening (Lauzon-Guay et al. 2005[a]). The elongation of shells (more filiform shapes) might also enable mussels to position themselves more favourably to expose their inhalant siphons to better access for food (Sénechal et al. 2008), this might be part of the food competitive adaptation to culture, i.e., exploitative competition. The strategy of attaining more elongated shells seems, therefore, to be advantageous in high density environments and is a common characteristic in mussels grown in suspended culture (Lauzon-Guay et al. 2005[a] and present study) and in other cultivation methods such as laboratory tanks (Alunno-Bruscia et al. 2001) and "mussel beds" (Seed 1968).

Nevertheless, no significant effect of the cultivation density on the energy distribution between shell and tissue was observed at any time during the study period. This does not imply that the individuals cultivated at lower densities do not obtain a larger quantity of energy, but rather that the energy distribution between shell and tissue is maintained in the same proportion for all densities. In fact, higher asymptotic values have been achieved in the size and weight growth curves of mussels cultivated at lower densities (Côté et al. 1993; Cubillo et al. submitted; Widman & Rhodes 1991; Xavier et al. 2007), as well as higher growth rates (Alunno-Bruscia et al. 2000; Cubillo et al. submitted; Gascoigne et al. 2005; Grant 1999). Differences in the growth of tissue and shell between densities are proportional and not observable when combined in the condition index. Other studies (Alunno-Bruscia et al. 2001; Mallet & Carver 1991) observed a density effect on the energy distribution in mussels. However, the different allocation energy index used and the differences in the experimental design issues (laboratory culture chambers) could explain, respectively, the discrepancies with our

results. Lauzon-Guay et al. (2005[b]) observed that prior to spawning mussels cultivated at higher density channelled a lower proportion of resources into tissue growth, with respect to those cultivated at lower densities. Nonetheless, these differences disappeared in post-spawning mussels, implying that the extra energy had been channelled into gonadal production (Lauzon-Guay et al. 2005[b]). This hypothesis is supported by Bayne et al. (1983) who observed a reduction in reproductive effort under environmental stress. This would also explain the lack of significant differences in the condition index between densities in this study, which took place after the main spawning period (spring) of this latitude (Cáceres-Martínez & Figueras 1998a,b; Peteiro et al. 2007; Snodden & Roberts 1997; Suárez et al. 2005; Villalba et al. 1995). In general, the condition index (CI) is considered to be a weak indicator for detecting stress in bivalve molluscs (Amiard et al. 2004; Duquesne et al. 2004; Guolan & Yong 1995; Hummel et al. 1996; Lauzon-Guay et al. 2005[a]; Waite et al. 2005) because most of the variability in the CI is associated with fluctuations in the gametogenic/reproductive cycle and to seasonal variations in food availability (Amiard et al. 2004; Boscolo et al. 2004; Hummel et al. 1996; Leung & Furness, 2001; Pampanin et al. 2005). Thus, individual variability in CI may mask the effect of density.

In our study, no effect of density on the slopes of the allometric Volume-Length and Projected area-Length relationships was observed until the last cultivation month (October). In this month a progressive increase was observed in the slopes of both allometric relationships with density, showing significant differences between extreme densities. However, the magnitude of the intercepts followed an inverse trend with density, whereby for the lowest densities the smallest individuals occupied a larger volume and surface area than at elevated densities, whereas the larger individuals occupied a similar volume and surface area at all tested densities. This alludes to the existence of asymmetric competition mechanisms due to the larger individuals obtaining a greater proportion of resources, thus affecting the growth of the smaller individuals (Weiner 1990). This behaviour has been observed in other studies at elevated densities (Bertness & Grosholz 1985; Fréchette et al. 1992; Fréchette & Despland 1999; Lauzon-Guay et al. 2005[b]). Our findings agrees with Fréchette et al. (1992) who hypothesized that asymmetric competition reflects an increase in the slope of Body mass-Shell length allometric relationships, as opposed to symmetric competition which exclusively affects the intercept. Little information exists on the

symmetric or asymmetric nature of intra-specific competition in suspended bivalves or on the underlying mechanisms of competition. Generally, asymmetric competition has been attributed to competition by physical interference between individuals, both in sessile invertebrates (Bertness & Grosholz 1985; Fréchette et al. 1992; Okamura 1986) and plants (Thomas & Weiner 1989; Weiner 1990). Symmetric competition has been more usually related to food limitation in plants (Thomas & Weiner 1989; Weiner 1990), infaunal (Peterson 1982) and epifaunal bivalves (Fréchette & Bourget 1985a,b) not subjected to physical limitations or spatial regulation. However, the results of Fréchette & Despland (1999) and Alunno-Bruscia et al. (2001) using mussels grown in the laboratory in the absence of physical interference suggest that local seston depletion can not be discarded as cause of asymmetric competition mechanisms.

Our results corroborate the notion of density-dependent morphological plasticity as noted in previous studies (Coe 1946 -*Mytilus edulis diegensis*-; Seed 1968, 1973; Richardson & Seed 1990 and Alunno-Bruscia et al. 2001 -*Mytilus edulis*-; Tanita & Kikuchi 1957 –*Pinctada martensii*-; Ohba 1956 –*Venerupis semidecussata*-; Wade 1967 –*Donax striatus*-; Lent 1967 –*Modiolus demissus*-; Brown et al. 1976). In addition to changes in morphology related to the ontogeny of the individuals, a clear effect of density on morphological parameters has been observed, leading to narrower and more elongated mussels at higher densities with respect to those grown at lower density. The significant interaction between density and time found in the present study reflects an increasing intra-specific competition as mussels grow, due to an increment of their space and food requirements.

Population density has been proposed to alter the morphology of mussels through competition for food (“exploitation”) or physical compression of the surrounding individuals (interference). However, due to multiple interactions between both factors, it is difficult to discriminate the principal driver of such morphological changes (Alunno-Bruscia et al. 2001; Guiñez & Castilla 1999; Guiñez 2005). Additional work is needed to clarify the degree to which each component (food limitation, food access or interference) contributes to the morphological changes of the individuals.

This work supports the hypothesis that morphological plasticity is a strategy to mitigate the effects of intra-specific competition at the individual level (Brown et al. 1976; Seed

1968, 1973). In addition, this plasticity seems to be a function of the size of individuals, leading to a greater morphological uniformity within sizes in populations cultured at lower density levels. Variations in shell morphology of mussels could have an effect on the acceptability and the value of the product in the market for fresh or frozen products, although this might not be the case for meat extraction. Our results may contribute to the adjustment of an appropriate cultivation density which would minimize intra-specific competition and optimize mussel production.

Capítulo 4. Evaluation of self-thinning models and estimation methods in multilayered sessile animal populations

Análisis de las relaciones de auto-raleo en *Mytilus galloprovincialis* en cultivo suspendido. Comparación de modelos y métodos de estimación.

Summary

Self-thinning (ST) models have been widely used in the last decades to describe population dynamics under intraspecific competition in plant and animal communities. Nevertheless, their applicability in animal populations is subjected to the appropriate inclusion of space occupancy and energy requirements. Specifically, the disposition of gregarious sessile animals in complex matrices makes difficult the application of classical ST models. This manuscript reviews the self-thinning models and regression methods currently used for gregarious sessile species by their application to the analysis of mussel populations (*Mytilus galloprovincialis)* grown in suspended culture. This work supports the necessity of incorporating the number of layers in the classical bidimensional ST model for the analysis of multilayered populations. Furthermore, the robustness of the tridimensional ST model was checked from two perspectives: (i) with respect to the measurement method of the variables involved in the model, and (ii) analyzing the congruence between the fits for biomass and individual mass. In addition, we explore the potential and applicability of the Stochastic Frontier Function (SFF) approach in the analysis of self-thinning relationships.

The estimated ST parameters depended on the measurement method of the variables involved in the model. This, together with the proximity between the SST and FST theoretical exponents, highlight the difficulties to discriminate the competition limiting factor (space/food) based on the self-thinning exponent. On the other hand, the SFF provided congruent results for biomass and individual mass analysis, on contrast with the lack of robustness observed for the central tendency regression methods. Furthermore, the SFF approach allowed a dynamic interpretation of the ST process providing insight into the temporal evolution of site occupancy. These results highlight the suitability of the stochastic frontier approach in the analysis of self-thinning in sessile animal populations.

4.1. Introduction

Intra-specific competition in plant and animal communities with high population densities leads to self-thinning mechanisms (hereafter ST), which play an important role in determining population dynamics and community structure (Fréchette & Lefaivre 1995; Fréchette et al. 1996; Petraitis 1995; Weller 1987a; Westoby 1984). Self-thinning is typically studied following the growth of even-aged populations at different densities through time (see Figure 1 in Alunno-Bruscia et al. 2000). This can be represented in biomass-density (B-N) or, equivalently, individual mean mass-density (m-N) diagrams. Traditionally, ST has been modeled by the allometric relationship $B=kN^{\beta}$ (Yoda et al. 1963). Most experimental and theoretical studies on ST relationships have been developed for plants, where competition for space or spatial self-thinning (SST) is assumed and the classical exponent $\beta = -1/2$ is suggested for a wide range of species (Westoby 1984; White 1981; Yoda et al. 1963). This exponent is obtained from the allometric relationships between individual area occupied (S), shell length (l) and weight (m). Assuming (i) isometric growth ($S \alpha l^2$ and $m \alpha l^3$), where shape does not change with the increase in size of individuals (Weller 1987b), (ii) 100% occupation of the sampling area (White 1981), and (iii) density is inversely related to the individual area occupied ($N \alpha S^{-1}$; Westoby 1984), the expressions: $m = kN^{-3/2}$ and $B = kN^{-1/2}$ were obtained.

On the other hand, Begon et al. (1986) suggested that the self-thinning process for mobile animals is better described due to food limitation or "food self-thinning" (FST). Accordingly, they associated the ST phenomenon with the metabolic rate of the population (MR), which itself is related to the individual mean weight ($MR \alpha N m^{3/4}$) and the environmental conditions (MR α F, where F is the overall energy flow through the population), leading to an exponent of $\beta = -1/3$ (Armstrong 1997; Bohlin et al. 1994; Dunham & Vinyard 1997; Latto 1994; Norberg 1988a). Assuming constant resource availability per unit area and stable environmental conditions, the relationships $m = kN^{-4/3}$ and $B = kN^{1-4/3}$ were obtained (Begon et al. 1986; Belgrano et al. 2002; Bohlin et al. 1994; Brown et al. 2004; Enquist et al. 1998).

However, the assumptions of the classical model for space limitations (SST) are not always fulfilled under natural field conditions. Multilayered disposition, which increases the surface area available to the organisms, and allometric growth, could cause

a deviation of the theoretical SST exponent (Hughes & Griffiths 1988; Norberg 1988a,b; Weller 1987; Westoby 1984; White 1981). These deviations have been included in more recent mussel self-thinning models (Fréchette & Lefaivre 1990; Guiñez & Castilla 1999; Guiñez et al. 2005). Guiñez & Castilla (1999) proposed the tridimensional ST approach (B-N-L) that incorporates the number of layers in the classical bidimensional model. Similarly, a wide range of exponents has been observed for the relationship between the metabolic rate and individual mean weight (Latto 1994) altering the theoretical FST relationship. Moreover, changes in the environmental conditions, as food availability and temperature, can also alter the FST slope (Armstrong 1997). Fréchette & Lefaivre (1990) proposed to discriminate the factor regulating competition (space/food) based on the comparison between the estimated and the theoretical ST exponents.

Mussel populations usually form highly dense multilayered beds (Alvarado & Castilla 1996; Guiñez & Castilla 1999; Hosomi 1985; Suchanek 1986). This crowding can lead to space and food limitations (Alvarado & Castilla 1996; Fréchette et al. 1992; Okamura 1986) and to self-thinning as the individuals grow (Fréchette & Lefaivre 1990, 1995; Guiñez & Castilla 1999; Guiñez et al. 2005; Hughes & Griffiths 1988; Petraitis 1995). Despite several authors have analyzed ST in mussel populations (Alunno-Bruscia et al. 2000; Alunno-Bruscia et al. 2001; Filgueira et al. 2008; Fréchette & Lefraive 1990; Fréchette et al. 1996; Fréchette et al. 2010; Guiñez & Castilla 1999; Hughes & Griffiths 1988; Lachance-Bernard et al. 2010; Petraitis 1995) an accurate approximation of the biomass/mass-density relationships is still lacking.

Aquaculture in suspended systems represents an extreme case of aggregation where the density of suspension feeders is maximized to achieve a greater commercial yield. Therefore, commercial farms provide an ideal scenario for the study of self-thinning mechanisms. In this study, we review the ST models currently used for gregarious sessile species by their application to the analysis of mussel populations grown at different densities in suspended cultivation systems. Firstly, the goodness-of-fit of bidimensional and tridimensional models are compared to evaluate the necessity of including the number of layers in the analysis of multilayered populations. Secondly, the robustness of the self-thinning model is studied from two perspectives: (i) with respect to the measurement method of the variables involved in the model and (ii) the relationship studied (B-N or m-N). In addition, several central tendency regression

techniques previously applied in the analysis of ST were compared and the estimated exponents were analyzed to identify the competition limiting factor (space/food). Finally, the stochastic frontier function (SFF) was fitted, including the effect of time in site occupancy in the analysis of sessile animal populations for the first time.

4.2. Material and methods

4.2.1. Experimental design

This study analyzes a dataset of density, biomass and individual weight of even-aged *Mytilus galloprovincialis* populations grown in suspended culture in the Ría de Ares-Betanzos (NW Spain). These data were obtained by sequential sampling of seven initial cultivation densities (220, 370, 500, 570, 750, 800 and 1150 individuals per meter of rope) randomly distributed over a commercial raft.

The experimental culture was carried out from late April to late November 2008. Monthly samplings were performed (7 samplings; from late May to late November). In each sampling, biomass (B1; g) was obtained by weighing the ropes in the water and applying a correction factor (weight of the rope in water × 5) in accordance with unpublished data. Furthermore, a sample of known length was taken from 4 ropes of each density treatment (28 ropes per sampling date). Each sample was cleaned of epibionts and weighed to obtain an alternative measure of population biomass (B2; g). The mussels were counted to calculate the density of the rope (N_0; ind/m), which was standardized to the number of individuals per square meter of rope (N; ind/m^2). Individual fresh mass (fm; g) was calculated by dividing the weight of subsamples containing 200-300 mussels by the number of individuals. Individual dry mass (dm; g), shell length (l; cm), height (H; cm), width (W; cm) and volume (V; ml) data were obtained from Chapter 3.

4.2.2. Measurement methods of the surface area occupied

Multilayered packing alters the surface area available to the individuals and, thus, can modify the ST exponent (Fréchette & Lefaivre 1990; Hosomi 1985; Hughes & Griffiths 1988). To account for this effect the effective surface area occupied (S_e) is required, that

is, the area that individuals would occupy if they were distributed in a single layer (Guiñez et al. 2005). The effective surface area was calculated assuming that the maximum anterio-posterior axis is disposed perpendicular to the substrate. Then, assuming that the volume occupied per mussel is a rectangular parallelepiped, the area projected onto the substrate was estimated by multiplying the width by the height of each individual (S_p; Guiñez & Castilla 1999). However, calculating the occupied area by the parallelepiped projection overestimates the real individual area occupied since overlapping is not considered. To overcome this problem, Filgueira et al. (2008) proposed the use of image analysis techniques to provide a more accurate approximation of mussel morphology. Therefore, apical photographs were taken to determine the individual area projected onto the substrate (S_{im}) using the software Image J 1.37v (Filgueira et al. 2008). Both procedures were performed for a subsample of 56 individuals (from 40 to 85 mm) per density treatment and sampling date. The allometric equations shell length (l; cm) vs. area occupied obtained by the parallelepiped projection (S_p; cm^2) ($S_p = 0.18 \times l^{1.94}$, N = 1444, $R^2 = 0.96$, $P < 0.001$) and by image analysis (S_{im}; cm^2) ($S_{im} = 0.10 \times l^{2.24}$, N = 1415, $R^2 = 0.92$, $P < 0.001$) were applied to the length frequency distribution to estimate the total area occupied by the population. In this work, the density was assumed not to affect the allometric relationship length vs. individual surface area occupied.

4.2.3. Effective density and number of layers

To account for the multilayered distribution of mussels the effective density (N_e) should be considered, that is, the density expected if the individuals formed a monolayer (Guiñez et al. 2005). N_e was calculated as N_0/S_e. In this work, $N_p = N_0/S_p$ and $N_{im} = N_0/S_{im}$ denote the effective density estimated by the parallelepiped projection and image analysis, respectively. The number of layers (L) was obtained as the quotient of sample density and effective density (i.e. N/N_e) (Guiñez & Castilla 2001), and is denoted by L_p (N/N_p) and L_{im} (N/N_{im}) depending on the method used to measure the surface area occupied. The number of layers (L) enables us to incorporate explicitly the effect of packing on the self-thinning model (Guiñez & Castilla 1999).

4.2.4. Mathematical formulation of self-thinning

4.2.4.1. Bidimensional model

Traditionally, ST has been described using a bidimensional model that defines the relationship between biomass (B) and population density (N):

$$B = k_2 N^{\beta_2} \tag{1}$$

where k_2 and $ß_2$ are the intercept and exponent of the allometric relationship, respectively.

Given the relationship between mean individual mass (m) and population biomass (m=B/N) we obtain:

$$m = k_2 N^{\beta_2 - 1} = k_2 N^{\gamma_2} \tag{2}$$

4.2.4.2. Tridimensional model

Guiñez & Castilla (1999) developed a tridimensional model incorporating the effect of multilayered disposition of sessile animal populations in the bidimensional model. In this model, density (N) was considered to be inversely proportional to the average area projected onto the substrate (S) and directly proportional to the number of layers (L), that is, $N \alpha L S^{-1}$. Therefore, if self-thinning is determined by packing geometry and allometric growth (Hughes & Griffiths 1988), the tridimensional model can be expressed as:

$$B = k_3 N^{\beta_3} L^{1-\beta_3} = k_3 \left(N/L\right)^{\beta_3} L \tag{3}$$

and

$$m = k_3 N^{\beta_3 - 1} L^{1-\beta_3} = k_3 \left(N/L\right)^{\beta_3 - 1} = k_3 \left(N/L\right)^{\gamma_3} \tag{4}$$

where the SST exponent is $\beta_3 = 1-[3(1-\alpha)/2(1-\omega)]$, being $3(1-\alpha)$ with $\alpha \neq 0$ and $2(1-\omega)$ with $\omega \neq 0$ correction factors for allometric growth that represent the population mean allometries shell length-weight and shell length-surface area occupied, respectively. In this study, according to the proportionality between the volume filled by biomass and

the surface area occupied established by Guiñez & Castilla (1999), this exponent was calculated as $\beta_3 = 1 - \delta$, where δ is the exponent of the population mean allometry volume-surface area occupied, adjusted by RMA (Reduced Major Axis) regression. On the other hand, the FST theoretical exponent was obtained from the literature (β_{FST}=-1.3).

Finally, considering the relationship between density and effective density, N_e=N/L, Eq. 3 reduces to:

$$B = k_3 N_e^{\beta_3} L \tag{5}$$

and Eq. 4 to:

$$m = k_3 N_e^{\beta_3 - 1} = k_3 N_e^{\gamma_3} \tag{6}$$

4.2.5. Data analysis

In each sampling, the biomass and area occupied by the mussels were obtained by two measurement methods. Prior to the ST analysis, the Wilcoxon test for paired samples was applied to check the equality between the different measurements of each variable. Furthermore, as self-thinning analysis has been conducted indistinctly for fresh and dry mass, the correlation between them was studied. In addition, the bidimensional and tridimensional self-thinning models for both measurements of the variables involved were fitted by linear regression (OLS, ordinary least squares) and their goodness-of-fit were compared using the F-test. In case of significant differences between fits, the best ST model and the more accurate measurement method was selected. Furthermore, the theoretical SST exponent was estimated for both measurements of surface area occupied.

Thereafter, several regression methods previously used for the estimation of the self-thinning slope were compared (Zhang et al. 2005; Guiñez & Castilla 1999; Lachance-Bernard et al. 2010):

- OLS (Ordinary Least Squares): linear least squares regression.
- RLM (Robust Linear Model): this model reduces the effect of outliers. In this work, the M-estimation method with bi-squared weights was applied (Bégin et al. 2001; Huber 1981; Lachance-Bernard et al. 2010).

- RMA (Reduced Major Axis): fits the line that best describes the relationship between two variables using PCA (Principal Components Analysis). The main objective of RMA is the estimation of the model parameters. Accordingly, Mohler et al. (1978) proposed to use this method in ST analysis instead of OLS, which goal is to predict a response Y from explanatory variables.
- NLM (non-linear model): this method was applied to the non-transformed tridimensional model (Eqs. 3-4). This fit allows the comparison of the tridimensional model (Eq. 3) with the unrestricted B-N-L model ($B=kN^{\beta}L^{\lambda}$) in order to check if the data fulfill the established relationship between N and L.

Finally, the exponents estimated by the previous fits were compared with the SST and FST theoretical exponents to determine the competition limiting factor.

Since the main objective of self-thinning analysis is to find the upper boundary ST line, the Stochastic Frontier Function (SFF) was estimated (Bi 2004; Bi et al. 2000). This function was first used in economy, where the concept of production is generally understood as the process that transforms a group of inputs to a group of outputs. This resembles the growth of mussels, which takes the food available in the local environment (inputs) to produce biomass (output). In our case, the frontier production function (Greene 1997) represents the maximum attainable mass or biomass given the density and the number of layers on each rope, that is, the carrying capacity of the system. Given a dataset comprising the observations of *I* ropes sampled at *T* time periods, the SFF was defined by the following general model (Batesse & Coelli 1992):

$$Y_{it} = \alpha + x_{it}\beta + \left(V_{it} - U_{it}\right), \quad i = 1,...,I,\ j = 1,...,T \tag{7}$$

where:

- Y_{it} is the (log-transformed) output or the dependent variable corresponding to the i-th rope at time t.
- X_{it}: is a vector k x 1 of (log-transformed) inputs or explanatory variables.
- (α, β): is the vector 1 x (k+1) of unknown parameters.
- V_{it}: random errors due to external factors. These are assumed to be independent and identically distributed $N(0,\sigma_v^2)$ and independent of the U_{it}.
- U_{it}: non-negative random variables associated with technical inefficiency. The term $0 \leq e^{-u} \leq 1$ is the technical efficiency and represents the site occupancy, that

is, the extent to which the mussels occupy the space and consume the available resources for growth within a given environment. When $e^{-u} = 1$, the site is fully occupied, i.e., the system has reached the maximum attainable biomass at a specific density, and any further growth will incur mortality.

According to the model proposed by Batesse & Coelli (1992), U_{it} is defined as:

$$U_{it} = \exp(-\eta(t_i - T))U_i \tag{8}$$

where η is an unknown parameter and U_i; i=1,…,I are obtained by truncation (at zero) of the normal distribution with unknown mean, μ, and unknown variance, σ_u^2. Before estimating the model parameters, the following hypotheses were tested:

- Firstly, the null hypothesis that there is no technical inefficiency is tested. This is expressed as H_0: γ=0, where $\sigma^2 = \sigma_v^2 + \sigma_u^2$ and $\gamma = \sigma_u^2 / \sigma^2$, according to the parameterization of the frontier library of R (Coelli & Henningsen 2011).
- The next step is testing whether the technical inefficiency effects are time invariant, that is, H_0 : η=0. If H_0 is accepted, Eq. 7 reduces to:

$$Y_i = \alpha + x_i\beta + (V_i - U_i), \quad i = 1,...,I \tag{9}$$

- Finally, we test the null hypothesis that U has half-normal distribution $|N(0,\sigma_u^2)|$ (Aigner et al. 1977), H_0 : μ=0, instead of truncated normal distribution $|N(\mu,\sigma_u^2)|$, as the general model proposes.

The three hypotheses were checked using generalized likelihood ratio tests. Once the distribution of U was selected, the parameters (α,β) were estimated by the maximum log-likelihood method proposed by Battese & Coelli (1992) implemented in the frontier library of R (Coelli & Henningsen 2011).

Data analysis was performed with the statistical package R 2.12.2 (R Development Core Team, 2011).

4.3. Results and discussion

4.3.1. Descriptive analysis

Figure 1 shows the box-plots that summarize the monthly evolution for each variable. Maximum densities (N) decreased over time suggesting mortality on the ropes with higher density. This was confirmed by the negative slope obtained in the linear fit of the natural logarithm of density vs. time for densities greater than 500 ind/m (F-test, $P < 0.05$). In addition, a trade-off between the exponential reduction in effective density (N_e) and the increase in the number of layers was observed in Fig. 1. This implies that the reorganization of growing individuals causes the formation of new layers and the subsequent reduction in the density per layer. However, whereas the number of layers increased with the initial density (K-W test, $p < 0.01$; Wilcoxon test, $p < 0.01$), except between 500 and 570, (Wilcoxon test, $p > 0.05$), there was no significant effect of initial density over N_e (Kruskall-Wallis test, $p > 0.1$). Therefore, in multilayered populations site occupancy is reflected by the degree of packing, measured as number of layers (L), which in our case increased until September and remained constant thereafter.

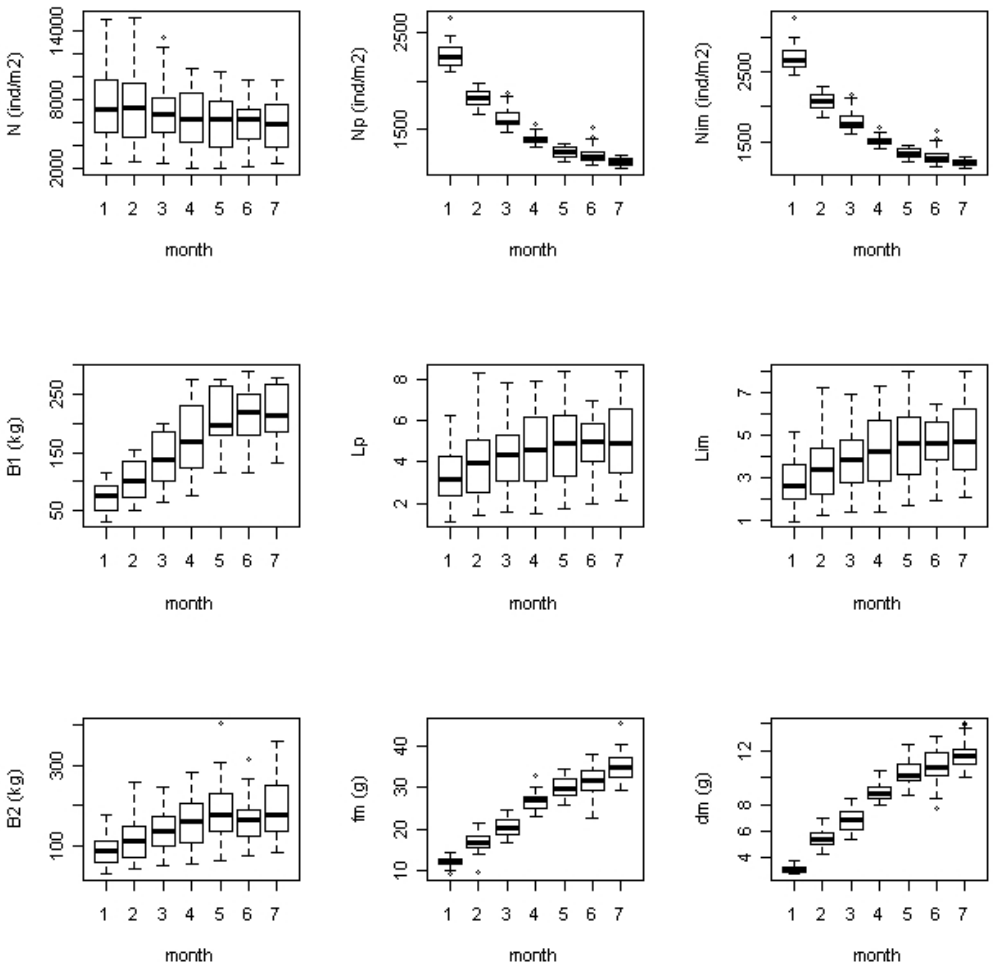

Fig. 1. Box-plots of density (N), effective density (N_p: parallelepiped projection; N_{im}: image analysis), biomass as weight of the ropes in water (B1); number of layers (L_p: parallelepiped projection; L_{im}: image analysis), estimated biomass from the sample weight (B2), fresh mass (fm) and dry mass (dm). (1: May, 2: June, 3: July, 4: August, 5: September, 6: October, 7: November).

Figures 2 and 3 show the Biomass-Density (B1-N and B2-N) and mass-Density (fm-N and dm-N) diagrams obtained from our data, where different growth and intra-specific competition temporal patterns are observed (Alunno-Bruscia et al. 2000; Fréchette et al. 1996). Initially (during the first month), the ecosystem was able to support a larger number of small individuals, as illustrated by the linear increase of biomass with density ($\beta>0$). At the same time, the mean individual mass was independent of density ($\gamma=0$).

Both facts indicate that competition and mortality were negligible even at higher densities, implying that growth was not regulated by the availability of resources.

As individuals grow, the higher density groups show a different pattern, whereby growth decreased indicating the presence of intra-specific competition. At this stage (June and July), the slope decreases until reaching a maximum in the B-N diagram ($\beta \rightarrow 0$, then $\gamma \rightarrow -1$) while density and competition increase, i.e., growth was density-dependent. This progressive decrease of γ is known as the competition-density or C-D effect (Hagihara 1999; Xue & Hagihara 1998) and is well-documented in plant populations (Westoby 1984). However, the question of whether the C-D effect also exists in animals has not yet been fully addressed. To our knowledge, only Hosomi (1985) for *Mytilus galloprovincialis* and Newell (1990) for *M. edulis* have detected this effect in molluscs. Further studies (Alunno-Bruscia et al. 2000; Fréchette & Bacher 1998) have not found any evidence of the C-D stage at intermediate competition levels, but instead Fréchette & Bacher (1998) observed a curvilinear trend.

From July, the processes of competition intensifies giving rise to mortality in higher density populations and leading to negative correlations between mean individual mass and density. This restricts the maximum attainable biomass at a specific density and is referred as the self-thinning region, where: $\beta < 0$ and $\gamma < -1$.

Most studies on the B-N curves in animals have centered on the ST region (Elliott 1993; Fréchette & Lefaivre 1990; Fréchette et al. 1992, 1996; Hughes & Griffiths 1988; Latto 1994) and little is known about the general shape of the B-N curves in these populations. Furthermore, recent studies on ST in animals (Armstrong 1997; Bohlin et al. 1994; Fréchette & Lefaivre 1990; Latto 1994) failed to provide a clear pattern of the ST function. Only Alunno-Bruscia et al. (2000) and Fréchette & Bacher (1998) have described, from experimental studies and hypothetical populations (respectively), the general shape of the B-N diagram in mussels. Yet, physical interference was avoided in both studies, such that growth was regulated exclusively by food availability. The present study is the first to describe the B-N and m-N curves of molluscs in natural conditions of suspended culture.

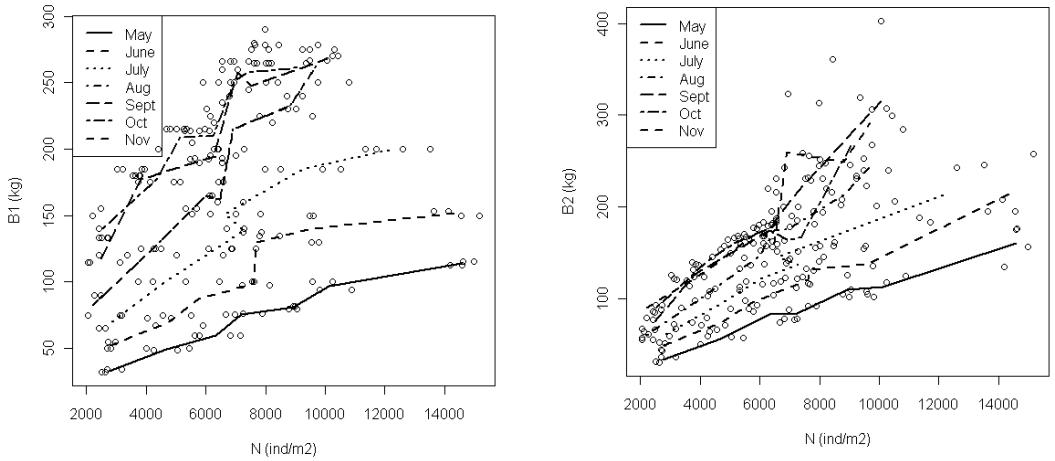

Fig. 2. B-N plots. (B1: rope weighed in water. B2: biomass estimated from sample weight).

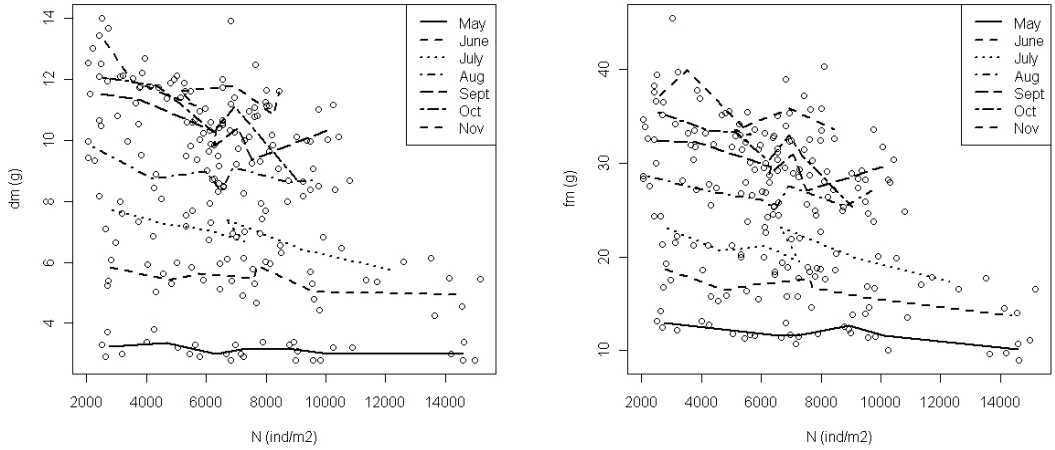

Fig. 3. m-N plots. (dm: individual dry mass; fm: individual fresh mass).

As explained in the "Data analysis" section, for each sampling time, two measurements of biomass (B1, B2), number of layers (L_p, L_{im}) and effective density (N_p, N_{im}) were obtained. The Wilcoxon test for paired samples rejects the homogeneity assumption for each pair of measurements. As expected B1>B2 ($p = 2.4x10^{-6}$), i.e. the estimation of biomass by weighing the ropes in water, that included the rope and attached epibionts, was higher than that obtained from the weight of the sample, where only mussels were considered. Since the surface area estimated by the parallelepiped projection was higher

than that estimated by image analysis ($S_p > S_{im}$), the number of layers was higher ($L_p > L_{im}$, $p < 2.2x10^{-16}$) and the effective density was lower ($N_p < N_{im}$, $P < 2.2x10^{-16}$). Finally, the correlation coefficient between individual dry mass (dm) and individual fresh mass (fm), R=0.9622, showed strong linear dependence, such that individual fresh mass can be estimated from individual dry mass by a linear model (OLS): fm=3.053+2.640dm, R^2=0.9255.

4.3.2. Bidimensional self-thinning model

The log-transformed bidimensional self-thinning models (Eqs. 1 and 2) for biomass (B1, B2) and individual mass (fm, dm), respectively, were fitted by linear regression (OLS) (Table 1). In all cases, the low proportion of variance explained (R^2= 0.172 for B1-N and R^2= 0.494 for B2-N; R^2=0.1082 for fm-N and R^2=0.083 for dm-N) and the diagnostic plots (Figures. A.1–A.4 in Appendix) showing that the residuals were no normal either homocedastic, indicate that the bidimensional fit does not satisfactorily explain the self-thinning process. On the other hand, the residuals showed a strong monthly trend, as well as an effect of initial density, that were not included in the model. Furthermore, dependence between the residuals and the number of layers was observed, indicating that this variable should be included in the model. In other words, the residual analysis suggests that the tridimensional model proposed by Guiñez & Castilla (1999) should be applied for multilayered populations.

Table 1. Linear fit of the log-transformed relationships B-N and m-N.

	B1-N		**B2-N**		**fm-N**		**dm-N**	
	$\mathbf{k_2}$	$\mathbf{\beta_2}$	$\mathbf{k_2}$	$\mathbf{\beta_2}$	$\mathbf{k_2}$	$\mathbf{\gamma_2}$	$\mathbf{k_2}$	$\mathbf{\gamma_2}$
Value	7.827	0.466	5.254	0.753	5.524	-0.274	4.494	-0.285
2.5%	6.584	0.323	4.319	0.646	4.576	-0.383	3.362	-0.415
97.5%	9.071	0.609	6.190	0.860	6.473	-0.165	5.626	-0.155
P	0.146	< 0.001	0.001	< 0.001	< 0.001	< 0.001	< 0.001	< 0.001
R^2	0.172		0.494		0.1082		0.0833	

Two aspects require consideration: (i) ST occurs in populations showing density-dependent mortality and (ii) the residuals of the bidimensional fits depend on the initial density. Furthermore, according to previous studies (Alunno-Bruscia et al. 2000) ST can be studied following the temporal evolution of the B-N or m-N relationship for each density group. Therefore, prior to including the number of layers in the model, the effect of initial density was included in the bidimensional model (Table 2). An improvement in the goodness of fit was obtained. Yet, the effect of initial density was only observed in the intercept while the ST slope remained constant (Tables 2-3). This improvement is due to the fact that initial density implicitly incorporates information on the degree of packing.

Table 2. Goodness of fit comparison (F-test) between the bidimensional model and models including the initial density (N_0) effect, where $N+N_0$ indicates the model without interaction density-initial density (effect of initial density included only in the intercept) and $N*N_0$ indicates the model with interaction density-initial density (effect of initial density included in both intercept and slope).

	B1		**B2**		**fm**		**dm**	
V. indep.	**R^2**	**p-value**	**R^2**	**p-value**	**R^2**	**p-value**	**R^2**	**p-value**
N	0.172		0.494		0.108		0.083	
$N+N_0$	0.507	<0.001	0.645	<0.001	0.367	<0.001	0.318	<0.001
$N*N_0$	0.501	0.699	0.644	0.496	0.364	0.504	0.311	0.673

Table 3. Linear fit of the bidimensional ST model for each initial density.

	$logK_2$							**β_2**	**R^2**
	220	**370**	**500**	**570**	**700**	**800**	**1150**		
B1	22.32	23.36	24.00	24.22	24.56	24.88	25.30	-1.403	0.507
B2	14.74	15.44	15.87	16.00	16.19	16.35	16.76	-0.471	0.645
fm	15.00	15.10	15.13	15.15	15.16	15.18	15.21	-1.497	0.367
dm	15.26	15.40	15.44	15.45	15.47	15.49	15.53	-1.674	0.318

4.3.3. Tridimensional self-thinning model

Table 4.a shows the linear fits of the log-transformed B-N-L model (Eq. 3) for the combinations of biomass (B1 and B2) and number of layers (L_p and L_{im}) measurements. Good fits of the model were obtained in all cases (R^2>0.9). The respective F-tests ($p < 2x10^{-16}$) confirmed a significant improvement over the bidimensional model. Furthermore, monthly trend or differences by initial density were no longer observed in the residuals.

As the relationship $\lambda=1-\beta_3$ imposed in the B-N-L model was only fulfilled by B2 (see CIs in Table 4.a), probably due to the overestimation of the biomass with B1, the former measurement method was selected for biomass estimation. On the other hand, the estimated parameters of the model depended on the measurement method of the number of layers. These results show that the fit of the self-thinning model and, therefore, the discrimination of the limiting factor (space or food), are affected by the measurement method of biomass and number of layers used.

Table 4.b shows the fits of the log-transformed m-N-L relationship (Eq. 4) corresponding to individual fresh mass (fm) and individual dry mass (dm), respectively. In both cases a good fit was obtained (R^2>0.95) with the two measurements of the number of layers (L_p and L_{im}). The F-tests comparing the bidimensional and tridimensional models ($p < 2.2x10^{-16}$) indicated that the inclusion of the number of layers provides a significantly better fit. With regards to the model parameters, the same result as for the relationship B-N-L was found, that is, the estimated exponents depended on the method used to calculate individual mass and the number of layers. For both dry and fresh mass, the theoretical relationship between density (N) and number of layers (L_p, L_{im}), $\gamma_3=-\lambda$ was met. However, only the fm-N-L exponents were consistent with those obtained for B2-N-L (Table 4). This meets our expectations since B2 was estimated from the fresh mass of each sample. The difference observed between the estimated parameters for the two measurements of mean individual mass may be due to the lack of proportionality between fm and dm (fm=3.053+2.640dm). Therefore:

$$dm = K_m N^{\beta_m} \Rightarrow fm = K_f N^{\beta_f} = a + bK_d N^{\beta_d}$$

Consequently, when a≠0 as in our case, there is no functional relationship between the self-thinning parameters of both fits. Thus, comparing the empirical fm and dm exponents with the same theoretical exponent is not meaningful. In this work, we selected the individual fresh mass (fm) as the fitted parameters were consistent with that obtained for the B2-N-L models. In future studies we suggest that the proportionality between both mass measurements should be tested prior to fitting the ST model, since different empirical parameters can be obtained.

Table 4. Linear fit for the tridimensional model of the B-N-L relationships (4.a) for both measurements of biomass (B1, B2) and number of layers (parallelepiped projection: L_p and image analysis: L_{im}), and the m-N-L (4.b) for both measurements of individual mass (dm, fm) and number of layers, for all densities pooled. Estimated parameters, 95 % confidence intervals and adjusted R^2.

4.a	**B1-N-L_p**			**B1-N-L_{im}**			**B2-N-L_p**			**B2-N-L_{im}**		
	k_3	**β_3**	**λ**	**k_3**	**β_3**	**λ**	**k_3**	**β_3**	**λ**	**k_3**	**β_3**	**λ**
Coef	20.23	-1.287	2.041	17.92	-0.948	1.702	14.29	-0.524	1.486	12.60	-0.277	1.240
2.5%	19.63	-1.367	1.960	17.39	-1.017	1.634	13.68	-0.604	1.404	12.07	-0.346	1.171
97.5%	20.83	-1.207	2.123	18.44	-0.880	1.770	14.89	-0.443	1.569	13.13	-0.208	1.308
R^2	0.939			0.939			0.933			0.933		

4.b	**fm-N-L_p**			**fm-N-L_{im}**			**dm-N-L_p**			**dm-N-L_{im}**		
	k_3	**γ_3**	**λ**	**k_3**	**γ_3**	**λ**	**k_3**	**γ_3**	**λ**	**k_3**	**γ_3**	**λ**
Coef	15.11	-1.628	1.577	13.32	-1.366	1.315	16.03	-1.916	1.899	13.88	-1.600	1.583
2.5%	14.73	-1.678	1.526	12.99	-1.410	1.272	15.67	-1.964	1.849	13.56	-1.642	1.542
97.5%	15.48	-1.578	1.628	13.65	-1.323	1.357	16.39	-1.867	1.948	14.20	-1.559	1.624
R^2	0.955			0.955			0.970			0.970		

Previous studies restricted the ST analysis to the densities showing mortality. Therefore, in this work, the self-thinning fits for B2 and fm including all densities where compared with those restricted to densities undergoing mortality. No significant differences were observed between the respective estimated parameters (compare CIs in Table 5). Thus, in our case the inclusion of densities without mortality would not introduce bias in the estimation of the ST exponent, in contrast to previous statements (Mohler et al. 1978; Weller 1987a; Osawa and Sugita 1989; Lonsdale 1990; Osawa and Allen 1993).

Table 5. Linear fits for the tridimensional model of the B-N-L and m-N-L relationships for both measurements of number of layers (parallelepiped projection: L_p and image analysis: L_{im}). Top: including all densities. Bottom: only densities undergoing mortality (N_0 >500 ind/m).

220-1150	**B2-N-L_p**			**B2-N-L_{im}**			**fm-N-L_p**			**fm-N-L_{im}**		
	k_3	**β_3**	**λ**	**k_3**	**β_3**	**λ**	**k_3**	**γ_3**	**λ**	**k_3**	**γ_3**	**λ**
Coef	14.29	-0.524	1.486	12.60	-0.277	1.239	15.10	-1.628	1.577	13.316	-1.366	1.315
2.5%	13.68	-0.604	1.404	12.07	-0.346	1.171	14.73	-1.678	1.525	12.985	-1.409	1.272
97.5%	14.89	-0.443	1.569	13.13	-0.208	1.308	15.48	-1.578	1.628	13.645	-1.323	1.357
p	<0.001	<0.001	<0.001	<0.001	0.001	<0.001	<0.001	<0.001	<0.001	<0.001	<0.001	<0.001
R^2	0.933			0.933			0.955			0.955		

570-1150	**B2-N-L_p**			**B2-N-L_{im}**			**fm-N-L_p**			**fm-N-L_{im}**		
	k_3	**β_3**	**λ**	**k_3**	**β_3**	**λ**	**k_3**	**γ_3**	**λ**	**k_3**	**γ_3**	**λ**
Coef	13.96	-0.486	1.481	12.27	-0.240	1.235	15.33	-1.654	1.581	13.54	-1.391	1.318
2.5%	12.89	-0.629	1.327	11.17	-0.370	1.107	14.74	-1.727	1.502	12.97	-1.458	1.253
97.5%	15.12	-0.343	1.634	13.38	-0.110	1.363	15.93	-1.581	1.659	14.10	-1.325	1.384
p	<0.001	<0.001	<0.001	<0.001	0.0004	<0.001	<0.001	<0.001	<0.001	<0.001	<0.001	<0.001
R^2	0.777			0.777			0.954			0.954		

4.3.4. Estimation of the theoretical SST exponents

The theoretical SST exponents were estimated by RMA from the log-transformed mean population allometry of individual volume vs. individual area occupied ($V=kS^{\tau}$). In previous studies, where the volume was not measured (Guiñez & Castilla 1999, 2001; Guiñez et al. 2005), the allometry of individual mass vs. individual area occupied was

used, given that mass is assumed to be proportional to volume. In our study, individual volume was measured providing a more accurate estimation of the SST exponent.

The estimated value of the allometric exponent of V on S_p was 1.4868 with a 95% confidence interval (CI) [1.4703, 1.5035] (R^2= 0.9538). Thus, the estimated SST exponent was $\beta_{p,SST}$= -0.49 and was assumed to be equal to the classical theoretical SST exponent (β_{SST}= -0.50). The estimated allometric exponent of V on S_{im} was 1.225 with 95% CI [1.210, 1.241] (R^2= 0.943). Therefore, the estimated SST exponent was $\beta_{im,SST}$= -0.23, which is significantly higher than -0.5 and the theoretical FST exponent (β_{FST}=-0.33). Therefore, the two measurements of area occupied provided significantly different SST exponents. The fact that the most accurate estimation of mussel morphology (image analysis) provided an exponent significantly different to the theoretical one, and that the relationship FST > SST was inverted (SST_{im}=-0.23 > FST=-0.33 > -0.50), casts doubt on the applicability of these theoretical exponents in mussel populations. Moreover, the proximity between the theoretical exponents complicates the discrimination between space and food competition.

4.3.5. Model comparison

Once the convenience of applying the tridimensional self-thinning model was demonstrated, the different regression methods proposed in the "Data analysis" section were compared. On the basis of the results obtained, B2 and individual fresh mass (fm) were used as dependent variables. Furthermore, using the effective density (N_e) instead of density (N), the tridimensional m-N-L model reduces to a more intuitive bidimensional model (Eq. 6). Thus, we propose the use of the effective density in the self-thinning fit for biomass and mass (Eqs. 5-6) to allow comparison of both relationships.

No significant differences between the regression methods applied in this work were found in the estimated slopes of the B2-N_e-L relationships, for both the parallelepiped projection and image analysis (see CIs in Table 6.a and OLS fit in Fig. 4). In particular, the comparison between the restricted (Eq. 5) and unrestricted ($B=kN_e^{\beta}L^{\lambda}$) non-linear fits (p = 0.672 for L_p and p = 0.671 for L_{im}) shows that they are equivalent confirming the relationship between N_e and L imposed in the tridimensional self-thinning model.

The comparison between the estimated and the theoretical exponents for the relationship B2-N_p-L_p, indicates competition for space ($\beta_{SST,p}$ =-0.49, Table 6.a), except for the robust fit (RM) where a significantly steeper slope was obtained ($p < 0.01$). On the other hand, for B2-N_{im}-L_{im}, both space ($\beta_{SST,im}$ =-0.23) and food limitations (β_{SST} =-0.33) are accepted, again with the exception of RM which indicates competition for food (Table 6.a). These differences in the discrimination of the limiting factor between the robust fit and the other methods are due to the smaller residuals of the former. Since robust regression gives smaller weights to extreme values of biomass and density, which are those of most interest in the fit of the upper boundary ST line, the suitability of this method for ST studies is questionable.

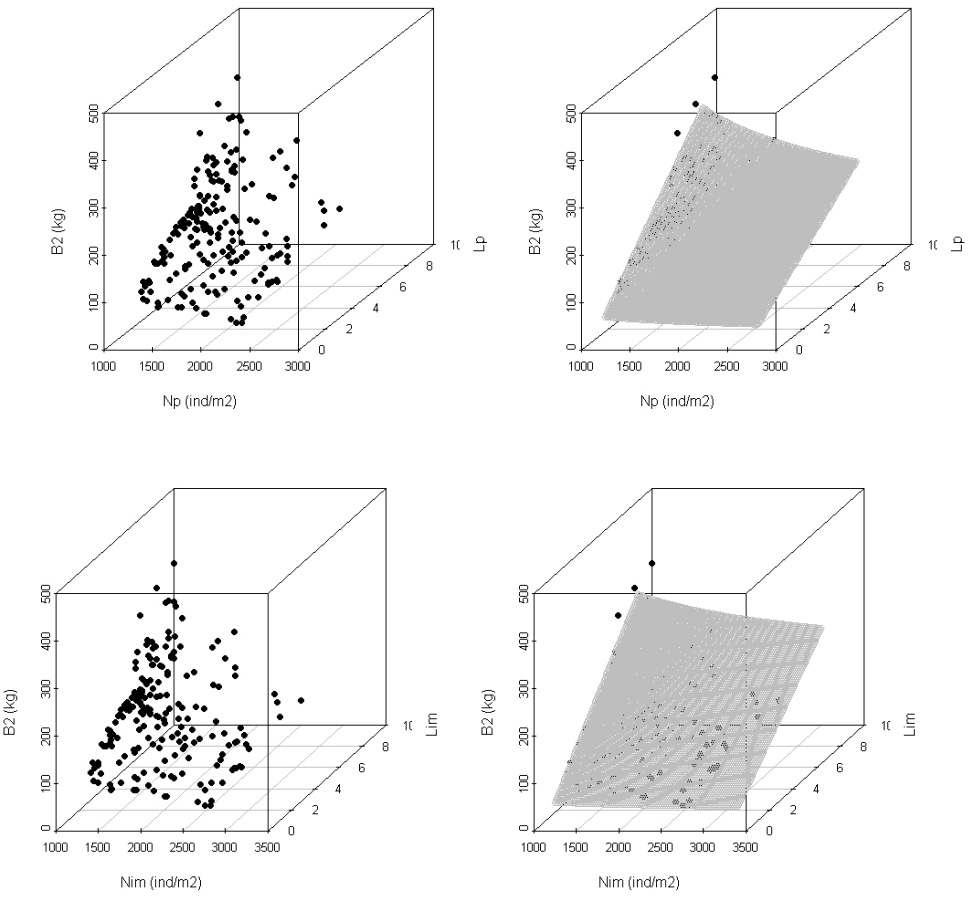

Fig. 4. Dispersion plot (left) and OLS fit (right) for the relationship B2-N_p-L_p (top) and B2-N_{im}-L_{im} (bottom).

The results obtained show that the estimated ST parameters (Table 6) depend on the measurement method of the surface area occupied, as observed by Filgueira et al. (2008). Furthermore, the proximity between the theoretical exponents obtained when image analysis (the more precise method) is used for SST estimation, exacerbates the difficulty in discriminating between food and space limitations found in previous studies (Alunno-Bruscia et al. 2000; Lachance-Bernard et al. 2010). On the other hand, our results would support the assumption of both limiting factors exerting a simultaneous effect on sessile animal populations, as suggested by Fréchette et al. (1992).

No significant differences in the estimated exponents of the fm-N_e relationship between the regression methods applied were found, for both occupied area measurements (Table 6.b). The estimated slope for the fm-N_p relationship was significantly lower than both theoretical exponents ($\gamma_{SST,p}$=-1.49 and γ_{FST}=-1.33), whereas the fm-N_{im} slope indicated FST. These results agree with those of Filgueira et al. (2008) with populations of the same specie. As pointed out above, the discrimination of the limiting factor depends on the measurement method of the occupied surface area. The fm-N_e fit leads to different conclusions to those obtained for the B2-N_e-L fit, demonstrating the lack of power of the current self-thinning models to discriminate the limiting factor. Finally, given that N_e=N/L, the fits with effective density were, as expected, equivalent to those using N and L, both for biomass (Eqs. 3-5; Table 4.a and 6.a) and individual mass (Eqs. 4-6; Table 4.b and 6.b).

Table 6. Tridimensional model fitted by the different regression methods proposed in this work. Estimated parameters and 95% confidence intervals for B2-N_e-L (6.a) and fm-N_e (6.b). T-test for comparison with the theoretical SST ($\beta_{SST,p}$= -0.49, $\beta_{SST,im}$= -0.23) and FST (β_{FST}= -0.33) exponents.

6.a	**B2-N_p-L_p**				**B2-N_{im}-L_{im}**			
	OLS	**RM**	**NLM1**	**NLM2**	**OLS**	**RM**	**NLM1**	**NLM2**
k_3	14.28	14.47	13.99	13.93	12.60	12.75	12.31	12.25
2.5%	13.68	14.20	13.15	13.14	12.07	12.51	11.58	11.58
97.5%	14.89	14.74	14.83	14.74	13.13	12.98	13.06	12.93
β_3	-0.523	-0.551	-0.486	-0.482	-0.277	-0.299	-0.241	-0.236
2.5%	-0.604	-0.587	-0.600	-0.594	-0.346	-0.330	-0.338	-0.329
97.5%	-0.443	-0.515	-0.375	-0.372	-0.208	-0.268	-0.146	-0.144
λ	0.963	0.973	0.985	1	0.963	0.972	0.985	1
2.5%	0.922	0.954	0.915		0.922	0.954	0.915	
97.5%	1.003	0.991	1.057		1.003	0.991	1.056	
p (SST)	0.285	0.0015	0.398	0.395	0.161	<0.001	0.389	0.396
p (FST)	<0.001	<0.001	0.01	0.011	0.126	0.056	0.077	0.053

Note: OLS (ordinary least squares), RM (robust linear model), NLM1 (unrestricted non-linear model), NLM2 (non-linear model with λ=1)

6.b	**fm-N_p**				**fm-N_{im}**			
	OLS	**RM**	**RMA**	**NLM**	**OLS**	**RM**	**RMA**	**NLM**
k_3	14.87	14.79	15.16	14.67	13.05	12.98	13.30	12.87
2.5%	14.49	14.47	14.79	14.19	12.73	12.71	12.98	12.46
97.5%	15.24	15.11	15.53	15.15	13.36	13.26	13.61	13.27
γ_3	-1.605	-1.595	-1.645	-1.578	-1.339	-1.331	-1.373	-1.314
2.5%	-1.656	-1.639	-1.595	-1.645	-1.382	-1.368	-1.331	-1.370
97.5%	-1.554	-1.551	-1.697	-1.511	-1.297	-1.294	-1.416	-1.258
p (SST)	<0.001	<0.001	<0.001	0.015	<0.001	<0.001	<0.001	0.005
p (FST)	<0.001	<0.001	<0.001	<0.001	0.363	0.399	0.046	0.341

Note: OLS (ordinary least squares), RM (robust linear model), RMA (reduced major axis), NLM (non linear model)

4.3.6. Stochastic frontier function (SFF).

The previous fits describe the central tendency of the relationship biomass/mass – density. Yet, the main goal of self-thinning analysis is to fit the upper limit of this relationship, that is, the upper boundary line. Therefore, in this work the stochastic frontier function (SFF) was fitted as proposed by Bi et al. (2000), Bi (2004) and Zang et al. (2005).

In the B2-N_e-L relationship, there were no differences between the SFF and the OLS fit (H_0: γ=0, p-value=1), implying full site occupancy. For the fm-N_e relationship, the previous tests to the SFF fit indicated that (i) full site occupancy was not reached ($p < 0.01$), i.e. SFF and OLS fits are significantly different (ii) the technical inefficiency effect or site occupancy varied over time ($p < 0.01$), and (iii) U had a half-normal distribution for fm-N_p ($p = 0.146$) and a truncated normal distribution for fm-N_{im} ($p = 0.047$). The maximum-likelihood estimate of the ST slope indicated space limitation for fm-N_p (γ_p = -1.483, $p = 0.3942$), whereas for fm-N_{im} both space (γ_p = -1.171, $p = 0.3636$) and food limitations ($p = 0.2041$) can be accepted. Thus, the difference between the SFF and the methods of central tendency in the fm-N_e relationship leads to different conclusions with regards to the limiting factor. However, the SFF for fm-N_e and B2-N_e-L provide the same conclusions, showing the robustness of this method in the discrimination of the limiting factor.

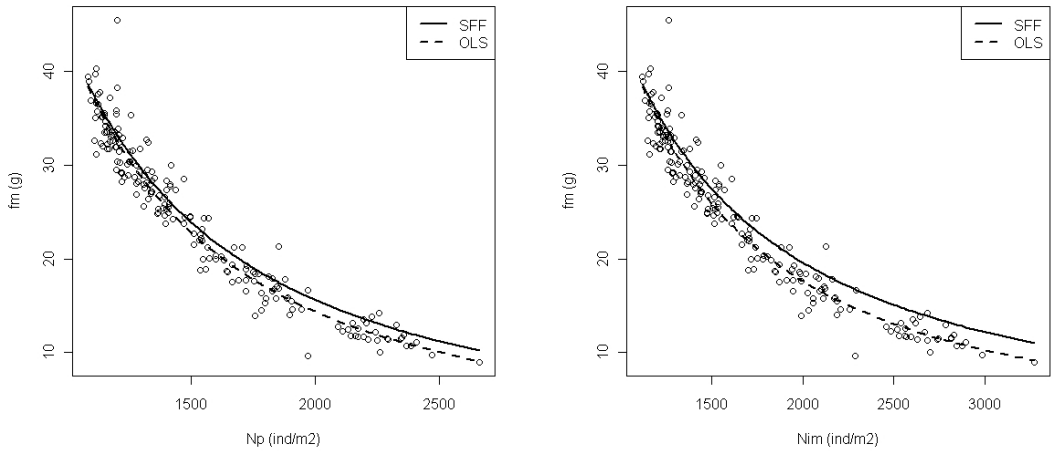

Fig. 5. Comparison between SFF and OLS fits for the relationship individual fresh mass-effective density. a) fm-N_p (SFF: $fm=14.018N_p^{-1.483}$, OLS: $fm=14.867N_p^{-1.605}$) and b) fm-N_{im} (SFF: $fm=11.873N_{im}^{-1.171}$, OLS: $fm=13.049N_p^{-1.339}$).

Table 7. Temporal evolution of site occupancy for the relationship fresh mass vs effective density (fm-N_e) for both measures of number of layers, parallelepiped projection (L_p) and image analysis (L_{im}).

Site occupancy	May	June	July	August	September	October	November
fm-N_p	0.9090	0.9326	0.9503	0.9635	0.9732	0.9804	0.9857
fm-N_{im}	0.8498	0.8917	0.9225	0.9449	0.9610	0.9724	0.9806

On the other hand, for the fm-N_e relationship, site occupancy increased with time for both measurements of N_e (η_p=0.3185 and η_{im}=0.3549) as confirmed by the monthly site occupancy levels (Table 7). The distance between the OLS and SFF lines increased with N_e (Fig. 5). Since N_e decreased with time, larger differences were observed in the first months where the site occupancy was lower. Consequently, (i) site occupancy increased progressively as individuals grew, and (ii) at the end of the experiment the system almost reached full site occupancy, in agreement with the results obtained for the B2-N_e-L relationship. These results highlight the suitability of the stochastic frontier approach in the analysis of ST dynamics in sessile animal populations, since it provides insight into the temporal evolution of site occupancy.

4.4. Conclusions

In this study, we analyzed the goodness of fit and consistency of current bidimensional and tridimensional self-thinning models by their application to mussel populations grown in suspended culture. We observed that for multilayered populations, crowding is reflected by the degree of packing measured as number of layers (L), whereas the density within layers (N_e) remained homogeneous over the density gradient. Furthermore, in contrast to previous studies (Alvarado & Castilla 1996; Hosomi 1985; Hughes & Griffiths 1988) a reduction in the number of layers due to intra-specific competition was not observed, although at the end of the study the formation of new layers had ceased.

The lack of fit of the bidimensional self-thinning model, demonstrated by the low proportion of variance explained by the model and the dependence between the residuals and the number of layers, confirmed that the tridimensional model proposed by Guiñez & Castilla (1999) should be applied in the analysis of multilayered populations.

This study improves the estimation of the theoretical SST exponent by using the mean population allometric relationship volume-area occupied, instead of using mass as an estimator of volume. Different theoretical SST exponents were obtained depending on the measurement method used to calculate the surface area occupied. Using the parallelepiped projection, the estimated exponent was equal to the classical SST exponent (-0.50), whereas with image analysis techniques the relationship $\beta_{FST}>\beta_{SST}$ was inverted ($\beta_{im,SST}$ =-0.23 > β_{FST} =-0.33 > -0.50). This casts doubt on the applicability of the classical theoretical exponents in mussel populations. Furthermore, the proximity between the SST and FST exponents, exacerbated in the more precise method (image analysis), can hinder the discrimination between both limiting factors.

In the application of the tridimensional model, significantly different fits were obtained depending on the measurement methods of the variables involved in the model. Firstly, the estimation of total biomass by weighing the rope in water (B1) should be discarded. Despite being a faster measure method, B1 does not fulfill the relationship between N and L established in the ST model. Secondly, the lack of proportionality between fresh and dry mass leads to differences between the estimated exponents and to different conclusions in the discrimination of the limiting factor. This suggests the need of assessing whether the current theoretical SST and FST exponents are valid for both measurements of individual mass, or if specific theoretical exponents should be defined for each measurement. Furthermore, significant differences between the estimated ST parameters were obtained depending on the measurement method of surface area occupied used, as previously observed in the estimation of the theoretical SST exponent. Finally, the inclusion of populations that do not exhibit density dependent mortality in the model fit did not introduce bias in the estimation of the ST exponent, in contrast to indications from previous studies (Lonsdale 1990; Mohler et al. 1978; Osawa & Sugita 1989; Osawa & Allen 1993 Weller 1987a).

In this study, the substitution of density (N) by effective density (N_e) provided equivalent fits and a simpler interpretation of the ST process. Furthermore, significant differences in the estimated parameters between the central tendency regression methods applied (OLS, RMA, RM, NLM) were not found, although the robust fit led to different conclusions with respect to the limiting factor. However, because the RM reduces the weight of the extreme values, its applicability in the ST study is limited. Furthermore, the competition limiting factor depends on the response variable (mass or biomass) and the measurement method of the surface area occupied (parallelepiped projection or image analysis). For individual mass, the slope estimated with the parallelepiped projection was significantly steeper than the theoretical ones, whereas the estimated slope with the most precise measurement (image analysis) agrees with FST. For biomass, under the parallelepiped projection the estimated slope indicated SST, whereas image analysis confirmed the difficulty in the discrimination of the limiting factor due to the closeness between the SST and FST theoretical exponents. On the other hand, these results may also suggest the interaction between competition for space and food, as indicated by Fréchette et al. (1992).

Traditionally, the self-thinning relationship has been fitted from data collected in successive samplings over time, such that the variables of interest present a temporal autocorrelation. This dependence has not been considered in current models and can cause bias in the estimation of the ST parameters. The alternative procedure of analyzing data obtained at a single sampling time (Alunno-Bruscia et al. 2000; Alunno-Bruscia et al. 2001) has the drawback of not allowing a proper dynamic interpretation of the self-thinning process. Therefore, we suggest that the temporal effect should be included in the ST models in future studies.

In this study, we applied frontier analysis methods (SFF) that allow (i) obtaining the upper boundary ST line without subjective data selection, (ii) studying the site occupancy, and (iii) a dynamic interpretation of the ST process through the analysis of temporal variability of site occupancy. For the B-N_e-L relationship there were no significant differences between SFF and central tendency fits, and full site occupancy could be assumed. In the relationship m-N_e, despite different frontier and central tendency fits were obtained, the mean site occupancy was higher than 90% and full occupancy was steadily approached. Finally, the SFF approach led to the same

conclusions in the discrimination of the limiting factor for both B-N_e-L and m-N_e relationships, highlighting the suitability of the SFF approach in the analysis of ST.

To summarize, significant differences were observed in the estimated ST parameters depending on the relationship studied (biomass or individual mass) and on the measurement methods of the variables involved in the model (biomass, individual mass and surface area occupied). This lack of robustness in ST analysis affects the discrimination between the competition limiting factors (space/food) and consequently the ecological interpretation of population dynamics. Therefore, we consider that both the current model and the discrimination criterion need to be revised.

4.5. APPENDIX

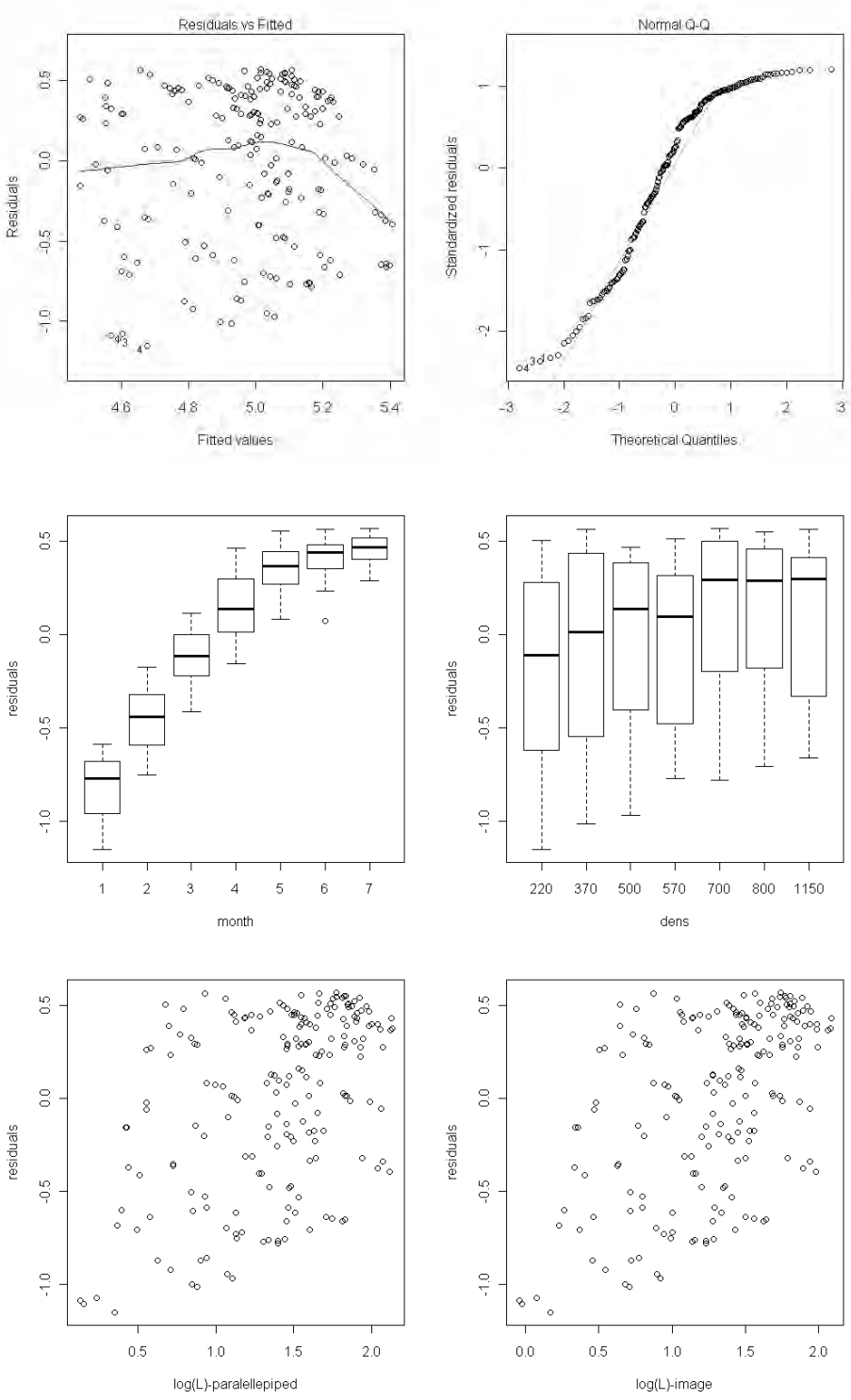

Fig. A1. Diagnostic plots of the linear fit of the relationship B1-N. Top: fitted values vs. residuals (left) and residuals QQ-plot. Center: residuals vs. month (1-7: months from May to November) and residuals vs. initial density. Bottom: residuals vs. number of layers.

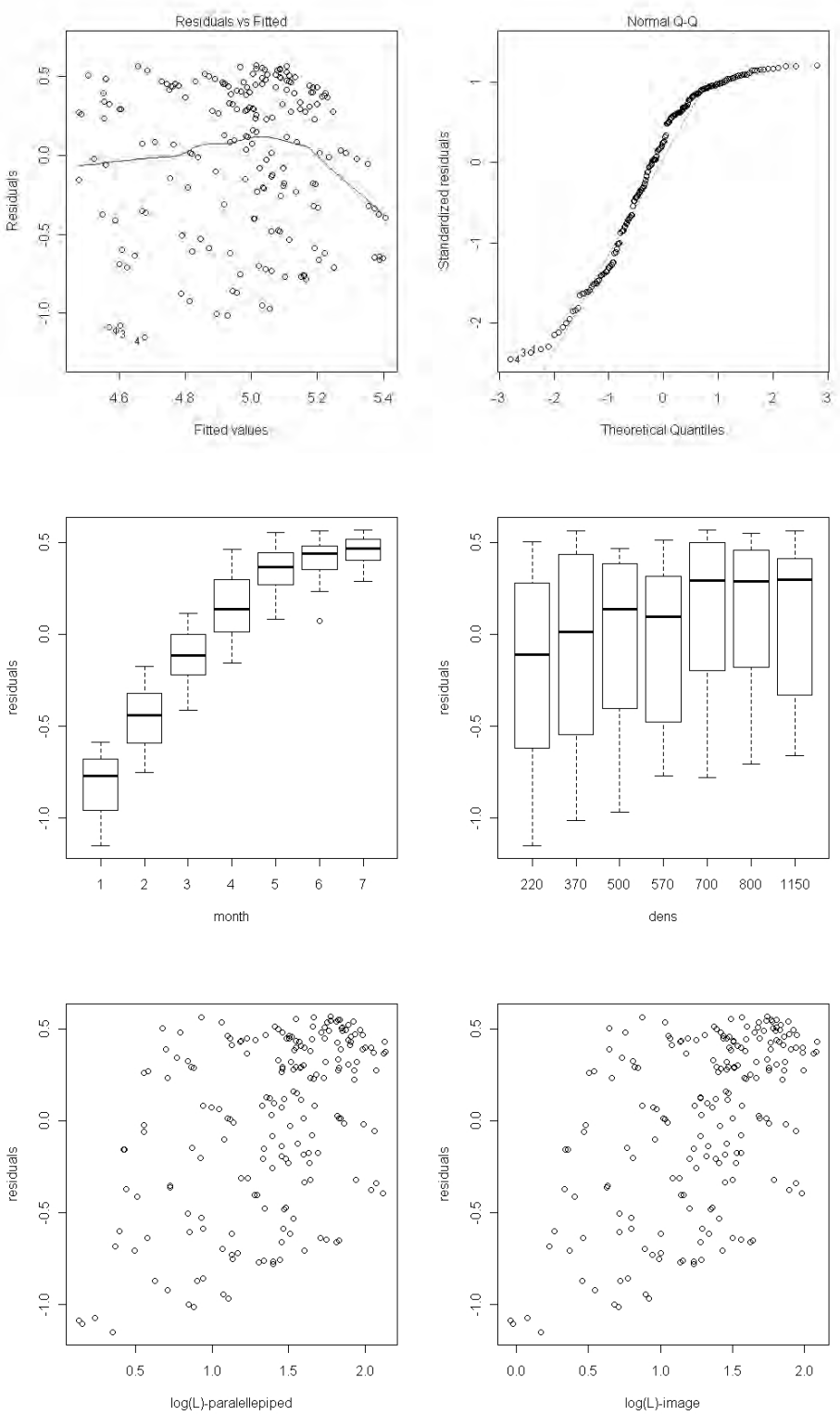

Fig. A2. Diagnostic plots of the linear fit of the relationship B2-N. Top: fitted values vs. residuals (left) and residuals QQ-plot. Center: residuals vs. month (1-7: months from May to November) and residuals vs. initial density. Bottom: residuals vs. number of layers.

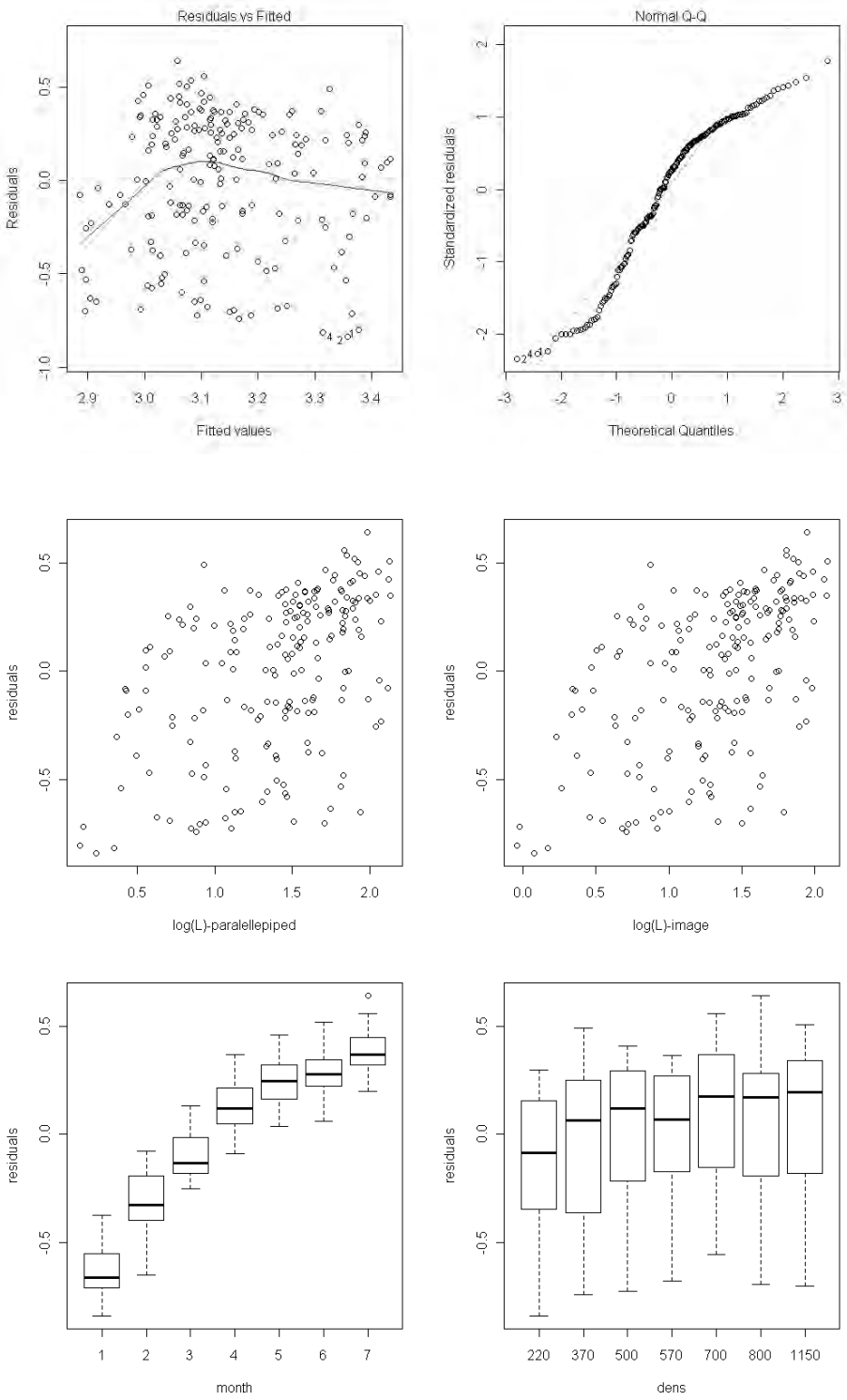

Fig. A3. Diagnostic plots of the linear fit of the relationship fm-N. Top: fitted values vs. residuals (left) and residuals QQ-plot. Center: residuals vs. month (1-7: months from May to November) and residuals vs. initial density. Bottom: residuals vs. number of layers.

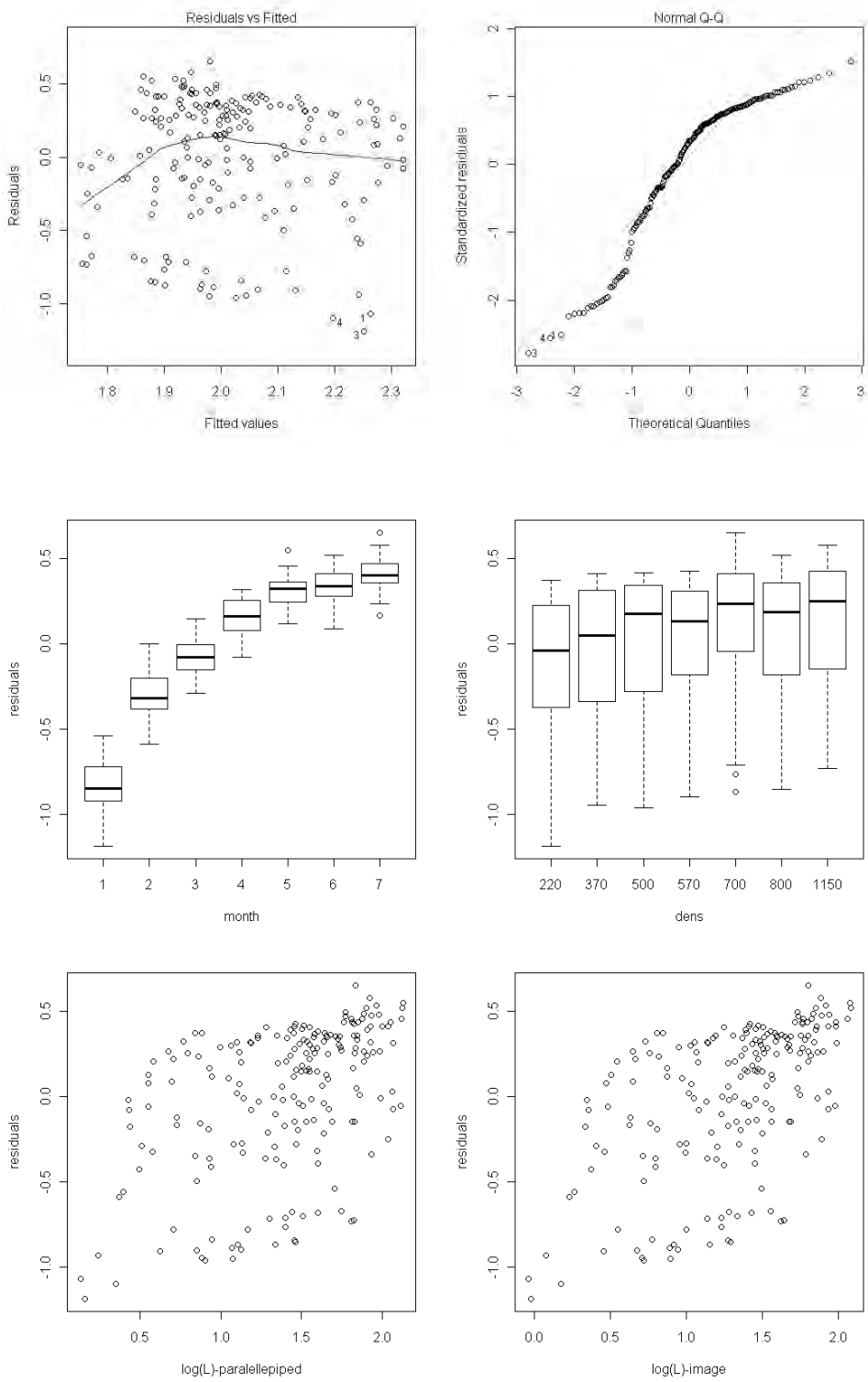

Fig. A4. Diagnostic plots of the linear fit of the relationship dm-N. Top: fitted values vs. residuals (left) and residuals QQ-plot. Center: residuals vs. month (1-7: months from May to November) and residuals vs. initial density. Bottom: residuals vs. number of layers.

Capítulo 5. Dynamic self-thinning model for sessile animal populations with multilayered distribution

Modelo dinámico de auto-raleo para poblaciones animales sésiles con distribución en múltiples capas

Summary

1. The main drawback of the traditional self-thinning model is how time is handled. Self-thinning (ST) has been formally recognized as a dynamic process, while the current ST models have not included the temporal effect. This restricts the analysis to the average competitive behavior of the population and produces a biased estimation of the self-thinning parameters.

2. In this study we extend the dynamic ST model introduced by Roderick & Barnes (2004) to the analysis of multilayered sessile animal populations. For this purpose, we incorporate the number of layers and the density per layer into the dynamical approach. This model is a generalization of the traditional ST model, which does not depend on predefined assumptions about the population.

3. In this study, the performance of the dynamic model was checked and compared with the classical ST model through the analysis of mussel populations grown at different density treatments. In addition, we provided insight into the ecological interpretation of the trajectory of the ST exponent.

4. The dynamic ST model allows studying the effect of population density on the competitive behavior of individuals and the temporal evolution of intraspecific competition, providing a more realistic description of population dynamics than the traditional model.

5.1. Introduction

The self-thinning process (ST) describes the inverse relationship between body size of individuals and population density when growth results in mortality through intraspecific competition (Westoby 1984). This mechanism, observed in plants and animals at high population densities, plays an important role in determining population dynamics and community structure (Fréchette & Lefaivre 1995; Fréchette et al. 1996; Guiñez & Castilla 1999, 2001; Guiñez et al. 2005; Marquet et al. 1995; Petraitis 1995; Puntieri 1993; Weller 1987; Westoby 1984).

Self-thinning can be analyzed by sequential sampling of even-aged populations growing at different densities (Fig. 1 in Alunno-Bruscia et al. 2000). This allows plotting biomass-density (B-N) or alternatively, individual mass-density (m-N) trajectories through time. Traditionally, ST has been represented by the allometric relationship $m=kN^{\beta}$ (Westoby 1984; White 1981; Yoda et al. 1963).

ST has been extensively studied in plant populations (Fréchette & Lefaivre 1995), where this process is attributed to competition for space (spatial self-thinning, SST) and the classic exponent $\beta_{SST}=-3/2$ was proposed (Westoby 1984). Begon et al. (1986) stated that in mobile animal populations the ST process would be regulated by food limitations (food self-thinning, FST) and suggested the exponent $\beta_{FST}=-4/3$.

Sessile bivalves are gregarious animals that form multiple layers over the substrate (Alvarado & Castilla 1996; Guiñez 1996; Guiñez & Castilla 1999, 2001; Hosomi 1985; Suchanek 1986). This multilayered disposition increases the surface area available to the organisms, which in turn would change the ST relationship (Fréchette & Lefaivre 1990; Guiñez & Castilla 1999; Hughes & Griffiths 1988). For this reason, Guiñez & Castilla (1999) proposed a tridimensional self thinning model (m-N-L) that incorporates the degree of packing (number of layers) to the bidimensional model:

$$\bar{m} = K\left(n/SL\right)^{\beta} = K\left(N/L\right)^{\beta} = KN_e^{\beta} \qquad (1)$$

where $\bar{m}$ is mean individual mass, n is number of individuals, S is total surface area occupied, N is density, L is number of layers, $N_e=N/L$ is the density per layer or effective density and (K, β) are the model parameters. The usual procedure in self-

thinning studies is to estimate (K, β) from sequential measurements of individual mass and density.

The main drawback of the traditional self-thinning model (Eq. 1) is how time is handled. While time is present implicitly due to (K, β) are estimated from sequential samplings, the time effect is not explicitly included in the model. This gives rise to two potential sources of error in the estimation of the ST parameters. First, β and K are assumed to be constant across the entire study period, while the self-thinning is a dynamic process and the ST exponent (β) would vary over time (Norberg 1988[a]; Westoby 1984; White 1981). Therefore, we would be estimating a mean value when we should be estimating a temporal trend. Secondly, the regression methods currently used for its study (reviewed by Zhang et al. 2005) assume that observations are independent, overlooking the temporal autocorrelation of the variables involved in the model and resulting in a biased estimation of the self-thinning parameters.

Thus, while self-thinning has been formally recognized as a dynamic process, the current analysis procedures have not been dynamic, failing to include the time effect. Roderick & Barnes (2004) highlighted this drawback and proposed a new formulation of self-thinning as a dynamic problem. The main assumption for this approach is that β can vary over time, but converges to -1 when total biomass is constant, given that:

$$\bar{m} = \frac{\sum m}{n} = \frac{\sum m}{SL}\frac{SL}{n} = \frac{\sum m}{SL}\left(\frac{n}{SL}\right)^{-1} = \frac{\sum m}{SL}N_e^{-1} = KN_e^{-1}$$

The main goal of this study was to extend the dynamic self-thinning model proposed by Roderick & Barnes (2004) for plant populations to the study of sessile animal populations with multilayered distribution. For this purpose, the number of layers (L) and effective density (N_e) were incorporated to the original model. Then, we tried to give insight into the dynamic interpretation for the different values of the ST exponent. Finally, the performance of the dynamic model was checked and compared with the classical ST model through the analysis of mussel (*Mytilus galloprovincialis* Lmk.) populations grown in suspended culture.

5.2. Materials and methods

5.2.1. Dynamic self-thinning model

We extended the dynamic model proposed by Roderick & Barnes (2004) for the analysis of self-thinning in plants to the study of multilayered sessile animal populations. For this purpose, we substituted the density or number of individuals per unit area (N) by the effective density or number of individuals per layer (N_e) defined in the tridimensional self-thinning model (Guiñez & Castilla 1999).

Assuming that the allometric relationship expressed in Eq. 1 is an identity, the unknown parameters (K, β) are uniquely determined by the effective density and mean individual mass observed in two instants of time. If $(\overline{m}_1, N_{e1})$ and $(\overline{m}_2, N_{e2})$ are the values observed at successive instants of time t_1 and t_2, substituting these values in the logarithmic transformation of Eq. 1 yields:

$$\begin{aligned} \ln \overline{m}_1 &= \log K + \beta \ln N_{e1} \\ \ln \overline{m}_2 &= \log K + \beta \ln N_{e2} \end{aligned} \tag{2}$$

The solution of Eq. 2 by elimination leads to:

$$\beta = \ln\left(\overline{m}_2 / \overline{m}_1\right) \Big/ \ln\left(N_{e2} / N_{e1}\right) \tag{3}$$

and

$$\ln K = \ln \overline{m}_1 - \beta \ln N_{e1} \tag{4}$$

Thus, the estimated values of K and β correspond to the same time interval as the measurements used to estimate them. This procedure was repeated for each pair of consecutive samplings to estimate the parameters corresponding to each time interval.

The procedure above would be used when observations are made for a finite number of points in time. However, from a theoretical viewpoint it is useful to extend the analysis to infinitesimal time intervals which allows an analytical treatment of self-thinning. For this purpose, we should note that:

$$\begin{aligned} \bar{m}_2 &= \bar{m}_1 + \delta\bar{m} \\ N_{e2} &= N_{e1} + \delta N_e \end{aligned} \tag{5}$$

where δ denotes a finite difference. Using Eq. 5, we can rewrite Eq. 3 as:

$$\beta = \ln\left(1+\delta\bar{m}/\bar{m}_1\right) \Big/ \ln\left(1+\delta N_e/N_{e1}\right) \tag{6}$$

For infinitesimal time increments, $\delta\bar{m} \to d\bar{m}$ and $\delta N_e \to dN_e$, as ln(1+x) → x for small values of x:

$$\beta = \frac{dm}{m}\frac{N_e}{dN_e} \tag{7}$$

Eq. 7 defines the self-thinning exponent (β) as the quotient between the rates of change of individual mean mass and density, which is very useful in interpreting the dynamic model.

In order to link the dynamic model with the self-thinning process we should note that, for a set of n individuals in a given area at time t, the total biomass of the area is:

$$B = m_1 + \ldots + m_n = n\bar{m} \tag{8}$$

Thus if N_e is the effective density, that is, the number of individuals per unit of area in each layer, the biomass per layer is:

$$B_L = \frac{n\bar{m}}{SL} = N_e\bar{m} \tag{9}$$

The biomass rate of change is then:

$$\frac{dB_L}{dt} = \bar{m}\frac{dN_e}{dt} + N_e\frac{d\bar{m}}{dt} \tag{10}$$

and when the biomass remains constant, $dB_L/dt = 0$, we have:

$$\bar{m}\frac{dN_e}{dt} = -N_e\frac{d\bar{m}}{dt} \tag{11}$$

Thus, since $\bar{m}$ and N_e are always positive, dN_e and $d\bar{m}$ must be of opposite signs, that is, an increase in mass implies a decrease in density, which can be due to mortality as well as reorganization of the individuals into new layers (migration), and viceversa.

Table 1. Ecological interpretation of self-thinning exponents (β).

Biomass		**Effective density**	**β**	**Interpretation**
$dB_L/dt=0$	$\frac{dN_e}{N_e} = -\frac{d\bar{m}}{\bar{m}}$		β = -1	Total biomass remains constant.
$dB_L/dt>0$	$\frac{dN_e}{N_e} > -\frac{d\bar{m}}{\bar{m}}$	$dN_e/dt < 0$	β < -1	dm/dt > 0, growth rate is greater than mortality-migration rate.
		$dN_e/dt > 0$	β > -1	If dm/dt < 0, individual mass loss is lower than density increase (-1< β < 0). If dm/dt > 0, both density and mass increase, no competition is observed (β > 0).
		$dN_e/dt = 0$	$\beta \to +\infty$	dm/dt > 0
$dB_L/dt<0$	$\frac{dN_e}{N_e} < -\frac{d\bar{m}}{\bar{m}}$	$dN_e/dt < 0$	β > -1	If dm/dt > 0, growth rate is lower than mortality/migration rate (-1< β < 0). If dm/dt < 0, both density and mass decrease (β > 0).
		$dN_e/dt > 0$	β < -1	dm/dt < 0, i.e. individual mass loss is greater than the rate of density increase.
		$dN_e/dt = 0$	$\beta \to -\infty$	dm/dt < 0

Comparing Eq. 7 and 10, we see that β is the ratio of the terms on the right side of Eq. 10. Thus, when biomass remains constant: β ≈ -1 (Eq. 11). This can reflect two situations: (i) dN_e/dt and dm/dt are bounded away from 0, and the rates of change of individual mass and effective density are equivalent, or (ii) $dN_e/dt \approx 0$ and dm/dt ≈ 0,

thus competition ameliorates and the system is stabilized. Generalizing, when $dN_e/dt < 0$, such as with mortality and/or migration, then $\beta < -1$ (e.g. -3/2, -4/3) if $dB_L/dt > 0$, that is, the growth rate is greater than the mortality rate; and $\beta > -1$ if $dB_L/dt < 0$, that is, the growth rate is lower than the mortality rate. The opposite holds for $dN_e/dt > 0$. When the effective density remains constant, $dN_e/dt = 0$, β tend to (either positive or negative) infinity (see Table 1).

5.2.2. Experimental design

We tested the validity of the dynamic self-thinning model through its application to the study of the mussel *Mytilus galloprovincialis* grown in suspended culture. This study analyzed seven density treatments (220, 370, 500, 570, 750, 800 and 1150 individuals per meter of rope) in the period from thinning-out to harvest (April-November 2008), following protocols and cultivation techniques used in the Galician Rías. In late April, for each density treatment, 28 ropes containing even-aged mussels were randomly distributed within the same raft in the Ría de Ares-Betanzos (NW of Spain). Monthly samples were taken until harvest (7 samplings, from late May to late November). In each sampling, a section of known length was taken from 4 ropes of each density treatment (28 ropes per sampling date). Each sample was cleaned of epibionts and weighed to obtain the population biomass (B; g). The mussels were counted to calculate the density as number of mussels per meter of rope (N_0; ind/m), which was standardized to the number of individuals per square meter of rope (N; ind/m^2). The individual fresh mass ($\bar{m}$; g) was obtained from sub-samples of 250-300 individuals, dividing the total mass by the number of individuals. Multilayered packing alters the surface area available to the individuals and, thus, could modify the ST exponent (Fréchette & Lefaivre 1990; Hosomi 1985; Hughes & Griffiths 1988). To account for this effect, the effective surface area occupied (S_e), that is, the surface the individuals would occupy if they were arranged in a single layer (Guiñez et al. 2005), is required. The effective surface area (S_e) was obtained by image analysis techniques (Filgueira et al. 2008) assuming that the maximum anterio-posterior axis of mussels is disposed perpendicular to the substrate. The effective density or number of individuals per layer ($N_e = N_0/S_e$) and the number of layers ($L=N/N_e$) of each sample were calculated according to Guiñez & Castilla (2001).

5.2.3. Statistical analysis

In this work, the dynamical approach proposed for multilayered populations was compared against the traditional tridimensional ST model. Firstly, for each density treatment, the traditional ST model (Eq. 1) was fitted using different regression methods (reviewed in Chapter 4). We tested the dependence of the estimated exponents on the density treatment to check whether the traditional model is able to detect different competition patterns. The estimated exponents were also compared with the theoretical food self thinning (FST) exponent (β_{FST}=-1.33) and the space self-thinning (SST) exponent obtained by image analysis techniques (β_{SST}=-1.23; Chapter 4), to discriminate the competition limiting factor.

In order to fit the dynamic model, for each time and density treatment, M=1000 replicates of effective density (N_e) and mean individual mass ($\bar{m}$) were obtained by Monte Carlo simulations. Then, the self-thinning exponent and its 95% confidence interval were estimated for each sampling interval (Eq. 7). Finally, Tukey tests were applied to determine whether β = -1, that is, whether the biomass remained constant between samplings. The statistical analysis was performed with the help of the statistical package R 2.12.2 (R Development Core Team, 2011).

5.3. Results

Fig. 1 shows the temporal evolution of density (N), effective density (N_e), biomass (B), biomass per layer (B_L), number of layers (L) and mean individual fresh mass ($\bar{m}$) for each density treatment (see tables in Appendix). We observe a trade-off between the exponential decrease in effective density and the increase in individual fresh mass, for all treatments. The density (N) plot shows that mortality occurred only in the higher initial densities (> 500 ind/m). Thus, for low-density populations the decrease in N_e would respond only to reorganization of individuals into new layers (migration), while for higher densities this would also include mortality. Mass, biomass, and biomass per layer increased in the first months and remained constant, or even decreased at higher densities in the last three months. Finally, for all densities an increase in the number of layers throughout the experimental period was observed. This increase was steadily at lower densities, while at higher densities the reorganization of growing individuals

caused a continuous readjustment between the number of layers and the effective density. Finally, in Fig.1 we observed that the density, number of layers, and biomass depended on the density treatment, while mean individual mass, effective density and biomass per layer were homogeneous over the density gradient. This implies that in multilayered populations crowding is reflected by the degree of packing measured as the number of layers (L).

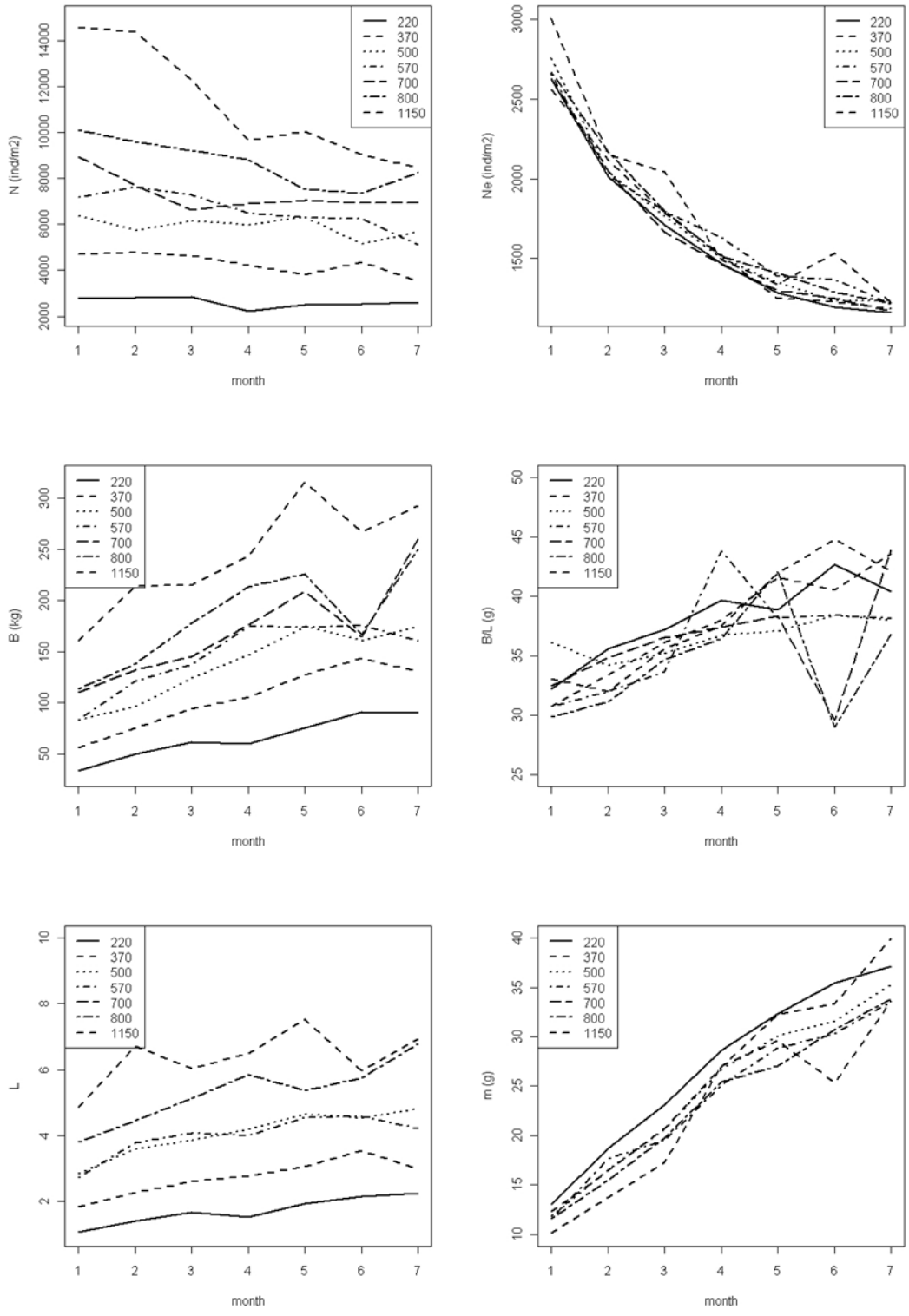

Fig. 1. Temporal evolution of density (N), effective density (N_e), biomass (B), biomass per layer (B_L), number of layers (L) and mean individual mass ($\overline{m}$) for each density treatment.

Table 2 shows the fits for the classical tridimensional self-thinning model (Eq. 1) for each density treatment. Since significant differences between the different regression methods applied in this study were not observed, only the results from linear regression (ordinary least squares, OLS) are shown. We obtained a good fit for m-N_e relationships ($R^2 > 0.94$). No significant effect of density treatment on the estimated exponents was observed (see CIs in Table 2). Likewise, comparison of the estimated exponents with the theoretical space (β_{SST}=-1.23) and food (β_{FST}=-1.33) ST exponents, did not allow discriminating the competition limiting factor for 220, 500, 700 and 800 ind/m density treatments, while concluded competition for food in mussels at 370, 570 and 1150 ind/m (see CIs for β in Table 2).

Table 2. OLS fit for the tridimensional model ($\bar{m} = KN_e^{\beta}$), estimated parameters and 95% confidence intervals for each density treatment.

Ind/m	K	CI	β	CI	R^2
220	12.402	[11.539, 13.265]	-1.2461	[-1.363, -1.129]	0.9464
370	13.488	[12.639, 14.336]	-1.3970	[-1.512, -1.282]	0.9585
500	12.640	[11.878, 13.401]	-1.2844	[-1.387, -1.182]	0.9606
570	13.300	[12.558, 14.043]	-1.3730	[-1.473, -1.273]	0.9672
700	12.684	[11.876, 13.491]	-1.2895	[-1.399, -1.180]	0.9558
800	13.011	[12.137, 13.886]	-1.3381	[-1.456, -1.220]	0.9527
1150	13.433	[12.413, 14.454]	-1.3944	[-1.531, -1.258]	0.9421

Table 3 shows the estimated self-thinning exponents obtained with the dynamic model, and Figs. 2-8 show the plots of the traditional and dynamic fits for each density treatment. The high variability observed for β in certain months was due to the lack of changes in effective density ($dN_e/dt \approx 0$).

During the first three months, mussels grown at lower initial density (220, 370 and 500 ind/m) presented higher growth rates than migration rates, giving rise to a progressive increase in biomass per layer and to a ST exponent lower than -1 (Figs. 2-4). As $dL/dt \geq 0$, population biomass also increased. In the next three months, both rates were fairly equivalent and β was ≈ -1. From September onwards the growth and migration rates tended to 0.

Mussels grown at 570 ind/m (Fig. 5) showed a different behavior. In June, $\beta < -1$, the growth rate was higher than the decrease in effective density, which from this treatment is attributable to both mortality and reorganization into new layers (migration) (Fig. 1). In July, the rate of growth and decrease in effective density were similar and, as $dL/dt \approx 0$, population biomass remained constant, obtaining a ST exponent close to -1. In August, the growth rate rose, probably as a result of the lower growth in July, giving rise to an increase in biomass and $\beta << -1$. From August onwards β was equal to -1. However, whereas in September and November both growth and density decrease rates were similar and bounded away from 0, in October both rates were close to 0.

The 700 and 800 ind/m density treatments (Figs. 6 and 7) showed a similar behavior. During the first months (up to September and August, respectively) the growth rate was higher than the decrease in effective density, leading to a progressive increase in both biomass per layer and population biomass ($\beta < -1$). Afterwards, both rates tended to 0 and $\beta = -1$, with the exception of November for 700 ind/m, where the growth rate was higher than 0 and $\beta < -1$.

Mussels grown at 1150 ind/m (Fig. 8) followed a different pattern than the previous density treatments. In June, the mortality-migration rate was higher than the growth rate ($\beta > -1$) indicating stronger intraspecific competition than at lower densities. This trend was reversed in the next two months and lead to self-thinning exponents lower than -1, being particularly low in July due to $dN_e/dt \rightarrow 0$. In September, the growth and N_e decrease rates were equivalent ($\beta = -1$) and the biomass per layer remained constant. The sign of dN_e/dt changed between the September-October and October-November samplings, leading to discontinuities in the ST trajectory. In October $\beta < -1$, but in this case the effective density grew due to a reduction in the number of layers (Fig. 1), being this density increase lower than the loss of individual mass. In the last month, $dN_e/dt < 0$ again and the rate of growth was higher than the decrease in effective density, leading to $\beta < -1$. In contrast to what occurred in the other density treatments, the point at which effective density stabilizes was never reached for 1150 ind/m treatment, and the system kept regulating itself at the end of the experiment.

Table 3. Estimated self-thinning exponents for the dynamical approach, 95% confidence intervals and p-values of Tukey test for H_0: $\beta = -1$.

		June	July	August	September	October	November
220	**β**	-1.370	-1.356	-1.495	-1.030	-1.863	-0.303
	2.5%	-1.403	-1.410	-1.536	-1.099	-2.352	-1.496
	97.5%	-1.338	-1.301	-1.453	-0.961	-1.375	0.892
	p	<0.0001	<0.0001	<0.0001	0.3964	0.0005	0.2525
370	**β**	-1.579	-1.415	-1.747	-0.940	-0.179	-2.649
	2.5%	-1.620	-1.457	-1.781	-0.963	-1.160	-4.553
	97.5%	-1.538	-1.373	-1.712	-0.918	0.802	-0.745
	p	<0.0001	<0.0001	<0.0001	<0.0001	0.1008	0.0895
500	**β**	-1.243	-1.503	-1.452	-1.483	-1.343	-0.271
	2.5%	-1.267	-1.574	-1.509	-1.875	-1.962	-0.954
	97.5%	-1.218	-1.433	-1.394	-1.091	-0.723	0.413
	p	<0.0001	<0.0001	<0.0001	0.0157	0.2781	0.0365
570	**β**	-1.539	-0.997	-3.021	-0.963	-0.814	-1.123
	2.5%	-1.561	-1.099	-3.247	-1.010	-1.578	-1.376
	97.5%	-1.517	-0.895	-2.795	-0.915	-0.050	-0.871
	p	<0.0001	0.954	<0.0001	0.1255	0.6327	0.3382
700	**β**	-1.148	-1.618	-1.412	-1.183	-1.464	-2.357
	2.5%	-1.181	-1.659	-1.501	-1.281	-2.383	-3.334
	97.5%	-1.115	-1.576	-1.323	-1.085	-0.545	-1.380
	p	<0.0001	<0.0001	<0.0001	0.0003	0.3220	0.0065
800	**β**	-1.484	-1.333	-1.502	-1.139	-1.177	-1.751
	2.5%	-1.536	-1.371	-1.533	-1.394	-1.734	-3.458
	97.5%	-1.432	-1.295	-1.470	-0.883	-0.619	-0.045
	p	<0.0001	<0.0001	<0.0001	0.2882	0.5341	0.3878
1150	**β**	-0.842	-5.690	-1.438	-0.975	-1.280	-1.249
	2.5%	-0.889	-7.834	-1.454	-1.066	-1.413	-1.285
	97.5%	-0.796	-3.545	-1.421	-0.885	-1.146	-1.214
	p	<0.0001	<0.0001	<0.0001	0.5946	<0.0001	<0.0001

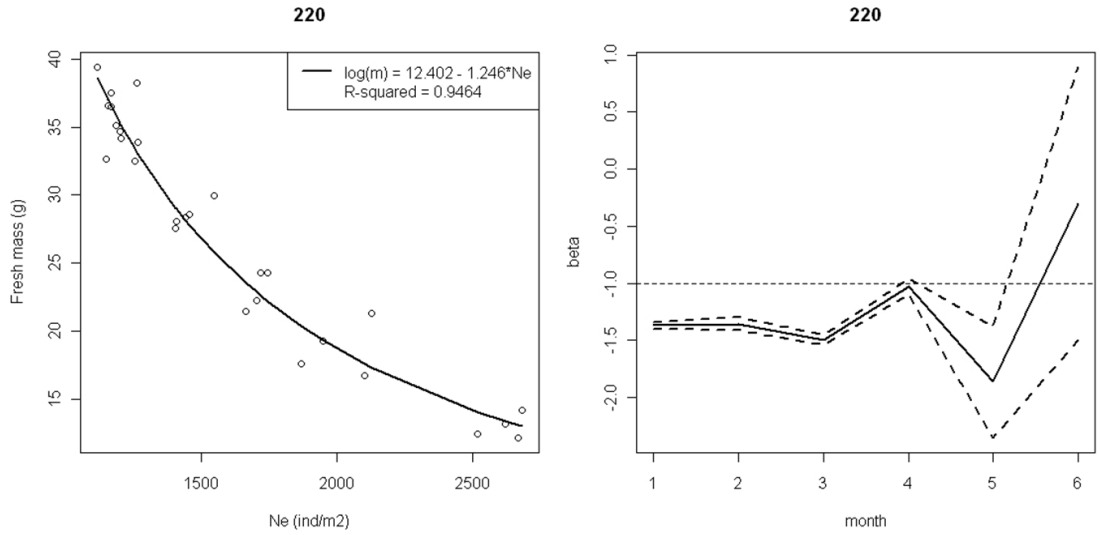

Fig. 2. Left: classical self thinning model. Right: dynamic self-thinning model, exponents (solid line) and 95% confidence band (dashed line) for 220 ind/m.

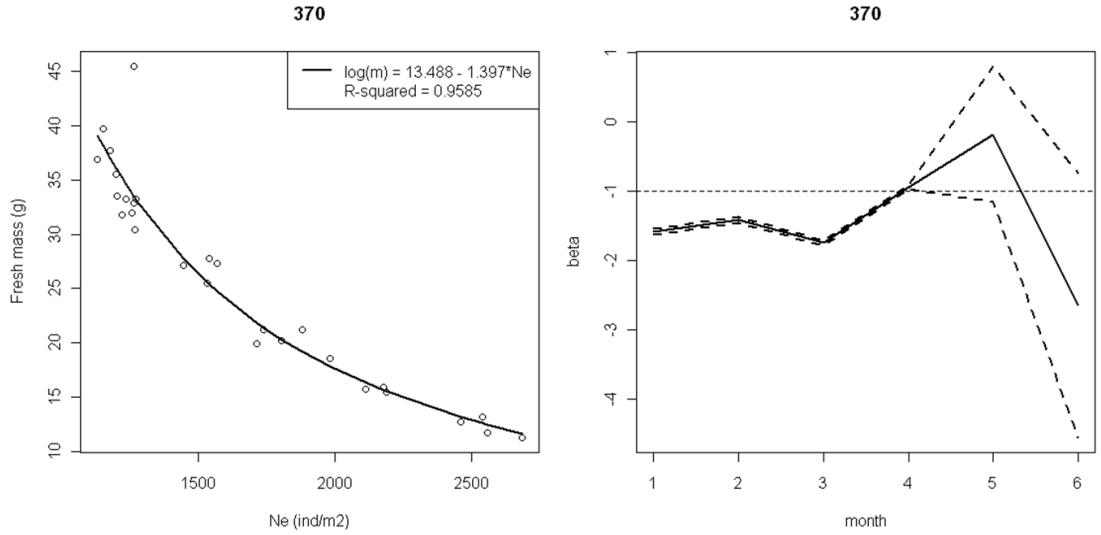

Fig. 3. Left: classical self thinning model. Right: dynamic self-thinning model, exponents (solid line) and 95% confidence band (dashed line) for 370 ind/m.

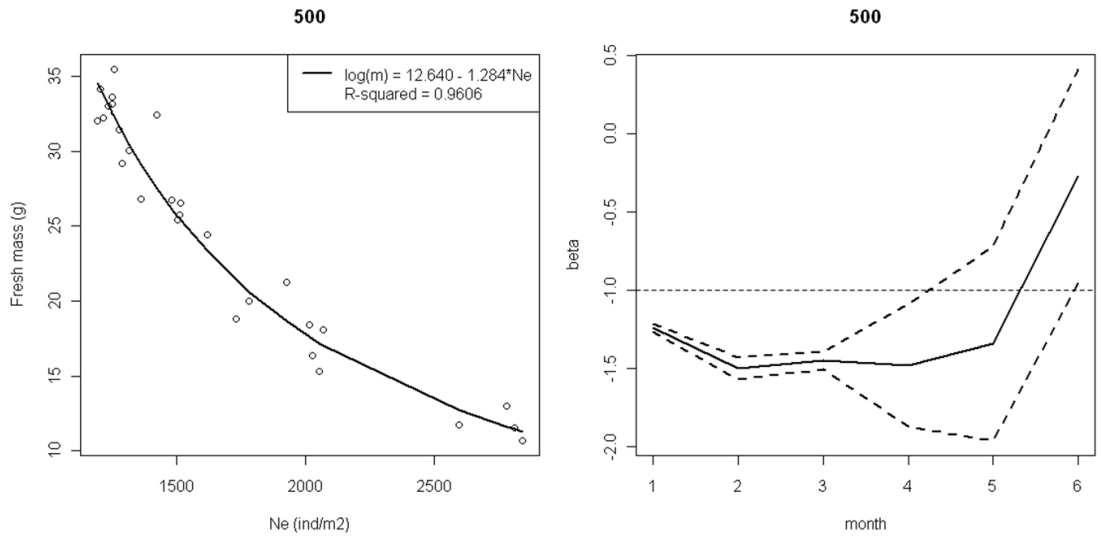

Fig. 4. . Left: classical self thinning model. Right: dynamic self-thinning model, exponents (solid line) and 95% confidence band (dashed line) for 500 ind/m.

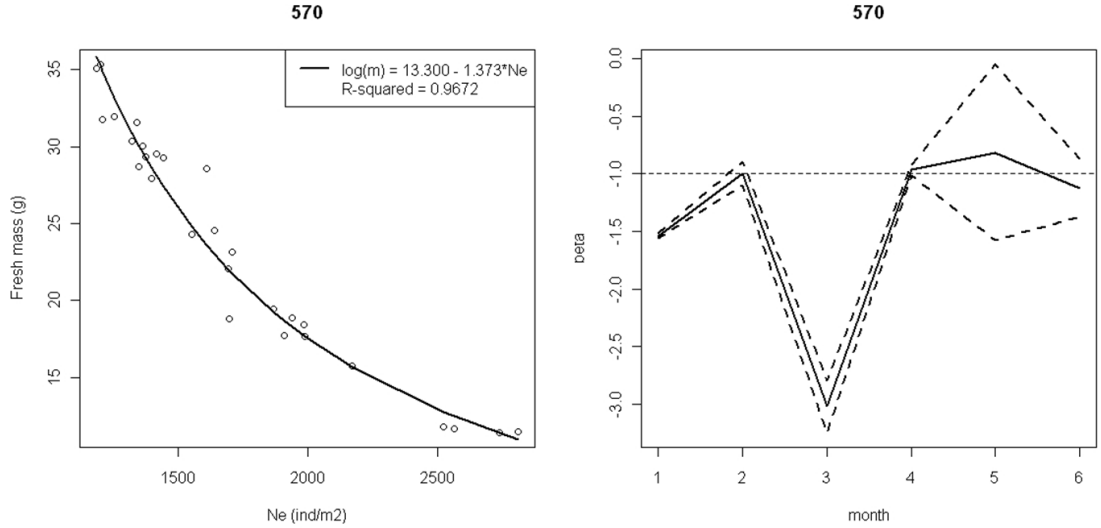

Fig. 5. Left: classical self thinning model. Right: dynamic self-thinning model, exponents (solid line) and 95% confidence band (dashed line) for 570 ind/m.

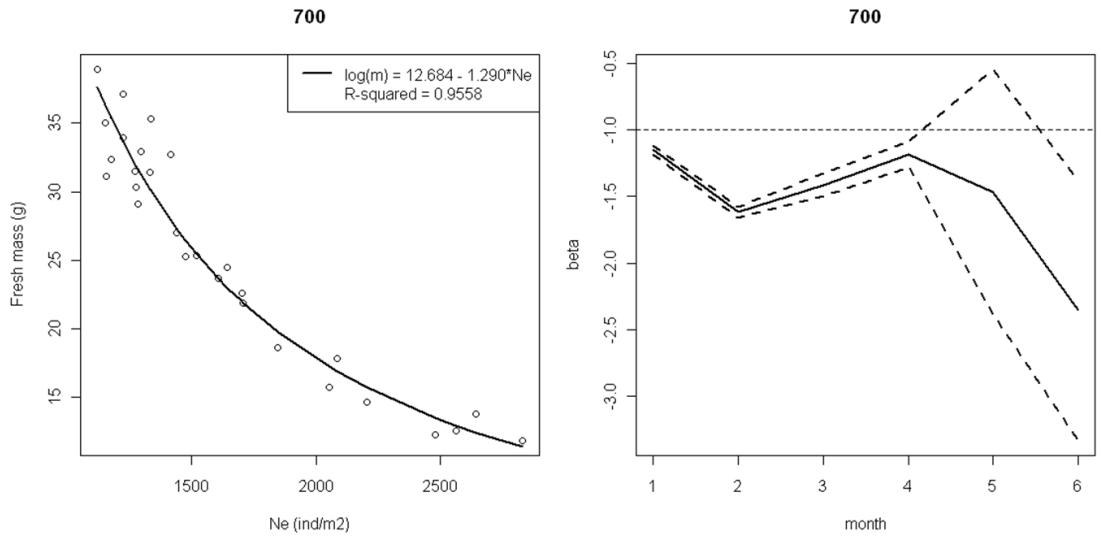

Fig. 6. Left: classical self thinning model. Right: dynamic self-thinning model, exponents (solid line) and 95% confidence band (dashed line) for 700 ind/m.

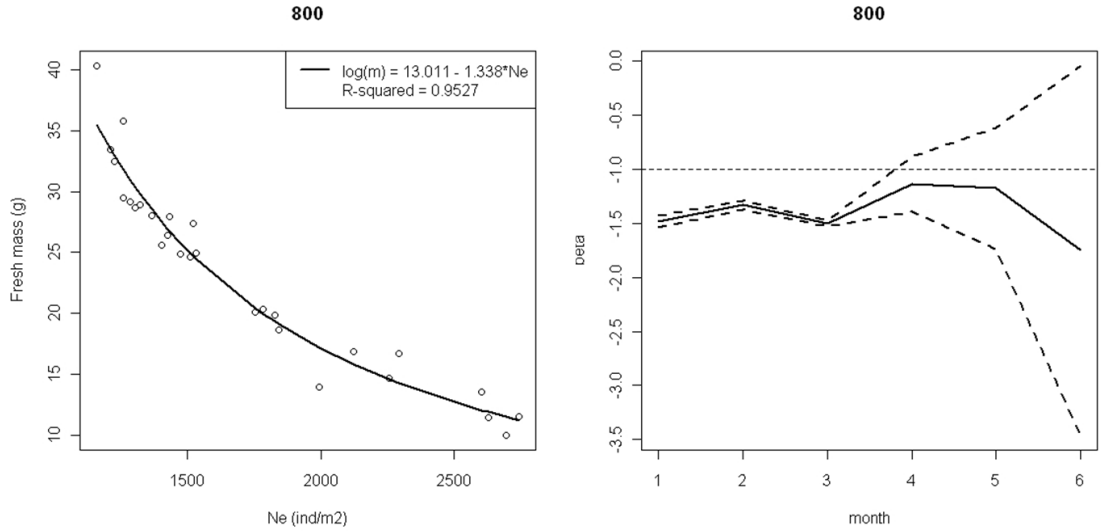

Fig. 7. Left: classical self thinning model. Right: dynamic self-thinning model, exponents (solid line) and 95% confidence band (dashed line) for 800 ind/m.

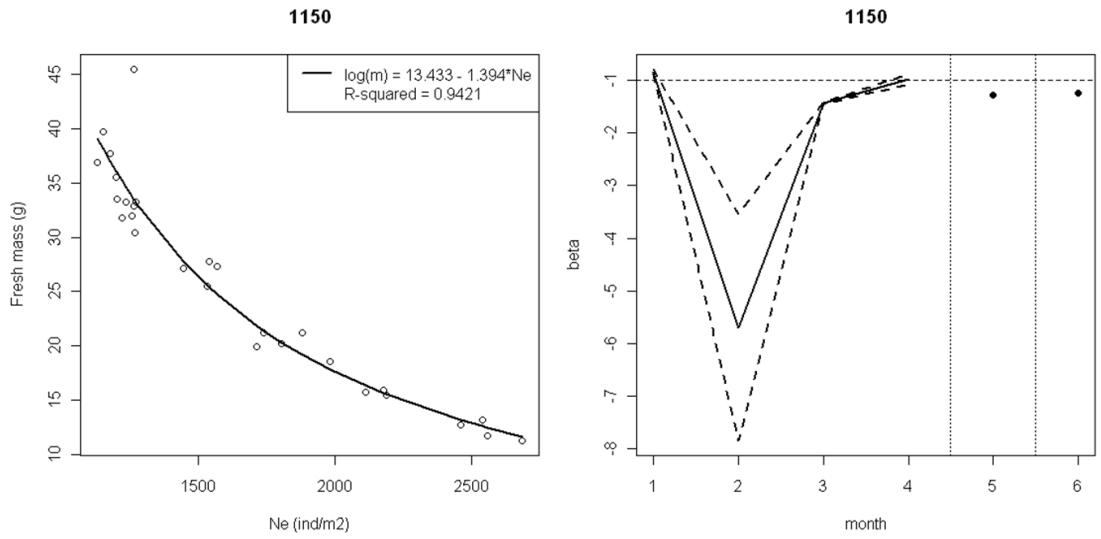

Fig. 8. Left: classical self thinning model. Right: dynamic self-thinning model, exponents (solid line) and 95% confidence band (dashed line) for 1150 ind/m.

5.4. Discussion

In this study we extend the dynamic self-thinning model proposed by Roderick & Barnes (2004) to the analysis of multilayered sessile animal populations. Comparison of this model against the classical tridimensional self-thinning model shows that the dynamical approach outperforms the traditional model in several points.

The estimation of the ST exponent trajectory by the dynamic model reflects the dynamic nature of the ST process (Westoby 1984; White 1981). However, the traditional model assumes that the ST parameters remain constant over time, being restricted to the analysis of the average competitive behavior of the population. Several authors (Begon et al. 2006; Chen et al. 2008; Nash et al. 2007; Xue & Hagihara 1998) have defined the "dynamic thinning line" as the temporal evolution of the mass-density relationship in a population. However, they have limited their study to the linear asymptote that this trajectory would approach, overlooking the time effect. From the methodological viewpoint, the assumption of independence for sequential autocorrelated data by the classical model leads to underestimate the error (overestimate the goodness of fit) and produces a biased estimation of the self-thinning parameters.

The dynamic model, which analyzes each sampling interval separately, overcomes this error.

In contraposition with the classical self-thinning model, the dynamical approach detected the effect of density treatment on the competitive behavior of individuals and population dynamics. Particularly, the exponent trajectories showed similar patterns among the 220- 800 ind/m treatments in contraposition with the density of 1150 ind/m. However, it should be noted that similar exponent trends could reflect different dynamics. Thus, for initial densities lower than 570 ind/m, the decrease in effective density was exclusively due to reorganization into new layers (migration), while at higher densities (570 - 1150 ind/m) it also included mortality. At the beginning of our study, mussel growth exceeded mussel migration-mortality rate in all density treatments analyzed, except for the 1150 ind/m. This indicates a greater intraspecific competition at high density levels and suggests that the carrying capacity of the system was reached. After the initial fall in N_e, the availability for limiting resources in 1150 ind/m treatment increased. And in the next two months, as for the lower densities, the individuals were able to grow at a greater rate than density decreased. In populations with initial densities below 1150 ind/m, from September onwards the biomass remained constant and both density decrease and individual growth tended to 0. This is probably due to the fact that the growth curve asymptote had been reached (Chapter 2). Therefore, intraspecific competition was no longer observed at these densities, while the 1150 ind/m population was still self-regulating at the end of the experiment. This suggests that populations grown at higher density levels, with stronger intraspecific competition, need more time to stabilize (Fig. 1).

The classical ST model is based on allometric relationships depending on a series of assumptions (Fréchette & Lefaivre 1990) that do not always hold, i.e. isometric growth and the 100% occupation of the sampling area. Conversely, the dynamic model is based on a mathematical axiom (Eq. 8) and therefore its validity does not depend on the empirical conditions. The dynamic model is a generalization of the traditional model but, as it is not based on the same allometric relationships, the estimated exponents are not comparable to the theoretical exponents of the classical model. Rather than discriminating the limiting factor, which has been one of the main goals in the ST analysis, the dynamic model focuses on analyzing the evolution of intraspecific competition over time (Table 1). Therefore, this new approach provides a more realistic

description of population dynamics. Moreover, the dynamic model allows the ecological interpretation of any possible value of β, while the traditional model can not explain any exponent different from the theoretical ones (-3/2 and -4/3). Finally, the results of our study confirm the difficulty of the classical model to achieve its main objective of distinguishing the competition limiting factor, as indicated in Chapter 4.

A crucial point in the application of the dynamical approach is to detect when the sign of dN_e/dt changes, as this change of sign introduces a discontinuity in the trajectory of the ST exponent. This should be considered when describing the ST process, since similar exponents can actually reflect opposite behaviors (Table 1), as observed for the 1150 ind/m density in the last two months (Fig. 8, Table 2).

In summary, this study demonstrates the applicability of the self-thinning dynamic model proposed by Roderick & Barnes (2004) to the analysis of multilayered sessile animal populations. Moreover, in contraposition with the classical self-thinning model, the dynamical approach allows studying the effect of population density on the competitive behavior of individuals and gives insight into the temporal evolution of intraspecific competition, providing a more realistic description of population dynamics. Nevertheless, it should be noted that for a correct ecological interpretation of self-thinning it is critical to analyze simultaneously the estimated exponents (β) and the variables involved in the process, i.e., density, total biomass and individual mass, as well as effective density, number of layers and biomass per layer for multilayered populations. This highlights the difficulty of interpreting an intricate process as self-thinning through a single parameter (β).

5.5. APPENDIX

Table A1. Mean and SD of density (N; ind/m^2), effective density (N_e; ind$(m^2L)^{-1}$), number of layers (L), mean individual fresh mass (m; g), total biomass (B; kg) and biomass per layer (B_L; kg) over the experimental period for 220 ind/m.

220		N	N_e	L	m	B	B_L
May	Mean	2759.50	2622.40	1.05	12.99	33.90	32.25
	SD	289.20	74.73	0.11	0.90	3.06	1.24
June	Mean	2799.77	2011.78	1.40	18.74	49.83	35.48
	SD	121.82	124.16	0.15	2.02	7.44	1.67
July	Mean	2835.44	1707.40	1.66	23.07	61.83	37.24
	SD	383.80	33.84	0.25	1.44	9.15	2.04
August	Mean	2218.35	1463.75	1.52	28.61	60.05	39.65
	SD	195.11	59.32	0.11	0.99	4.85	1.69
September	Mean	2493.67	1283.57	1.93	32.28	75.05	38.99
	SD	613.28	87.43	0.34	2.94	11.40	1.08
October	Mean	2550.63	1194.06	2.14	35.42	91.05	42.34
	SD	402.62	53.49	0.32	2.50	20.58	3.10
November	Mean	2591.77	1159.85	2.23	37.16	90.18	40.42
	SD	140.34	28.73	0.11	1.79	3.42	1.17

Table A2. Mean and SD of density (N; ind/m^2), effective density (N_e; ind$(m^2L)^{-1}$), number of layers (L), mean individual fresh mass (m; g), total biomass (B; kg) and biomass per layer (B_L; kg) over the experimental period for 370 ind/m.

370		N	N_e	L	m	B	B_L
May	Mean	4689.88	2559.75	1.83	12.26	56.15	30.90
	SD	669.97	92.89	0.21	0.86	4.05	2.62
June	Mean	4778.48	2114.39	2.25	16.45	75.18	33.30
	SD	822.26	94.65	0.31	1.45	12.62	1.79
July	Mean	4643.99	1784.59	2.61	20.67	94.23	35.97
	SD	800.32	74.40	0.48	0.68	19.94	1.07
August	Mean	4219.62	1520.97	2.77	26.94	105.23	37.97
	SD	285.48	53.70	0.09	0.98	5.74	0.88
September	Mean	3817.72	1248.79	3.06	32.26	127.20	41.64
	SD	213.27	32.70	0.16	1.42	10.94	4.14
October	Mean	4351.27	1228.51	3.54	33.36	143.55	40.59
	SD	796.19	28.11	0.64	1.57	25.23	1.06
November	Mean	3517.18	1181.08	2.99	39.95	130.45	44.25
	SD	455.92	58.66	0.49	3.84	8.07	5.80

Table A3. Mean and SD of density (N; ind/m^2), effective density (N_e; ind$(m^2L)^{-1}$), number of layers (L), mean individual fresh mass (m; g), total biomass (B; kg) and biomass per layer (B_L; kg) over the experimental period for 500 ind/m.

500		N	N_e	L	m	B	B_L
May	Mean	6342.70	2759.13	2.30	11.73	82.95	36.52
	SD	750.91	111.82	0.22	0.94	5.80	5.87
June	Mean	5750.00	2041.44	2.82	17.06	96.30	33.91
	SD	911.18	24.84	0.45	1.46	21.60	3.14
July	Mean	6144.62	1762.92	3.52	21.14	123.85	35.04
	SD	814.83	128.43	0.67	2.42	27.50	1.59
August	Mean	5991.46	1501.06	3.99	26.13	146.58	36.74
	SD	594.01	14.25	0.38	0.63	13.80	0.20
September	Mean	6334.50	1346.27	4.71	29.63	174.43	37.13
	SD	581.04	59.31	0.36	2.31	8.93	1.08
October	Mean	5142.09	1230.78	4.17	33.26	160.23	38.44
	SD	503.83	40.78	0.33	1.87	10.20	0.73
November	Mean	5664.56	1234.90	4.59	33.00	174.25	38.02
	SD	363.17	17.44	0.25	0.57	7.54	0.57

Table A4. Mean and SD of density (N; ind/m^2), effective density (N_e; ind$(m^2L)^{-1}$), number of layers (L), mean individual fresh mass (m; g), total biomass (B; kg) and biomass per layer (B_L; kg) over the experimental period for 570 ind/m.

570		N	N_e	L	m	B	B_L
May	Mean	7192.60	2660.65	2.71	11.57	83.35	30.77
	SD	514.96	136.99	0.29	0.15	8.23	1.29
June	Mean	7626.27	2022.27	3.78	17.67	120.90	31.95
	SD	373.49	102.35	0.33	1.39	23.58	5.30
July	Mean	7272.15	1793.32	4.08	19.49	137.08	33.57
	SD	465.61	111.37	0.47	1.84	19.48	1.34
August	Mean	6487.34	1628.62	3.99	25.12	174.70	43.96
	SD	513.19	64.97	0.38	2.38	18.51	4.70
September	Mean	6281.65	1385.94	4.54	28.86	173.45	38.21
	SD	738.80	28.98	0.58	0.72	23.07	0.94
October	Mean	6246.84	1368.73	4.58	30.30	175.60	38.43
	SD	363.58	52.19	0.43	0.96	12.34	1.09
November	Mean	5113.93	1214.18	4.21	33.52	160.30	38.12
	SD	573.22	29.61	0.36	1.95	13.64	1.49

Table A5. Mean and SD of density (N; ind/m^2), effective density (N_e; ind$(m^2L)^{-1}$), number of layers (L), mean individual fresh mass (m; g), total biomass (B; kg) and biomass per layer (B_L; kg) over the experimental period for 700 ind/m.

700		N	N_e	L	m	B	B_L
May	Mean	8936.70	2630.53	3.41	12.63	110.50	32.42
	SD	109.39	149.70	0.18	0.83	10.54	1.79
June	Mean	7694.30	2048.47	3.78	16.72	131.90	34.92
	SD	669.19	148.59	0.56	1.84	18.51	1.47
July	Mean	6621.84	1664.80	3.98	23.17	145.48	36.45
	SD	995.50	47.66	0.59	1.14	26.31	2.01
August	Mean	6898.74	1461.62	4.71	27.58	175.88	37.42
	SD	1237.58	45.95	0.71	3.53	24.17	1.61
September	Mean	7055.38	1296.67	5.45	30.94	208.83	38.32
	SD	1074.40	23.54	0.91	1.64	34.92	1.27
October	Mean	6934.18	1246.34	5.57	32.98	164.75	29.59
	SD	366.46	75.80	0.26	2.02	46.98	8.18
November	Mean	6929.21	1169.08	5.93	35.86	260.10	43.87
	SD	366.28	43.29	0.19	2.84	45.55	7.56

Table A6. Mean and SD of density (N; ind/m^2), effective density (N_e; ind(m^2L)$^{-1}$), number of layers (L), mean individual fresh mass (m; g), total biomass (B; kg) and biomass per layer (B_L; kg) over the experimental period for 800 ind/m.

800		N	N_e	L	m	B	B_L
May	Mean	10126.60	2667.28	3.80	11.61	113.38	29.82
	SD	576.59	64.30	0.27	1.46	9.91	1.01
June	Mean	9603.48	2166.36	4.44	15.53	138.17	31.00
	SD	121.12	136.69	0.24	1.45	24.26	4.47
July	Mean	9224.68	1800.66	5.13	19.73	177.70	34.49
	SD	1179.69	41.57	0.69	0.73	31.38	1.53
August	Mean	8821.20	1508.45	5.85	25.45	212.95	36.45
	SD	775.75	24.50	0.46	1.28	16.60	1.27
September	Mean	7531.65	1406.15	5.36	27.01	225.70	42.64
	SD	896.57	31.23	0.70	1.20	5.89	5.64
October	Mean	7372.15	1284.94	5.74	30.74	166.60	29.40
	SD	546.22	32.36	0.48	3.41	37.43	8.28
November	Mean	8268.99	1219.98	6.77	33.86	249.38	36.78
	SD	744.01	51.11	0.45	4.69	52.37	6.65

Table A7. Mean and SD of density (N; ind/m^2), effective density (N_e; ind$(m^2L)^{-1}$), number of layers (L), mean individual fresh mass (m; g), total biomass (B; kg) and biomass per layer (B_L; kg) over the experimental period for 1150 ind/m.

1150		N	N_e	L	m	B	B_L
May	Mean	14588.63	3007.03	4.87	10.13	160.78	33.18
	SD	323.78	182.61	0.32	0.96	19.18	4.84
June	Mean	14373.42	2149.96	6.71	13.70	214.38	31.93
	SD	645.57	113.28	0.56	2.92	29.67	2.80
July	Mean	12286.39	2042.59	6.05	17.28	215.05	35.48
	SD	974.49	113.84	0.79	0.58	33.70	1.51
August	Mean	9683.23	1491.20	6.49	27.05	243.75	37.52
	SD	1076.51	45.10	0.67	1.59	29.26	1.39
September	Mean	10056.01	1338.80	7.52	29.62	315.43	42.02
	SD	403.61	42.42	0.49	1.72	62.80	8.78
October	Mean	9061.08	1530.06	5.96	25.31	266.93	46.04
	SD	782.88	106.10	0.79	2.74	33.20	13.00
November	Mean	8452.88	1221.20	6.93	33.57	292.00	42.26
	SD	925.28	47.87	0.77	1.50	53.44	7.22

Capítulo 6. Conclusiones generales

El cultivo de mejillón tiene una gran importancia ecológica y socio-económica en las Rías Gallegas y se encuentra determinado en gran medida por la densidad de las unidades de cultivo (bateas), su distribución espacial, las características ecológicas y oceanográficas y, en particular, la disponibilidad de alimento en el área de cultivo. Además, la densidad en cada unidad de cultivo (número de cuerdas) y la densidad por cuerda (individuos por cuerda) es un factor fundamental que afecta al rendimiento y la productividad de la cosecha y por lo tanto, es de extrema importancia para el desarrollo de estrategias de explotación y gestión de los cultivos.

Desde el punto de vista ecológico, la densidad juega un papel importante en la dinámica poblacional de los organismos sésiles. La especie *Mytilus galloprovincialis* tiene una gran capacidad de filtración que puede ocasionar la depleción de las partículas de seston en la columna de agua y provocar limitaciones de alimento. Esto puede conllevar a la aparición de fenómenos de competencia intraespecífica que darán lugar a limitaciones en el crecimiento de los individuos. Además, al aumentar la densidad, los individuos pueden sufrir efectos negativos sobre su capacidad de la apertura valvar para alimentarse y restricciones en el crecimiento causadas por limitaciones espaciales (Bertness & Grosholz 1985; Fréchette & Despland 1999). Todo esto puede desencadenar la aparición de una mortalidad denso-dependiente o self-thinning (ST) que finalmente regula el tamaño poblacional en función de la disponibilidad de recursos.

La existencia de competencia por espacio y alimento ha sido observada en poblaciones de mejillones, tanto naturales (Bertness & Grosholz 1985; Harger 1972; Kautsky 1982; Okamura 1986; Seed 1969) como cultivadas (Ceccherelli & Barboni 1983; Fréchette & Lefaivre 1990; Fréchette et al. 1992; Mueller, 1996; Taylor et al. 1997). La acuicultura en cultivo suspendido representa un caso especial de agregación donde se maximiza la densidad de estos suspensívoros para conseguir un mayor rendimiento comercial. Esto nos proporciona un escenario ideal para el estudio de los efectos de la densidad y la competencia intraespecífica en condiciones naturales.

En este trabajo se aborda el estudio de la influencia de la densidad poblacional sobre el crecimiento, la plasticidad morfológica y la supervivencia de *Mytilus galloprovincialis* en una situación de cultivo suspendido en la Ría de Ares-Betanzos. Además, se revisan los distintos modelos y métodos de regresión empleados actualmente en el análisis del self-thinning mediante su aplicación al estudio de poblaciones animales sésiles con disposición multicapa. Para ello, se ha realizado la evaluación temporal de poblaciones

de *Mytilus galloprovincialis* cultivadas a diferentes densidades (220, 370, 500, 570, 750, 800 y 1150 individuos por metro lineal de cuerda) durante ocho meses (abril-noviembre de 2008), abarcando el periodo de desdoble a cosecha. En base a los resultados obtenidos en los distintos capítulos que conforman este trabajo, se establecieron las siguientes conclusiones:

Capítulo 2:

De nuestros resultados se concluye, de forma general, que **existe un efecto negativo de la densidad de plantado sobre el crecimiento del mejillón *Mytilus galloprovincialis* en una situación de cultivo suspendido.** Esta síntesis se deriva de las siguientes conclusiones extraídas de las observaciones y correspondientes análisis.

Del análisis de las curvas de crecimiento y las tasas de crecimiento en talla y peso se concluye que los individuos cultivados a densidades elevadas presentan un crecimiento más lento y consecuentemente alcanzan un peso y una talla máximos significativamente menores que los cultivados a menor densidad. Por lo tanto, las densidades elevadas contienen una mayor proporción de individuos pequeños y una menor proporción de mejillón de mayor tamaño, en relación a densidades menores. **La existencia de un crecimiento diferencial a lo largo del gradiente de densidad sugiere diferencias en el nivel de competencia intraespecífica por los recursos limitantes (espacio/alimento), que hacen que a menor densidad los individuos obtengan una mayor proporción de recursos, favoreciendo su crecimiento.**

El efecto negativo de la densidad sobre las tasas de crecimiento de la talla y peso se acentúa con el crecimiento de los individuos. Así, los efectos sobre la tasa de crecimiento se vuelven significativos a partir de tallas en torno a los 66 mm. Esto indica que, a medida que los individuos crecen, sus requerimientos por los recursos limitantes aumentan y los fenómenos de competencia intra-específica se intensifican. Este hecho debería ser considerado en la gestión de la acuicultura, ya que si se limita el tamaño del mejillón en la cosecha, los cultivos pueden soportar densidades más elevadas sin que lleguen a observarse efectos negativos sobre el crecimiento.

A su vez, un ajuste de la densidad de cultivo a la disponibilidad de alimento de cada zona permitirá minimizar la competencia intraespecífica y por tanto, mejorar el crecimiento y rendimiento del mejillón, optimizando la producción y los beneficios económicos.

Capítulo 3:

Nuestros resultados permiten concluir que **existe una variación en la morfología de los mejillones asociada al crecimiento**, observándose una disminución en las relaciones alto/largo y alto/ancho (H/L y H/W) y un incremento en la relación ancho/largo (W/L) al aumentar la talla. Por lo tanto, aunque se registra crecimiento en todas las dimensiones, estos cambios no son uniformes a lo largo del tiempo, sino que se producen cambios progresivos en las proporciones relativas al aumentar la talla. Este crecimiento diferencial entre las distintas dimensiones de la concha se refleja en un cambio gradual en su forma, de tal manera que los mejillones de mayor tamaño presentarán una morfología más elongada en la cual el alto excederá al ancho, en una proporción cada vez menor.

Nuestro trabajo apoya la hipótesis de que la plasticidad morfológica es una estrategia para mitigar los efectos de la competencia intra-específica a nivel individual. Se ha observado que los mejillones plantados a mayor densidad disminuían su relación H/L y W/L, dando lugar a conchas más elongadas o filiformes y estrechas que los que crecen a bajas densidades. **La estrategia de alcanzar formas más elongadas resulta ser ventajosa en ambientes de elevada densidad**, al reducir la interferencia física entre individuos favoreciendo la tasa de aclaramiento (Jørgensen et al. 1988) y permitir una mejor exposición de su sifón inhalante y por lo tanto, un mejor acceso al alimento (Sénechal et al. 2008).

No se observaron diferencias asociadas a la densidad en la relación H/W. Esto indica que la competencia intraespecífica, aunque provoca restricciones en el crecimiento en altura y anchura de los mejillones, lo hace siempre en la misma proporción a lo largo del gradiente de densidad.

La interacción significativa entre densidad y tiempo observada en la relación H/L y W/L refleja un **aumento progresivo de la competencia intraespecífica con el crecimiento de los organismos**, **debido al incremento de sus requerimientos de espacio y alimento,** como se observa en las tasas de crecimiento en talla y peso (Capítulo 2).

Nuestros datos indican que no existe un efecto significativo de la densidad de cultivo sobre la distribución de energía entre concha y tejidos. Aunque los individuos cultivados a menor densidad obtienen una mayor cantidad de energía (Capítulo 2), el reparto de esta entre la concha y el tejido se mantiene en la misma proporción a lo largo del gradiente de densidad estudiado, para una misma época. Esto corrobora que **el índice de condición (IC) es un indicador débil para detectar el efecto de la densidad en moluscos bivalvos**, probablemente porque la mayor parte de su variabilidad se asocia a fluctuaciones en el ciclo gametogénico y a variaciones estacionales en la disponibilidad de alimento.

Al final del periodo experimental del presente estudio se constata la existencia de fenómenos de competencia asimétrica en densidades elevadas, debidos a que los individuos de mayor tamaño obtienen una mayor proporción de recursos e interfieren en el crecimiento de los individuos más pequeños. Por este motivo, se obtiene una mayor uniformidad morfológica entre tallas en las poblaciones cultivadas a menor densidad, lo que puede ser de interés para la industria miticultora.

Capítulo 4:

De los resultados obtenidos se concluye que en poblaciones con disposición en múltiples capas, el nivel de ocupación o hacinamiento (“crowding”) se refleja en el grado de empaquetamiento, medido como número de capas (L), mientras que la densidad de cada capa (N_e) se mantiene estable a lo largo del gradiente de densidad estudiado.

El empleo de la relación alométrica volumen-superficie ocupada, en lugar de usar la masa como estimador del volumen, mejora la estimación del exponente teórico del self-thinning espacial (SST).

La estimación del exponente teórico del SST depende del método de medida empleado en el cálculo de la superficie ocupada, lo que cuestiona la aplicabilidad de los exponentes teóricos del ST en el estudio de poblaciones animales sésiles. Así, la estimación de superficie ocupada obtenida por el método del paralelepípedo (S_p) proporciona un exponente igual al teórico ($\beta_{p,SST}$ = -0.50), mientras que con la estimación por imagen (S_{im}), más precisa, se invierte la relación establecida entre los exponentes por espacio y alimento ($\beta_{FST}>\beta_{SST}$) ($\beta_{im,SST}$ =-0.23 > β_{FST} =-0.33).

L**a proximidad encontrada entre los exponentes teóricos estimados para espacio -por imagen- y alimento (-0.23 y -0.33, respectivamente) dificulta la discriminación entre ambos tipos de competencia.**

Por otra parte, nuestros resultados descartan el empleo del modelo bidimensional en el estudio del self-thinning debido a la baja proporción de varianza explicada y la dependencia entre los residuos y el número de capas. **Se confirma la necesidad de aplicar el modelo tridimensional de self-thinning propuesto por Guiñez & Castilla (1999) cuando se analizan poblaciones animales sésiles con disposición multicapa.**

La inclusión de las densidades que no presentan mortalidad en el análisis de self-thinning no introdujo sesgo en la estimación del exponente, en contra de lo indicado en estudios previos (Lonsdale 1990; Mohler et al. 1978; Osawa & Sugita 1989; Osawa & Allen 1993; Weller 1987[a]), con lo que se evita realizar una selección subjetiva de los datos.

La sustitución de la densidad (N) por la densidad efectiva (N_e) en el modelo tridimensional de ST proporciona ajustes equivalentes y reduce el modelo tridimensional (m-N-L) a uno bidimensional (m-N_e), simplificando la interpretación del modelo.

El empleo de distintos métodos de regresión (regresión lineal simple-OLS, regresión de eje máximo-RMA, ajuste robusto-RM y modelo no lineal-NLM**) no conlleva diferencias significativas en la estimación de los parámetros de ST (k, ß)**,

aunque el ajuste robusto aporta conclusiones distintas respecto al factor limitante. Sin embargo, el hecho de que el RM reduzca el peso de los valores extremos limita su aplicabilidad en el estudio de self-thinning.

La estimación de los parámetros del modelo tridimensional y las conclusiones sobre el factor limitante de la competencia (espacio/alimento) dependen de la relación estudiada (masa o biomasa) y del método de medida de las variables del modelo (biomasa, masa y superficie ocupada). Esta falta de consistencia del modelo de ST dificulta la discriminación del tipo de competencia, y en consecuencia, la interpretación ecológica de la dinámica poblacional.

Se recomienda el empleo de métodos de análisis de frontera (Stochastic Frontier Function, SFF) en el análisis de ST, ya que i) permiten estimar el límite/línea superior de ST (upper boundary line) incluyendo todos los valores, sin necesidad de realizar una selección subjetiva de datos, ii) permiten estudiar el nivel de ocupación del sistema, iii) aportan una interpretación dinámica del proceso de ST mediante el análisis de la variabilidad temporal del nivel de ocupación y iv) se obtienen las mismas conclusiones respecto al factor limitante al utilizar las relaciones para biomasa y masa (es un método más robusto).

Capítulo 5:

Con el objetivo de resolver la falta de consistencia del modelo tridimensional, en este capítulo **se demuestra la aplicabilidad del modelo dinámico de self-thinning, propuesto por Roderick & Barnes (2004), en el análisis de poblaciones animales sésiles con disposición en múltiples capas.** La comparación de este método con el modelo tradicional de self-thinning muestra que **el enfoque dinámico mejora al modelo tridimensional tradicional en varios aspectos:**

- El modelo dinámico, al estimar la trayectoria del exponente de self-thinning, refleja la naturaleza dinámica del proceso. Mientras que el modelo tradicional, al suponer que los parámetros de ST se mantienen constantes, se limita a estudiar el comportamiento medio de la población.

- **El modelo dinámico evita el error de estimación** que comete el modelo tradicional al aplicar métodos de regresión que suponen medidas independientes a datos secuenciales, y por tanto autocorrelacionados, evitando así la estimación sesgada de los parámetros de ST.

- **El modelo dinámico, a diferencia del modelo tradicional de ST, permite estudiar el efecto de la densidad poblacional en el comportamiento competitivo y la evolución temporal de la competencia intraespecífica, aportando una descripción más realista de la dinámica poblacional.**

- **El modelo dinámico es capaz de interpretar cualquier posible valor de β**, mientras que el modelo tradicional no ofrece explicación para exponentes distintos a los teóricos (-0.5 ó -0.33). Además, los resultados de este trabajo confirman la dificultad del modelo clásico para discriminar el factor limitante, como ya se indicaba en el Capítulo 4.

Por otro lado, en la aplicación del modelo dinámico de ST hay que tener en cuenta varios aspectos:

- Para interpretar correctamente el comportamiento de la población en cada momento es imprescindible **conocer los intervalos de tiempo donde el signo de la derivada de la densidad (dN_e/dt) cambia**, ya que exponentes similares pueden ser el reflejo de comportamientos/dinámicas opuestas.

- Se confirma la dificultad de explicar un proceso tan complejo como el self-thinning mediante un único parámetro (β). **Para una correcta interpretación ecológica del self-thinning es imprescindible analizar conjuntamente el exponente de ST (β) y las variables que intervienen en el modelo:** masa individual, densidad y biomasa poblacional, además de la densidad efectiva, número de capas y biomasa por capa en poblaciones con distribución en múltiples capas.

Bibliografía

Aigner D.J, Lovell C.A.K, Schmidt P. 1977. Formulation and estimation of stochastic frontier production function models. Journal of Econometrics 6:21-37.

Akester, R.J., Martel, A.L., 2000. Shell shape, dysodont tooth morphology, and hinge-ligament thickness in the bay mussel *Mytilus trossulus* correlate with wave exposure. Canadian Journal of Zoology-Revue Canadienne De Zoologie 78(2): 240-53.

Alunno-Bruscia, M., Petraitis, P.S., Bourget, E., Fréchette, M. (2000) Body size-density relationship for *Mytilus edulis* in an experimental food-regulated situation. Oikos 90(1): 28-42.

Alunno-Bruscia, M., Bourget E., Fréchette, M. 2001. Shell allometry and length-mass-density relationship for *Mytilus edulis* in an experimental food-regulated situation. Mar Ecol Prog Ser 219: 177-188.

Alvarado, J.L., Castilla, J.C. (1996) Tridimensional matrices of *Perumytilus purpuratus* on intertidal platforms with varying wave forces in central Chile. Marine Ecology Progress Series 133: 135–141.

Álvarez-Salgado, X.A., Labarta, U., Fernandez-Reiriz, M.J., Figueiras, F.G., Roson, G., Piedracoba, S., Filgueira, R., Cabanas, J.M., 2008. Renewal time and the impact of harmful algal blooms on the extensive mussel raft culture of the Iberian coastal upwelling system (SW Europe). Harmful Algae 7(6), 849-855.

Álvarez-Salgado, X. A., Figueiras, F. G., Fernandez-Reiriz, M. J., Labarta, U., Peteiro, L., Piedracoba, S., 2011. Control of lipophilic shellfish poisoning outbreaks by seasonal upwelling and continental runoff. Harmful Algae 10(2), 121-129.

Amiard, J.C., Bacheley, H., Barille, A.L., Barille, L., Geffard, A., Himery, N., 2004. Temporal changes in nickel and vanadium concentrations and in condition index and metallothionein levels in three species of molluscs following the "Erika" oil spill. Aquat. Living Resour. 17(3): 281-8.

Armstrong, J.D. 1997. Self-thinning in juvenile sea trout and other salmonid fishes revisited. Journal of Animal Ecology 66: 519–526.

Banavar, J.R., Maritan, A., Rinaldo, A., 1999. Size and form in efficient transportation networks. Nature. 399: 130-132.

Battese, G.E., Coelli, T. 1992. Frontier production functions, technical efficiency and panel data: with application to paddy farmers in India. Journal of Productivity Analysis 3: 153-169.

Bayne, B.L., Salkeld, P.N., Worrall, C.M., 1983. Reproductive effort and value in different populations of the marine mussel, *Mytilus edulis* L. Oecologia. 59(1): 18-26.

Bégin, É., Bégin, J., Bélanger, L., Rivest, L.P., Tremblay, S. 2001. Balsam fir self-thinning relationship and its constancy among different ecological regions. Canadian Journal of Forest Research 31: 950–959.

Begon, M., Firbank, L., Wall, R. (1986) Is there a self-thinning rule for animal populations? Oikos 46: 122–124.

Begon, M., Townsend, C.R. & Harper, J.L (2006) Ecology: from individuals to ecosystems. 4th edn. Blackwell Publishing, Oxford.

Belgrano, A., Allen, A.P., Enquist, B.J. and Gillooly, J.F. 2002. Allometric scaling of maximum population density: a common rule for marine phytoplankton and terrestrial plants. Ecology Letters 5: 611–613.

Bertness, M.D., Grosholz, E., 1985. Population dynamics of the ribbed mussel, *Geukensia demissa*: the costs and benefits of an aggregated distribution. Oecol. 67(2): 192-204.

Bi, H., Wan, G., Turvey, N.D. 2000. Estimating the self-thinning boundary line as a density-dependent stochastic biomass frontier. Ecology 81: 1477–1483.

Bi, H. 2004. Stochastic frontier analysis of a classic self-thinning experiment. Austral Ecology 29: 408–417.

Bohlin, T., Dellefors, C., Faremo, U., Johlander, A. 1994. The energetic equivalence hypothesis and the relation between population density and body size in stream living salmonids. American Naturalist 143: 478–493.

Boromthanarat, S., Deslous-Paoli, J.M., 1988. Production of Mytilus edulis L. reared on bouchots in the Bay of Marennes-Oléron: Comparison between two methods of culture. Aquaculture 72: 255-263.

Boscolo, R., Cacciatore, F., Berto, D., Marin, M.G., Giani, M., 2004. Contamination of natural and cultured mussels (*Mytilus galloprovincialis*) from the northern Adriatic Sea by tributyltin and dibutyltin compounds. Applied Organometallic Chemistry 18: 614-618.

Box, G.E.P., Hunter, W., Hunter, J.S., 1978. Statistics for experimenters. An introduction to design, data analysis and model building. John Wiley & Sons, Inc., New York.

Branch, G.M., Steffani, C.N., 2004. Can we predict the effects of alien species? A case-history of the invasion of South Africa by Mytilus galloprovincialis (Lamarck). 300 (1-2): 189-215.

Briones, C., Guinez, R., 2005. Bilateral asymmetry of shell shape and spatial position in matrices of the mussel *Perumytilus purpuratus* (Lamarck, 1819) (Bivalvia : Mytilidae). Revista Chilena De Historia Natural 78(1): 3-14.

Brown, R.A., Seed, R., O'Connor, R.J., 1976. A comparison of relative growth in *Cerastoderma (=Cardium) edule, Modiolus modiolus* and *Mytilus edulis* (Mollusca: Bivalvia). J. Zool. 179: 297-315.

Brown J.H., Gillooly J.F., Allen, A.P., Savage, V.A. West, G.B. 2004. Toward a metabolic theory of ecology. Ecology 85: 1771-1789.

Caceres-Martinez, J., Figueras, A., 1998a. Long-term survey on wild and cultured mussels (*Mytilus galloprovincialis* Lmk) reproductive cycles in the Ria de Vigo (NW Spain). Aquaculture 162(1-2): 141-56.

Caceres-Martinez, J., Figueras, A., 1998b. Distribution and abundance of mussel (*Mytilus galloprovincialis* Lmk) larvae and post-larvae in the Ria de Vigo (NW Spain). J. Exp. Mar. Biol. Ecol. 229(2): 277-87.

Caro, A.U., Castilla, J.C., 2004. Predator-inducible defences and local intrapopulation variability of the intertidal mussel *Semimytilus algosus* in central Chile. Mar. Ecol. Prog. Ser. 276, 115-23.

Ceccherelli, V.U., Barboni, A., 1983. Growth, survival and yield of *Mytilus galloprovincialis* Lamk, on fixed suspended culture in a bay of the Po River Delta. Aquaculture 34 (1-2): 101-114.

Chen, Y., Jackson, D.A., Harvey, H.H., 1992. A comparison of von Bertalanffy and polynomial functions in modeling fish growth data. Can. J. Fish. Aquat. Sci. 49: 1228-1235.

Chen, K., Kang H.M, Bai, J., Fang, X.W. & Wang G. (2008) Relationship between the Virtual Dynamic Thinning Line and the Self-Thinning Boundary Line in Simulated Plant Populations. Journal of Integrative Plant Biology, 50: 280-290.

Chinzei, Y., White, B.N., Wyatt, G.R., 1982. Vitellogenin messenger-rna in locust fat-body - identification, isolation, and quantitative changes induced by juvenile-hormone. Can. J. Biochem. 60(3): 243-51.

Cigarria, J., Fernandez, J., 1998. Manila clam (*Ruditapes philippinarum*) culture in oyster bags: Influence of density on survival, growth and biometric relationships. J. Mar. Biol. Assoc. U.K. 78(2): 551-560.

Coe, W.R., 1946. A resurgent population of the California bay-mussel (*Mytilus edulis digenesis*). J. Morphol. 78(1): 85-103.

Coelli, T. and Henningsen, A. 2011. frontier: Stochastic Frontier Analysis. R package version 0.997-2. http://CRAN.R-project.org/package=frontier

Cote, J., Himmelman, J.H., Claereboudt, M., Bonardelli, J.C., 1993. Influence of density and depth on the growth of juvenile sea scallops (*Placopecten magellanicus*) in suspended culture. Can. J. Fish. Aquat. Sci. 50(9): 1857-69.

Dame, R.F., Prins, T.C., 1998. Bivalve carrying capacity in coastal ecosystems. Aquat. Ecol. 31: 409-421.

Dickie, L.M., Boudreau, P.R., Freeman, K.R., 1984. Influences of stock and site on growth and mortality in the blue mussel (*Mytilus edulis*). Can. J. Fish. Aquat. Sci. 41 **(**1): 134-140.

Dolmer, P., 2000. Feeding activity of mussels *Mytilus edulis* related to near-bed currents and phytoplankton biomass. J. Sea Res. 44: 221-231.

Dunham, J.B., Vinyard, G.L. 1997. Relationships between body mass, population density, and the self-thinning rule in stream-living salmonids. Canadian Journal of Fisheries and Aquatic Sciences 54:1025–1030.

Duquesne, S., Liess, M., Bird, D.J., 2004. Sub-lethal effects of metal exposure: Physiological and behavioural responses of the estuarine bivalve *Macoma balthica*. Mar. Environ. Res. 58(2-5): 245-50.

Enquist, B.J., Brown, J.H. and West, G.B. 1998. Allometric scaling of plant energetics and population density. Nature 395:163-165.

Figueiras, F.G., Labarta, U., Fernández-Reiriz, M.J., 2002. Coastal upwelling, primary production and mussel growth in the Rías Baixas of Galicia. Hydrobiologia 484: 121-131.

Filgueira, R., Labarta, U., Fernandez-Reiriz, M. J. (2008) Effect of condition index on allometric relationships of clearance rate in *Mytilus galloprovincialis* Lamarck, 1819. Revista De Biología Marina y Oceanografia 43(2): 391-8.

Filgueira, R., Peteiro, L.G., Labarta, U., Fernández-Reiriz, M.J. 2008. The self-thinning rule applied to cultured populations in aggregate growth matrices. Journal of Molluscan Studies 74:415–418.

Fréchette, M., Bacher, C. 1998. A modelling study of optimal stocking density of mussel populations kept in experimental tanks. Journal of Experimental Marine Biology and Ecology 219: 241– 255.

Fréchette, M., Bourget, E., 1985a. Energy-flow between the pelagic and benthic zones - factors controlling particulate organic-matter available to an intertidal mussel bed. Can. J. Fish. Aquat. Sci. 42(6): 1158-65.

Fréchette, M., Bourget, E., 1985b. Food-limited growth of *Mytilus edulis* L. in relation to the benthic boundary-layer. Can. J. Fish. Aquat. Sci. 42(6): 1166-70.

Fréchette, M. Despland, E., 1999. Impaired shell gaping and food depletion as mechanisms of assymetric competition in mussels. Ecoscience 6(1): 1-11.

Fréchette, M., Lefaivre, D., 1990. Discriminating between food and space limitation in benthic suspension feeders using self-thinning relationships. Mar. Ecol. Prog. Ser. 65(1): 15-23.

Fréchette, M., Lefaivre, D., 1995. On self-thinning in animals. Oikos 73(3): 425-428.

Fréchette, M., Aitken, A.E., Page, L., 1992. Interdependence of food and space limitation of a benthic suspension feeder: consequences for self-thinning relationships. Mar. Ecol. Prog. Ser. 83(1): 55-62.

Fréchette, M., Bergeron, P., Gagnon, P. 1996. On the use of self-thinning relationships in stocking experiments. Aquaculture 145: 91–112.

Fréchette, M., Lachance-Bernard, M., Daigle, G. 2010. Body size, population density and factors regulating suspension-cultured blue mussel (*Mytilus spp.*) populations. Aquatic Living Resources 23: 247-254.

Fuentes, J., Morales, J., Villalba, A., 1998. Growth, mortality and parasitization of mussels cultivated in the Ria de Arousa (NW Spain) from two sources of seed: intertidal rocky shore vs. collector ropes. Aquaculture 162: 231–240.

Fuentes, J., Gregorio, V., Giráldez, R., Molares, J., 2000. Within-raft variability of the growth rate of mussels, *Mytilus galloprovincialis*, cultivated in the Ria de Arousa (NW Spain). Aquaculture 189: 39-52.

Funk, A., Reckendorfer, W., 2008. Environmental heterogeneity and morphological variability in *Pisidium subtruncatum* (Sphaeriidae, Bivalvia). Int. Rev. Hydrobiol. 93(2): 188-99.

Gascoigne, J.C., Beadman, H.A., Saurel, C., Kaiser, M.J., 2005. Density dependence, spatial scale and patterning in sessile biota. Oecologia 145(3): 371-81.

Gibbs, M.M., James, M.R., Pickmere, S.E., Woods, P.H., Shekespeare, B.S., Hickman, R.W., Illingworth, J., 1991. Hydrodynamics and water column properties at six stations

associated with mussel forming in Pelorus Sound, 1984-85. NZ. J. Mar. Fresh. Res. 25: 239-254.

Gosling, E., 2003. Bivalve molluscs. Biology, ecology and culture. Blackwell Publishing Ltd., Oxford. 443 pp.

Grant, J., 1996. The relationship of bioenergetics and the environment to the field growth of cultured bivalves. J. Exp. Mar. Biol. Ecol. 200: 239-256.

Grant, J., 1999. Ecological constraints on the sustainability of bivalve aquaculture. Dissertation, Leiden; Schipholweg 107C, PO Box 447, 2316 SC Leiden, Netherlands: A. A. Balkema Publishers.

Greene, W.H. 1997. Frontier production functions. Pages 81-166 *in* M.H. Pesaran and P. Schmidt, editors. Handbook of applied econometrics: microeconomics. Blackwell, Oxford, UK.

Griffiths, C.L., Hockey, P.A.R., 1987. A model describing the interactive roles of predation, competition and tidal elevation in structuring mussel populations. S. Afr. J. Mar. Sci. 5: 547-556.

Guiñez, R. (1996) Dinámica poblacional del chorito maico, *Perumytilus purpuratus* (Lamarck 1819) (Bivalvia: Mytilidae), en gradientes de exposición al oleaje. Ph.D. thesis. Pontificia Universidad Católica de Chile, Santiago.

Guiñez, R., 2005. A review on self-thinning in mussels. Revista De Biologia Marina y Oceanografia 40(1): 1-6.

Guiñez, R., Castilla, J.C., 1999. A tridimensional self-thinning model for multilayered intertidal mussels. Am. Nat. 154(3): 341-57.

Guiñez, R., Castilla, J.C. 2001. An allometric tridimensional model of self-thinning for a gregarious tunicate. Ecology 82: 2331–2341.

Guiñez, R., Petraitis, P.S., Castilla, J.C. 2005. Layering, the effective density of mussels and mass–density boundary curves. Oikos 110: 186–190.

Guolan, H, Yong, W., 1995. Effects of tributyltin chloride on marine bivalve mussels. Water Res. 29(8): 1877-84.

Hagihara, A., 1999. Theoretical considerations on the C-D effect in self-thinning plant populations. Researches on Population Ecology (Kyoto) 41: 151-159.

Harger, J.R.W., 1972. Competitive coexistence: maintenance of interacting associations of the sea mussels *Mytilus edulis* and *Mytilus californianus.* Veliger 14: 387-410.

Hosomi, A. 1985. On the persistent trend of constant biomass and the constant total occupation area of the mussel *Mytilus galloprovincialis* (Lamarck). Japanese Journal of Malacology 44: 33-48.

Huber, P.J. 1981. Robust Statistics. Wiley, New York, USA.

Hughes, R.N., Griffiths, C.L. 1988. Self-thinning in barnacles and mussels: the geometry of packing. American Naturalist 132: 484–491.

Hummel, H., Amiard-Triquet, C., Bachelet, G., Desprez, M., Marchand, J., Sylvand, B., Amiard, J.C., Rybarczyk, H., Bogaards, R.H., Sinke, J. et al., 1996b. Sensitivity to stress of the estuarine bivalve *Macoma balthica* from areas between the Netherlands and its southern limits (Gironde). J. Sea. Res. 35(4): 315-21.

Jeffrey, S.W., Humphrey, G.F., 1975. New spectrophotometric equations for the determining chlorophylls a, b, c_1, and c_2 in higher plants, algae and natural phytoplankton. Biochem. Physiol. Pflanz., 167:191-194.

Jørgensen, C.B., Larsen, P.S., Møhlenberg, F., Riisgård, H.U., 1988. The mussel pump: properties and modelling. Mar. Ecol. Prog. Ser. 45: 205-216.

Karayucel, S., Karayucel, I., 2000. Influence of stock and site on growth, mortality and shell morphology in cultivated blue mussels (*Mytilus edulis* L.) in two Scottish sea lochs. Israeli Journal of Aquaculture-Bamidgeh 52(3): 98-110.

Kautsky, N., 1982. Growth and size structure in a Baltic *Mytilus edulis* population. Mar. Biol. 68(2): 117-33.

Labarta, U. 2004. El mejillón, un paradigma bioeconómico. In Bateeiros, Mar, Mejillón. Una Perspectiva Bioeconómica. Ed. by Centro de Investigación Económica y Financiera. Fundación Caixa Galicia. ISBN: 84-95491-69-9. 262 pp.

Lachance-Bernard, M., Daigle, G., Himmelman, J.H., Fréchette, M. 2010. Biomass-density relationships and self-thinning of blue mussels (*Mytilus* spp.) reared on self-regulated longlines, Aquaculture 308: 34-43

Latto, J. 1994. Evidence for a self-thinning rule in animals. Oikos 69: 531–534.

Lauzon-Guay, J.S., Hamilton, D.J., Barbeau, M.A., 2005a. Effect of mussel density and size on the morphology of blue mussels (*Mytilus edulis*) grown in suspended culture in Prince Edward Island, Canada. Aquaculture 249(1-4): 265-274.

Lauzon-Guay, J., Dionne, M., Barbeau, M.A., Hamilton, D.J., 2005b. Effects of seed size and density on growth, tissue-to-shell ratio and survival of cultivated mussels (*Mytilus edulis*) in Prince Edward Island, Canada. Aquaculture 250(3-4): 652-65.

Lauzon-Guay, J.S., Barbeau, M.A., Watmough, J., Hamilton, D.J., 2006. Model for growth and survival of mussels *Mytilus edulis* reared in Prince Edward Island, Canada. Mar. Ecol. Prog. Ser. 323: 171-183.

Lent, C.M., 1967. Effect of habitat on growth indices in the ribbed mussel, *Modiolus (arcuatula) demissus*. Chesapeake Science 8(4): 221-7.

Leonard, G.H., Bertness, M.D., Yund, P.O., 1999. Crab predation, waterborne cues, and inducible defenses in the blue mussel, *Mytilus edulis*. Ecology 80(1): 1-14.

Lesser, M.P., Shumway, S.E., Cucci, T., Smith, J., 1992. Impact of fouling organisms on mussel rope culture: Interspecific competition for food among suspension-feeding invertebrates. J. Exp. Mar. Biol. Ecol. 165: 91-102.

Leung, K.M.Y., Furness, R.W., 2001. Metallothionein induction and condition index of dogwhelks *Nucella lapillus* (L.) exposed to cadmium and hydrogen peroxide. Chemosphere 44(3): 321-5.

Lin, J., 1991. Predator-prey interactions between blue crabs and ribbed mussels living in clumps. Estuar. Coast. Shelf. Sci. 32: 61-69.

Lonsdale, W.M. 1990. The self-thinning rule: dead or alive? Ecology 71: 1373-1388.

Mallet, A.L., Carver, C.E., 1991. An assessment of strategies for growing mussels in suspended culture. J. Shellfish Res. 9: 87-93.

Marquet, P.A., Navarrete, S.A., Castilla, J.C., 1990. Scaling population-density to body size in rocky intertidal communities. Science 250(4984): 1125-7.

Marquet, P.A., Navarrete, S.A. & Castilla, J.C. (1995) Body size, population density, and the energetic equivalence rule. Journal of Animal Ecology, 54: 325-332.

Maximovich, N.V., Sukhotin, A., Minichev, Y.S., 1996. Long-term dynamics of blue mussel (*Mytilus edulis* L.) culture settlements (the White Sea). Aquaculture 147: 191-204.

McGrorty, S., Goss-Custard, J.D., 1995. Population dynamics of *Mytilus edulis* along environmental gradients: Density-dependent changes in adult mussel numbers. Mar. Ecol. Prog. Ser. 129: 197-213.

Mohler, C.L., Marks, P.L., Sprugel, D.G. 1978. Stand structures and allometry of trees during self-thinning of pure stands. Journal of Ecology 66: 599-614.

Motulsky, H., Christopoulos, A. C. 2004. Fitting Models to Biological Data using Linear and Nonlinear Regression: a Practical Guide to Curve Fitting. Oxford University Press, Oxford. 351 pp.

Mueller, K.W., 1996. A preliminary study of the spatial variation in growth of raft-cultured blue mussels *Mytilus trossulus* in northern Puget Sound, Washington. J. World Aquacult. Soc. 27: 240-246.

Nash, R.D.M, Geffen, A.J., Burrows, M.T. & Gibson, R.N. (2007) Dynamics of shallow-water juvenile flatfish nursery grounds: application of the 'self-thinning rule'. Marine Ecology Progress Series, 344: 231–244.

Navarro, E., Iglesias, J.I.P., Camacho, A.P., Labarta, U., Beiras, R., 1991. The physiological energetics of mussels (*Mytilus galloprovincialis* Lmk) from different cultivation rafts in the Ria de Arosa (Galicia, N.W. Spain). Aquaculture 94: 197–212.

Newell, C.R., 1990. The effects of mussel (*Mytilus edulis* Linnaeus 1758) position in seeded bottom patches on growth at subtidal lease sites in Maine. J. Shellfish Res. 9: 113-118.

Norberg R.Å. 1988*a*. Theory of growth geometry of plants and self-thinning of plant populations: geometry similarity, elastic similarity, and different growth modes of plants parts. American Naturalist 131: 220-256.

Norberg, R.Å., 1988*b*. Self-thinning of plant populations dictated by packing density and individual growth geometry and relationships between animal population density and body mass governed by metabolic rate. pp. 259-279 *in* Size structured populations. Ecology and Evolution. B. Ebenman and L. Persson, editors. Springer-Verlag, Berlin, Heidelberg.

Ohba, S., 1956. Effects of population density on mortality and growth in an experimental culture of a bivalve, *Venerupis semidecussata*. Biological Journal of Okayama University. 112, 169.

Okamura, B., 1986. Group living and the effects of spatial position in aggregations of *Mytilus edulis*. Oecologia 69(3): 341-347.

Osawa, A., Sugita, S. 1989. The self-thinning rule: another interpretation of Weller's results. Ecology 70: 279- 283.

Osawa, A., Allen, R. 1993. Allometric theory explains self-thinning relationships of mountain beech and red pine. Ecology 74: 1020–1032.

Paine, R.T., 1974. Intertidal Community Structure. Experimental Studies on the Relationship between a Dominant Competitor and Its Principal Predator. *Oecologia* 15 (2): 93-120.

Pampanin, D.M., Volpato, E., Marangon, I., Nasci, C., 2005. Physiological measurements from native and transplanted mussel (*Mytilus galloprovincialis*) in the canals of Venice. Survival in air and condition index. Comparative Biochemistry and Physiology 140(1): 41-52.

Parsons, G.J., Dadswell, M.J., 1992. Effect of stocking density on growth, production, and survival of the giant scallop *Placopecten magellanicus*, held in intermediate suspension culture in Passamaquoddy Bay, New Brunswick. Aquaculture 103: 291-309.

Pérez Camacho, A., Labarta, U. 2004. Rendimientos y producción del mejillón: bases biológicas para la innovación. In Bateeiros, Mar, Mejillón. Una Perspectiva Bioeconómica. Ed. by Centro de Investigación Económica y Financiera. Fundación Caixa Galicia. ISBN: 84-95491-69-9. 262 pp.

Pérez Camacho, A., González, R., Fuentes, J., 1991. Mussel culture in Galicia (N.W. Spain). Aquaculture 94: 263- 278.

Pérez Camacho, A., Labarta, U., Navarro, E., 2000. Energy balance of mussels *Mytilus galloprovincialis*: the effect of length and age. Mar. Ecol. Prog. Ser. 199: 149-158.

Peteiro, L.G., Filgueira, R., Labarta, U., Fernández-Reiriz, M.J., 2007. Settlement and recruitment patterns of *Mytilus galloprovincialis* L. in the Ría de Ares-Betanzos (NW Spain) in the years 2004/2005. Aquaculture Research 38 (9): 957-964.

Peterson, C.H., 1982. The importance of predation and intraspecific and interspecific competition in the population biology of 2 infaunal suspension-feeding bivalves, *Protothaca staminea* and *Chione undatella*. Ecol. Monogr. 52(4): 437-75.

Peterson, C.H. Beal, B.F., 1989. Bivalve growth and higher-order interactions - importance of density, site, and time. Ecology 70(5): 1390-1404.

Petraitis, P.S., 1995. The role of growth in maintaining spatial dominance by mussels (*Mytilus edulis*). Ecology 76(4): 1337-1346.

Puntieri, J.G. (1993) The self-thinning rule: bibliography revision. Preslia, 65, 243–267.

R Development Core Team (2011). R: A language and environment for statistical computing. R Foundation for Statistical Computing, Vienna, Austria. ISBN 3-900051-07-0, URL http://www.R-project.org/

Ratkoskwy, D. A. 1990. Handbook of Nonlinear Regression Models. Ed. by D. B. Owen, R. G. Cornell, W. J. Kennedy, A. M. Kshirsagar, and E. G. Schilling. Marcel Dekker, Inc., New York. 241 pp.

Reimer, O., Tedengren, M., 1996. Phenotypical improvement of morphological defences in the mussel *Mytilus edulis* induced by exposure to the predator *Asterias rubens*. Oikos 75(3): 383-90.

Reimer, O., Tedengren, M., 1997. Predator-induced changes in byssal attachment, aggregation and migration in the blue mussel, *Mytilus edulis*. Mar. Freshwat. Behav. Physiol. 30 (4): 251-266.

Reimer, O., Olsson, B., Tedengren, M., 1995. Growth, physiological rates and behaviour of *Mytilus edulis* exposed to the predator *Asterias rubens*. Mar. Freshwat. Behav. Physiol. 25(4): 233-44.

Richardson, C.A., Seed, R., 1990. Predictions of mussel (*Mytilus edulis*) biomass on an offshore platform from single population samples. Biofouling 2: 289-297.

Roderick, M. L. & Barnes, B. (2004) Self-thinning of plant populations from a dynamic viewpoint. Functional Ecology. 18: 197–203.

Román, G., Campos, M.J., Acosta, C.P., Cano, J., 1999. Growth of the queen scallop (*Aequipecten opercularis*) in suspended culture: influence of density and depth. Aquaculture 178 (1-2): 43-62.

Rosland, R., Bacher, C., Strand, Ø., Aure, J., Strohmeier, T., 2011. Modelling growth variability in longline mussel farms as a function of stocking density and farm design. J. Sea Res. 66(4): 318-330.

Scarrat, D.J., 2000. Development of the mussel industry in eastern Canada. Bull. Aquacul. Assoc. Canada 100 (2): 37-40.

SCOR-UNESCO, 1966. Determination of photosynthetic pigments in seawater. Monogr. Oceanog. Method. UNESCO, Paris, vol. 1; 11-18 pp.

Seed, R., 1968. Factors influencing shell shape in the mussel *Mytilus edulis*. J. Mar. Biol. Assoc. U.K. 48: 561-584.

Seed, R., 1969. The ecology of *Mytilus edulis* L. (Lamellibranchiata) on exposed rocky shores. I. Breeding and settlement. Oecologia (Berlin) 3: 277-316.

Seed, R., 1973. Absolute and allometric growth in the mussel, *Mytilus edulis* L. (Mollusca, Bivalvia). Proc. Malacol. Soc. London 40: 343-357.

Seed, R., 1980. Variations in the shell-flesh relationships of *Mytilus*- value of sea mussels as items of prey. Veliger 22(3): 219-21.

Seed, R., Suchanek, T.H., 1992. Population and community ecology of *Mytilus*, in: Gosling E. (Ed.) The Mussel *Mytilus*: Ecology, Physiology, Genetics and Culture. Elsevier, Amsterdam, pp 87-170.

Sénéchal, J., Grant, J., Archambault, M.C., 2008. Experimental manipulation of suspended culture socks: Growth and behavior of juvenile mussels (*Mytilus* spp.). J. Shellfish Res. 27 (4): 811-826.

Smaal, A., van Stralen, M., 1990. Average annual growth and condition of mussels as a function of food source. Hydrobiologia 195: 179-188.

Snedecor, G.W., Cochran, W.G., 1989. Statistical methods, 8th ed. Iowa State University Press, Ames, Ia.

Snodden, L.M., Roberts, D., 1997. Reproductive patterns and tidal effects on spat settlement of *Mytilus edulis* populations in Dundrum bay, Northern Ireland. J. Mar. Biol. Assoc. U.K. 77(1): 229-43.

Steffani, C.N., Branch, G.M., 2003. Growth rate, condition, and shell shape of *Mytilus edulis*: Responses to wave exposure. Mar. Ecol. Prog. Ser. 246: 197-209.

Stillman, R.A., McGrorty, S., Goss-Custard, J.D., West, A.D., 2000. Predicting mussel population density and age structure: The relationship between model complexity and predictive power**.** Mar. Ecol. Prog. Ser. 208: 131-145.

Stirling, H.P., Okumus, I., 1994. Growth, mortality and shell morphology of cultivated mussel (*Mytilus edulis*) stocks cross planted between two Scottish sea lochs. Mar. Biol. 119: 115-124.

Stiven, A.E., Kuenzler, E.J., 1979. The response of two molluscs: *Littorina irrorata* and *Geukensia demissa*, to field manipulations of density and *Spartina litter*. Ecol. Monogr. 49: 151-171.

Suarez, M.P., Alvarez, C., Molist, P., San Juan, F., 2005. Particular aspects of gonadal cycle and seasonal distribution of gametogenic stages of *Mytilus galloprovincialis* cultured in the estuary of Vigo. J. Shellfish Res. 24(2): 531-40.

Suchanek, TH. 1986. Mussels and their role in structuring rocky shore communities. pp. 70-96 *in* The ecology of rocky coasts. P.G. Moore & R. Seed, editors. Columbia University Press, New York.

Tanita, S., Kikuchi, S., 1957. On the density effect of the raft cultured oysters. I. The density effect within one plate. Bull. Tohoku Reg. Fish. Lab. Res. 9: 133–142.

Taylor, J.J., Rose, R.A., Southgate, P.C., 1997. Effects of stocking density on the growth and survival of juvenile silver-lip pearl oysters (*Pinctada maxima*, Jameson) in suspended and bottom culture. J. Shellfish Res. 16: 569-572.

Thomas, S.C., Weiner, J., 1989. Including competitive asymmetry in measures of local interference in plant-populations. Oecologia 80(3): 349-55.

Tonn, W. M., Holopainen, I. J. and Paszkowski, C. A. 1994. Density-dependent effects and the regulation of crucian carp populations in single-species ponds. Ecology 75: 824–834.

Villalba, A., 1995. Gametogenic cycle of cultured mussel, *Mytilus galloprovincialis*, in the bays of Galicia (NW Spain). Aquaculture 130(2-3): 269-277.

Wade, B.A., 1967. On taxonomy morphology and ecology of beach clam *Donax striatus* linne. Bull. Mar. Sci. 17(3): 723-

Waite, L., Grant, J., Davidson, J., 2005. Bay-scale spatial growth variation of mussels *Mytilus edulis* in suspended culture, Prince Edward Island, Canada. Mar. Ecol. Prog. Ser. 297: 157-167.

Weiner, J., 1990. Asymmetric competition in plant-populations. Trends in Ecology & Evolution 5(11): 360-4.

Weller, D.E. 1987a. A reevaluation of the -3/2 power rule of plant self-thinning. Ecological Monographs 57: 23-43.

Weller, D.E. 1987b. Self-thinning exponent correlated with allometric measures of plant geometry. Ecology 68: 813-821.

Westoby, M. 1984. The self-thinning rule. Advances in Ecological Research 14: 167–225.

West, G.B., Brown, J.H., Enquist, B.J., 1997. A General Model for the Origin of Allometric Scaling Laws in Biology. Science 276(5309): 122-126.

White, J. 1981. The allometric interpretation of the self-thinning rule. Journal of Theoretical Biology 89: 475–500.

Widman, J.C., Rhodes, E.W., 1991. Nursery culture of the bay scallop, *Argopecten irradians irradians*, in suspended mesh nets. Aquaculture 99(3-4): 257-267.

Xavier, B.M., Branch, G.M., Wieters, E., 2007. Abundance, growth and recruitment of *Mytilus galloprovincialis* on the west coast of South Africa in relation to upwelling. Mar. Ecol. Prog. Ser. 346: 189-201.

Yoda, K., Kira, T., Ogawa, H., Hozumi, K. 1963. Self-thinning in overcrowded pure stands under cultivated and natural conditions (Intraspecific competition among higher plants XI). Journal of Biology, Osaka City University 14: 107–129.

Xue, L & Hagihara, A. (1998) Growth analysis of the self-thinning stands of *Pinus densiflora* Sieb. et Zucc. Ecological Research, 13: 183–191.

Zar, J.H., 1999. Biostatistical Analysis. Prentice Hall, Inc., Upper Saddle River, New Jersey. 663 pp.

Zhang, L., Bi, H., Gove, J.H. and Heath, L.S. 2005. A comparison of alternative methods for estimating the self-thinning boundary line. Canadian Journal of Forest Research 35: 1507-1514.

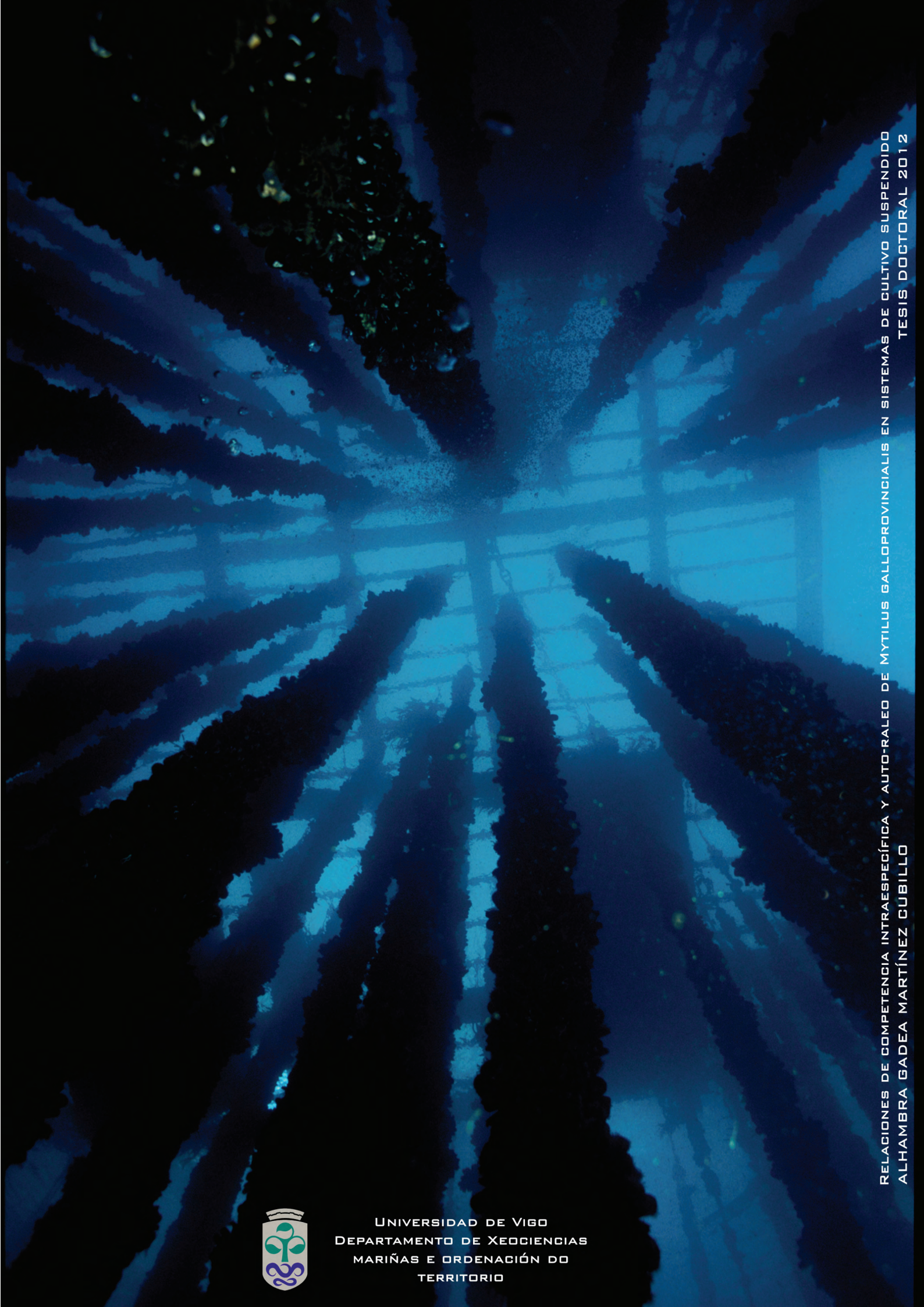

Relaciones de competencia intraespecífica y auto-raleo de Mytilus galloprovincialis en sistemas de cultivo suspendido

TESIS DOCTORAL 2012

ALHAMBRA GADEA MARTÍNEZ CUBILLO

Universidad de Vigo
Departamento de Xeociencias mariñas e ordenación do territorio